The Reliability of Weight Optimised Steel Portal Frames

by

Willem Stolk

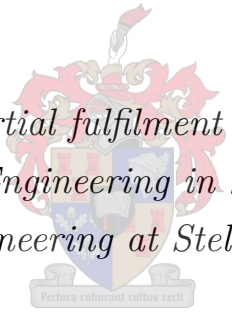

Thesis presented in partial fulfilment of the requirements for the degree of Master of Engineering in Structural Engineering in the Faculty of Engineering at Stellenbosch University

Department of Structural Engineering,
University of Stellenbosch,
Private Bag X1, Matieland 7602, South Africa.

Supervisor: Mr. E. van der Klashorst
Co-Supervisor: Dr. C. Viljoen

December 2015

The financial assistance of the National Research Foundation (NRF) towards this research is hereby acknowledged. Opinions expressed and conclusions arrived at, are those of the author and are not necessarily to be attributed to the NRF.

Declaration

By submitting this thesis/dissertation electronically, I declare that the entirety of the work contained therein is my own, original work, that I am the sole author thereof (save to the extent explicitly otherwise stated), that reproduction and publication thereof by Stellenbosch University will not infringe any third party rights and that I have not previously in its entirety or in part submitted it for obtaining any qualification.

Date: December 2015

Abstract

Steel portal frame structures are traditionally designed in accordance with ultimate limit state criteria and then typically evaluated in terms of the serviceability limit state. The serviceability limit state often governs the design process, therefore it is important that appropriate deflection limits are used for the design of steel portal frames. The origin of deflection limits specified in some current codes of practice are unknown, while some codes do not even specify serviceability limit state deflections for portal frames, but rather leave the judgement of deflection limits to the engineer.

The design of portal frame structures in accordance with certain deflection limits have no direct effect on the serviceability of the frame itself, however the deflection limits are used to protect the structure against other complicated serviceability demands. These demands include structural damage to non-structural members and connections as well as noticeable distressing deflections. When considering ultimate limit state, the definition of failure is fairly clear, however the distinction between serviceable and unserviceable are vague. It is therefore evident that the SCI advisory desk specified deflection limits, which are widely adopted, are mostly defined on experience. These specified limits may have a direct effect on the optimal weight and reliability of the structure.

For the proposed study, a real-coded Genetic Algorithm which is part of the evolutionary algorithm family is used to determine the optimal or near optimal weight of steel portal frames. The proposed Genetic Algorithm based on the natural process, known as survival-of-the-fittest, selects the optimal universal beam section from a discrete set of available sections for columns and rafters. Furthermore, the algorithm will determine the optimal length of the haunch at the eaves as well as the optimal roof pitch. With the use of these four design variables, each portal frame has a possible 28.83×10^6 number of solutions.

A total of 119 portal frames of different span to height ratios were optimised with the use of the proposed Genetic Algorithm. These 119 analyses were used to investigate the effect of the haunch length and roof pitch of the portal frame on the optimal weight. An overall average decrease in total weight of 9% were obtained when haunched rafters were used for portal frames. In terms of the roof pitch of portal frames, the conclusion was made that the roof pitch only has a significant effect on the optimal weight of portal frames with a span to height ratio larger than two. From the 119 analyses, 87% of the frames subjected to wind load were governed by

the serviceability limit state.

The reliability or safety index of each optimal steel portal frame will then be calculated with the use of the First Order Reliability Method (FORM), and compared to specified reliability values accepted in design codes of practice for ultimate and serviceability limit states. The value of the reliability index is dependent on the amount and quality of information that is available, therefore the theory and philosophy emphasize that the reliability or safety index becomes a design variable during the design phase of a structure.

An average reliability index of $\beta = 3.3$ were obtained for optimal portal frames governed by the ultimate limit state which is greater than the target reliability index of $\beta = 3.0$ specified in SANS 10160-1:2011. For frames governed by the horizontal deflection limit, an average reliability index of $\beta = 0.6$ were obtained which is far less than the allowable target reliability index of $\beta = 2.0$ specified in SANS 10160-1:2011 for irreversible deflections.

Uittreksel

Staal portaalrame word tradisioneel in terme van die uiterste limietstaat ontwerp en daarna in terme van die diensbaarheid limietstaat geëvalueer. Die diensbaarheid limietstaat is gewoonlik die bepalende faktor tydens die ontwerp van portaalrame, daarom is dit belangrik geskikte defleksielimiete gebruik word. Die oorsprong van defleksielimiete wat in huidige ontwerpkodes gespesifiseer word, is onbekend, terwyl sommige ontwerpkodes die defleksielimiete aan die ingenieur se oordeel oorlaat.

Die ontwerp van portaalrame, volgens sekere defleksielimiete, het geen direkte impak op die diensbaarheid van die raam self nie. Die defleksielimiete word wel gebruik om die portaalraam teen ander ingewikkelde diensbaarheidseise te beskerm. Hierdie eise sluit strukturele skade aan niestrukturele elemente en konneksies sowel as merkbare kommerwekkende defleksies in. Wanneer die uiterste limietstaat in ag geneem word, is die definisie van faling duidelik. Die onderskeid wat tussen die terme diensbaar en ondiensbaar getref word, is vaag. Dit is daarom verstaanbaar dat die defleksielimiete wat deur die SCI se adviserende instansie aanvaar is, meestal op ervaring gebaseer is. Hierdie limiete het 'n direkte invloed op die optimale gewig en betroubaarheid van die struktuur.

Vir die voorgestelde studie word 'n Genetiese Algoritme, wat deel uitmaak van die evolusionêre algoritmiese familie, gebruik om 'n optimale portaalraam te vind. Die voorgestelde genetiese algoritme wat op die natuurlike proses, bekend as oorlewing van die sterkste, gebaseer is, kies 'n optimale universele balk vanuit 'n lys van beskikbare groottes. Dit word vir beide kolomme en balke gedoen. Die Genetiese Algoritme bepaal voorts die optimale lengte van die kolomskouers by die dakrante asook die optimale helling van die dak.

'n Totaal van 119 portaalrame van verskillende span tot hoogte verhoudings was geoptimiseer met behulp van die voorgestelde Genetiese Algoritme. Die 119 analises was gebruik om die effek van die kolomskouers en dakhelling van 'n portaalraam op die optimale gewig te ondersoek. 'n Totale afname in totale gewig van 9% is verkry wanneer kolomskouers gebruik was. In terme van die dakhelling van 'n portaalraam was die gevolgtrekking gemaak dat die dakhelling slegs 'n beduidende invloed op die optimale gewig van 'n portaal raam het vir rame met 'n span tot hoogte verhouding groter as twee. Van die 119 portaalrame word 87% van die rame beheer deur die diensbaarheid limietstaat.

Die betroubaarheidsindeks, óf veiligheidsindeks, van die optimale portaalraam word deur die Eerste Orde Betroubaarheidsmetode (EOBM) bereken. Die voorgeskrewe betroubaarheidsindeks in ontwerpkodes vir die uiterste-en diensbaarheid limietstaat word dan hiermee vergelyk. Die waarde van die betroubaarheidsindeks is van die hoeveelheid en kwaliteit van inligting wat beskikbaar is afhanklik. Sodoende dui die teorie en filosofie daarop aan dat die betroubaarheidsindeks of veiligheidsindeks 'n ontwerpsveranderlike word tydens die ontwerpfase van 'n struktuur.

'n Gemiddelde betroubaarheidsindex van $\beta = 3.3$ was verkry vir rame wat beheer word deur die uiterste limietstaat. Hierdie betroubaarheidsindex is groter as die teiken betroubaarheidslimiet van $\beta = 3.0$ wat voorgeskryf is in SANS 10160-1:2011 en daarom aanvaarbaar. Vir rame wat beheer word deur die horisontal defleksie limietstaat, 'n gemiddelde betroubaarheidsindex van $\beta = 0.6$ was verky. Hierdie betroubaarheidsindex is laer as die teiken betroubaarheidsindex van $\beta = 2.0$ wat voorgeskryf is in SANS 10160-1:2011 vir onomkeerbare defleksies en daarom onaanvaarbaar.

Acknowledgements

- Thank you to my main supervisor, Mr. Etienne van der Klashorst, for his support and guidance.
- Thank you to my co-supervisor, Dr. Celeste Viljoen, for her support and guidance.
- Thank you to my fiancé, Mackayla Hanna Heneke, for all her support, love and guidance.
- Thank you to my parents, Dr. Willem Stolk and Elba Stolk, for their support, love and guidance.
- Thank you to CDSS for financial support.
- The financial assistance of the National Research Foundation (NRF) towards this research is hereby acknowledged. Opinions expressed and conclusions arrived at, are those of the author and are not necessarily to be attributed to the NRF.

Contents

List of Figures

List of Tables

Chapter 1

Introduction

1.1 Overview

The reliability of portal frames of different span to height ratios and wind loading conditions can only be compared to target reliability values accepted in design codes given that each portal frame structure is an optimal or near optimal design. An optimal design of a portal frame structure would mean that the frame is at its ultimate capacity either in terms of the ultimate or serviceability limit state depending on which limit state governs the design.

During the late 1950's and early 1960's, the idea of evolutionary computation as an optimisation tool led to great research opportunities to improve the time it takes to obtain an optimal solution when there is a very large population of possible solutions. The main idea was to use the basic principles of evolution known as survival-of-the-fittest and natural selection to obtain an optimal solution from a very large population of possible solutions [24].

With the development of the digital computer, evolutionary algorithms which include evolutionary programming, evolution strategies and Genetic Algorithms were developed and used for the optimisation of structures where a large number of possible solutions exist [23].

In order to obtain an optimal portal frame given a specified span and height, a searching algorithm like Genetic Algorithms have to be used because of the large number of possible solutions. When an optimal solution is obtained, the design is governed by either the ultimate or serviceability limit state function, depending on which limit state function is closest to its maximum capacity i.e. deflection or member failure.

Given that the optimal solution of a portal frame can be obtained considering the member sizes, haunch length and roof pitch as design variables, the reliability of the frame is calculated with a non-linear Newton Raphson First Order Reliability Method (FORM). The obtained reliability index values for an optimal portal frame can then be compared to target reliability values accepted in design codes.

1.2 Objectives

The main objective of this study is to obtain an optimal portal frame structure with the use of a Genetic Algorithm. The probability of failure of any optimal frame can then be calculated depending on the governing limit state function. These values can then be compared for different span to height ratios to determine if current deflection limits and partial factors used for design variables of steel portal frames are sufficient to obtain target reliability values specified in SANS 10160-1:2011.

During the optimisation phase, the aim is to also determine the importance of haunched rafters and roof pitch on the optimal weight of portal frames as well as the governing limit state function being either the ultimate or serviceability limit state.

1.3 Methodology

A real-coded Genetic Algorithm will be programmed in JAVA to obtain an optimal solution of a portal frame with the member sizes, haunch length and roof pitch chosen as design variables. The Genetic Algorithm will consist of a loading section, a finite element method and a portal frame design section.

The wind loading section will be responsible for calculating the applied distributed loads on the portal frame because of wind loading for all possible wind load cases. The linear finite element method will then make use of the direct stiffness method and calculate reaction forces and moments as well as deflections resulting from the applied loading. A portal frame design section will calculate the member capacities and evaluate if failure of each member will occur.

The Genetic Algorithm use all the results from the finite element method, the design section and loading conditions to determine which solution from a very large group of possible solutions is the best solution. When an optimal portal frame of specified dimensions is obtained, the reliability index of the frame can be calculated.

A First Order Reliability Method is then used to determine the reliability index of the entire frame depending on the weakest member of the frame and which limit state function governs the design. An optimal frame means that the frame has no reserve capacity for the limit state function governing the design and that any increase in loading will result in failure. Given that an optimal frame is obtained from the Genetic Algorithm, the reliability of such a frame can then be compared to target reliability values in SANS 10160-1:2011 corresponding to the governing limit state. Conclusions can thus be drawn on the suitability of current deflection limits, design partial factors, target reliability values and sensitivity of certain design variables.

1.4 Exposition

The study is divided into five chapters, starting with an introduction chapter above giving a broad overview of the study and the principle aim thereof.

Chapter two consists of a literature study regarding the methods and techniques used to obtain an optimal portal frame and subsequently determine the reliability index of the optimal portal frame as well as a motivation for this study.

Chapter three consists of a description of the methods used for the program created in JAVA including Genetic Algorithms, wind loading, finite element method, portal frame design and reliability aspects.

Chapter four includes all the results and discussions for the optimal weight of portal frames, the importance of roof pitch and haunched rafters as well as the reliability results for optimal portal frames.

A full and in depth conclusion as well as recommendations for further studies are given in Chapter five.

The JAVA program created for this study is attached on a CD in Appendix C.

Chapter 2

Literature Study

2.1 Structural Optimisation

2.1.1 Introduction

The design process of a portal frame structure is subdivided into several subtasks which include a problem definition, a conceptual design, a selection of alternatives and a selection of the best design. To determine the reliability of an optimal portal frame, the best solution of a portal frame of specified span and height dimensions has to be obtained with the use of structural optimisation [42].

To use formal optimisation methods to find the best solution, the definition of the best design has to be clearly stated. According to Schoofs [42], this definition can be reached by answering the following three questions:

1. How are different designs described?
2. What is the criterion for the best design?
3. What are the design constraints and requirements?

The first of these three questions is based on defining a system which includes design variables, parameters and constants used in the design and optimisation phase. Secondly the criterion for an optimal structure (objectives) in terms of performance are defined. These objectives are based on a characteristic which defines the best or optimal design, for example cost, weight or performance. Lastly the third question involves a set of requirements, so-called design constraints, which have to be satisfied for an acceptable design. These design constraints are related to the objective set for the problem at hand [42].

In general, the optimisation process can be stated as changing a set of design variables subjected to specified constraints and objectives in order to obtain the optimal solution [46].

The use of optimisation techniques to find an optimal solution to a problem are summarized by Schoofs [42] as follows:

1. A selection of a set of design variables that describe the design and optimisation phase of a project.
2. A selection of an objective function which will be used to find the optimal solution.
3. A selection of specific constraints which have to be satisfied by the design.
4. The determination of a set of values which satisfy the objective function subjected to the specified constraints.

Optimisation techniques and methods have been used as early as the days of Newton, Lagrange and Cauchy. These methods mainly consist of mathematical programming techniques using gradient-based search methods [42, 26]. Although these methods created huge research and development opportunities, the gradient-based optimisation methods may suffer from slow convergence and might not converge to the global optimum at all. This gave way to the development of optimisation techniques such as evolutionary and genetic algorithms which are based on probabilistic searching and not mathematical gradient-based methods [26]. The use of genetic algorithms for optimisation are discussed in Section 2.2.

Optimisation techniques in the field of structural engineering have several applications from the sizing and topology optimisation of large scale three dimensional frames to the shape optimisation of two dimensional mechanical parts [26]. Some of these types of structural optimisation methods are discussed in more detail in Section 2.1.3.

As in Vanderplaats [46] and Papadrakakis, Lagaros, and Tsompanakis [26], a general structural optimisation problem can be formulated as follows:

$$Minimize\ F(x) \tag{2.1}$$

subject to;

$$g(x) \leq 0 \tag{2.2}$$

$$h(x) = 0 \tag{2.3}$$

$$x_L \leq x \leq x_U \tag{2.4}$$

where Equation (2.1) is the objective function, Equations (2.2) and (2.3) are inequality and

equality constraints respectively and Equation (2.4) defines the upper and lower bounds of the design variable x.

2.1.2 History of Structural Optimisation

With the development of the digital computer during the mid 1950's, the introduction of the finite element method created the opportunity for new research into structural optimisation. Since the work done by Newton, Lagrange and Cauchy, this was the first real breakthrough in the world of structural optimisation [42].

Following several years of study in the field of the finite element methods and structural optimisation, Schmit [41] proposed a new approach in 1960 in terms of the techniques used for structural optimisation. A paper published by Schmit called Structural Design by Systematic Synthesis acted as a basis for all future structural optimisation methods. The 3-bar truss structure in Figure 2.1 was analysed by Schmit and the conclusion was made that the middle bar number two is never stressed to its limit under either of the load conditions for its optimal design. This observation and conclusion violated traditional assumptions that each member of the truss structure should be fully stressed to its limit under at least one of the load conditions. This caused a huge increase in research in terms of structural optimisation [46].

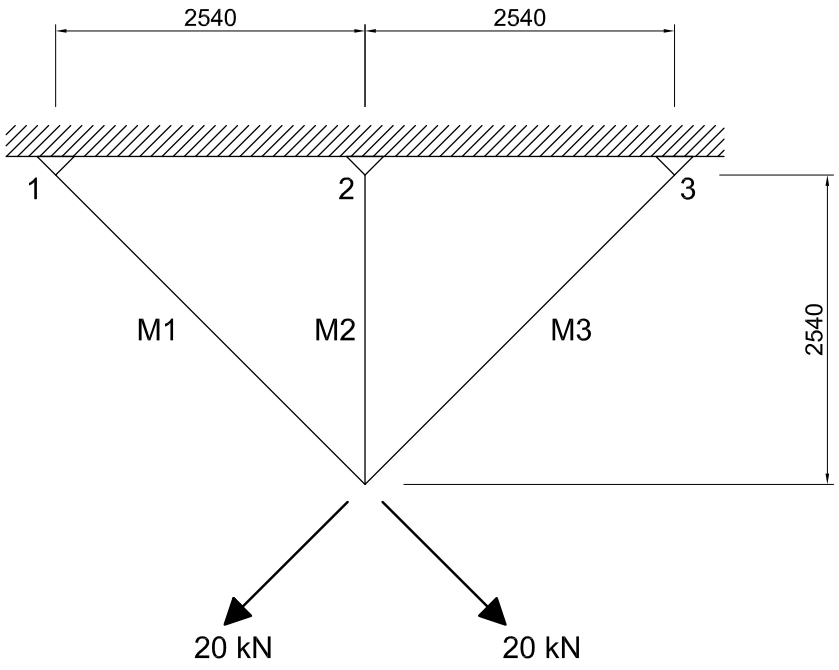

Figure 2.1: Presentation of the three bar truss analysed by Schmit [46].

Even though the new approach by Schmit [41] was significant in terms of structural optimisation techniques, these methods were not embraced by the professional community. The main reason

for the lack of enthusiasm for this new approach was due to the fact that even simple structures with only a few members had to be analysed several hundred times in order to obtain an optimal solution. With the large finite element models needed to simulate real structures, these methods were highly time consuming and expensive and were limited to only a few design variables with the mathematical programming techniques available at the time [42].

During the late 1960's, an alternative approach to the methods proposed by Schmit [41] were presented in analytical and numerical form by Prager and Taylor [30] and Venkayya, Khot, and Reddy [47] respectively. This new technique known as the optimality criteria approach make use of the basic principles of structural synthesis with the main difference being that the structural synthesis method directly minimized an objective function while the new optimality criteria method make use of constraints and restrictions applied to the problem at hand.

In 1972, Sobieszczanski and Loendorf [44] made use of a combination of the mathematical programming methods proposed by Schmit [41] and the optimality criteria method developed by Prager and Taylor [30] in the design of fuselage structures. The component design problem is dealt with by the mathematical programming methods while the optimality criteria methods dealt with the large number of design variables. The combination of these methods gave researchers greater possibility in finding an optimal relationship between the structural synthesis and optimality criteria methods.

During the latter parts of the 1970's, several researchers were working on ways to improve the effectiveness and efficiency of the mathematical programming methods. In 1976, Schmit and Hirokazu [40] presented a new and improved form of structural synthesis by making use of formal approximation concepts. This method made use of approximation functions when an original problem is created and used these approximations in order to obtain an optimal solution. Once an optimal solution is obtained, a finite element analysis is performed and more accurate approximation functions are created for the next iteration until the final optimal solution is obtained [42].

2.1.3 Types of Structural Optimisation Techniques

There are three basic types of structural optimisation techniques that can be used to find an optimal or near optimal portal frame structure subject to specified constraints and objective functions. Saka [39] did a study to obtain the optimum design of pitched roof steel frames with haunched rafters by using a size optimisation technique which selects an optimum universal beam section for both the columns and rafters as well as an optimum haunch length and depth.

Furthermore did Saka [39] mention that for economical reasons, pinned-base stanchions were used for portal frames as well as the use of haunched rafters at the eaves in order to withstand large moments. The formulation of the design problem analysed by Saka [39] was based on an elastic design method, taking into account both ultimate and serviceability limit state criteria.

Due to the large number of possible solutions to one single portal frame, Saka [39] made use of genetic algorithms which are discussed in Section 2.2.

Phan et al. [29] was also interested in obtaining an optimal design of steel portal frames in order to investigate what effect serviceability limits have on these optimal designs. Phan et al. [29] also made use of size optimisation as well as the use of genetic algorithms as a searching method to obtain the optimal design.

Following the two studies done by Saka [39] and Phan et al. [29], it is clear that the use of size optimisation for the determination of an optimal portal frame design where a universal beam section for the columns and rafters as well as an optimal haunch length and roof pitch are needed, will be sufficient in order to calculate the reliability of weight optimized steel portal frames. Size optimisation which will be used as part of the JAVA program created for the reliability calculation of optimal portal frames as well as the other two optimisation techniques namely shape and topology optimisation are briefly discussed below.

2.1.3.1 Size Optimisation

Size optimisation is based on minimizing the weight of a structure, subjected to given constraints in terms of stresses and displacements [22]. During size optimisation, the design variables are dependent on the cross-sectional properties of each member of the structure. By selecting the best possible configuration of members in terms of each member's size, the lightest and most cost effective structure is obtained. Although a configuration where each member is different might result in the lightest possible structure, engineering practice demands that members are divided into groups in order to sustain symmetry and uniformity of the structure. The use of sizing optimisation for steel structures is commonly done with discrete design variables due to the availability of specific profiles [26].

When structural size optimisation is used, the weight of the structure is commonly the objective function $F(x)$ as in Equation (2.1), although constraints like stresses, stiffness, deflections, buckling and dynamic responses also have to be considered.

2.1.3.2 Shape Optimisation

Shape optimisation is used in structural engineering to improve the shape of a given structure by optimizing an objective function subjected to specified constraints. The objective function is frequently directly related to the coordinates of start and end nodes of given members, therefore changing the overall shape of the structure [26].

2.1.3.3 Topology Optimisation

Topology optimisation is a type of structural optimisation which is often used in structural engineering and design and is based on taking the cross-sectional areas of each member of the structure as design variables. In order to achieve an optimal or near optimal solution, the cross-sectional areas of some members are then set equal to zero, with the structure subjected to specified constraints like stress and displacement limits, therefore removing those members from the structure [22].

2.2 Genetic Algorithms for Structural Optimisation

2.2.1 Introduction

The use of optimisation techniques as discussed in Section 2.1 lead to the problem of finding an optimal solution from a very large population of possible solutions. For the structural optimisation of steel portal frame structures where the column size, rafter size, haunch length and roof pitch are all design variables, the size of the population of possible solutions are in the order of 28.83×10^6 given that the column and rafter sizes are selected from the list of I and H-section profiles in the South African Steel Construction Handbook [38] and the haunch length and roof pitch are continuous design variables. Due to this extremely large number of possible solutions, an algorithm like Genetic Algorithms as were used by Saka [39] and Phan et al. [29] has to be developed to find the most suitable, economical and cost effective solution.

Genetic Algorithms referred to as GA's are only one of several algorithms better known as evolutionary algorithms and are well suited to most computational problems in many fields [24]. The main characteristic of all evolutionary algorithms are the use of the biological phenomenon known as survival-of-the-fittest.

Genetic Algorithms used for optimisation purposes in this study are based on random and genetic inspired techniques such as natural selection in order to evolve a large set of possible solutions and use bits and pieces of the best solutions of each generation to create the solutions of the next generation with an occasional creation of an entirely new solution for good measure [14]. According to Goldberg [14], Genetic Algorithms efficiently use historical information of previous generations in order to find new search points with an improved performance.

The technique known as natural selection upon which GA's are based, eliminate the greatest problem and hurdle faced in computational programming and design: identifying and specifying all features of a problem and the ways to solve and deal with these problems in advance [18].

According to Holland [18], Genetic Algorithms make use of two processes by which natural organisms evolve: natural selection and sexual reproduction. Natural selection determine which solutions of the population survive and are used for reproduction while sexual reproduction

refer to the mixing and combination of genes in order to obtain the next generation of solutions. Sections 2.2.3 to 2.2.7 include brief descriptions about the processes and techniques used in Genetic Algorithms to ensure that an optimal solution is obtained. Section 2.2.2 includes a short history of genetic algorithms and the development thereof.

2.2.2 History of Genetic Algorithms

The main concept of Genetic Algorithms arose from the early studies done by Barricelli [3] in 1962 by using genetic systems of digital computers. These studies proved that the use of artificial genetic systems were similar to biological evolution by using self-reproducing numerical entities with full control of their properties. The conclusion from these studies were that in order to create and develop these evolutionary processes, certain properties had to be assigned to the numerical self reproducing entities. These two properties were as follows: (1) The numerical entities had to be self producing, and (2) the numerical entities had to undergo changes with the means of mutations to their physical properties to ensure evolution and survival-of-the-fittest.

Professor Holland, the father of Genetic Algorithms, was the first to apply genetic like operators to artificial problems in adaptation in 1962. Holland's main goal was to develop a program capable of adapting to any arbitrary environment and recognized that the fundamental role of unnatural selection is based on the principle of survival-of-the-fittest. Holland not only discovered the need for natural selection, he introduced the principle of population searching methods rather than the single solution searching methods [14].

Although Professor Holland hinted to the importance of genetic operators like crossover and other recombination operators in 1962, the first written acknowledgements to the importance of these operators were made in 1965.

2.2.3 Representation

Each possible solution used in a genetic algorithm is represented as a chromosome. A chromosome in a living organism is a string of DNA which serves as a blueprint of that organism. Each chromosome consists of multiple genes, where each gene stores the information about a specific trait of that organism, e.g. eye colour. In genetic algorithm terms, each solution represented as a chromosome has a number of genes equal to the number of design variable involved in the problem [24].

The most general representation of a chromosome in a genetic algorithm is with the use of binary strings where each design variable (gene) is represented by a combination of ones and zeros defining a specific value. For the purpose of this study, each gene will be represented with the use of a real number as oppose to binary strings for the simple reason that each gene holds a real valued number indicating a position on a discrete list of possibilities. This will eliminate the processing computational effort needed to transform each binary string to a real value.

According to Goldberg [14], some multidimensional optimisation problems require long binary strings in order to represent a solution vector. Long binary strings result in large search spaces, which cause Genetic Algorithms to struggle with convergence to an optimal solution. Therefore real valued Genetic Algorithms are more efficient in terms of structural optimisation with several design variables.

Figure 2.2 shows an individual solution representation as a chromosome with n number of genes where each gene contains a design variable.

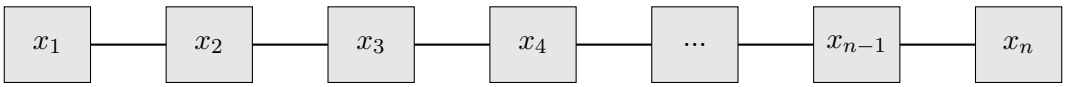

Figure 2.2: Individual solution represented with a chromosome consisting of genes [1].

2.2.4 GA Operators

As mentioned in Section 2.2.1, the biological mechanism known as sexual reproduction is used to create new solutions from the combination of bits and pieces of previous solutions. An initial population is created by randomly selecting values for each design variable of each solution represented as a chromosome. The progression of the initial population into new generations depends on the effectiveness of the Genetic Algorithm operators, operating on the individual solutions selected for reproduction. The selection process is described in Section 2.2.4.1. The Genetic Algorithm operators are responsible for determining how individual solutions from the current population reproduce to create solutions in the next generation. Effective and efficient Genetic Algorithm operators will ensure that better solutions are produced in each new generation and will ensure that premature convergence does not occur [1]. With the use of this mechanism, the best traits of solutions from the current generation will be carried over to the next generation while unfavourable traits are not [24]. There are two methods used in the Genetic Algorithm for this purpose: crossover and mutation, which are briefly discussed in Sections 2.2.4.2 and 2.2.4.3 respectively.

2.2.4.1 Selection

Selection is a Genetic Algorithm process that selects a set of promising solutions from the current population to undergo reproduction. There are several available techniques that can be used for the selection process, but they are all based on a basic idea of selecting solutions that perform better at the expense of solutions that perform worse. The use of selection is an imitation of natural selection, as it selects and gives better performing solutions a greater chance to survive to the next generation [7].

Two widely used selection processes in genetic algorithms are tournament selection and rank-based selection which are briefly discussed below.

Tournament Selection

Tournament selection is a process where tournaments are held between randomly selected individual solutions to ensure that the best performing solutions get selected for reproduction. By having the same number of tournaments as the size of the population, it will ensure that the worst performing solutions will not be selected for reproduction, thus not be carried over into the next generation of solutions [19].

Rank-Based Selection

Rank-based selection is based on selecting the best performing individual solutions by ranking them in terms of their fitness. The solutions are ranked from the most favourable solutions with the best fitness to the least favourable solutions with the worst fitness. A portion of the population with the most favourable fitness values are selected for reproduction [9]. The principle of fitness evaluation is explained in Section 2.2.6.

2.2.4.2 Crossover

Crossover is a Genetic Algorithm operator responsible for producing two new individual solutions in the new generation of solutions. The new solutions have a combination of genes (traits) from two or more individual solutions from the current population [1, 49]. Several crossover techniques exist of which a few are discussed below.

One-Point Crossover

According to Adewuya [1], the one-point crossover technique is where a crossover point between two genes is randomly selected. With the use of this technique, two new individual solutions (child chromosomes) are created from two current solutions (parent solutions) selected at random from the current population.

Figure 2.3 is a graphical representation of one-point crossover with a single crossover point indicated with a dashed line.

Two-Point Crossover

The two-point crossover technique is based on exactly the same principle as the one-point crossover technique, with the only difference being that the two-point crossover technique has two crossover points.

Figure 2.4 is a graphical representation of the two-point crossover technique where two new individual solutions are created from two current individual solutions with the two crossover points indicated with dashed lines [1].

Uniform Crossover

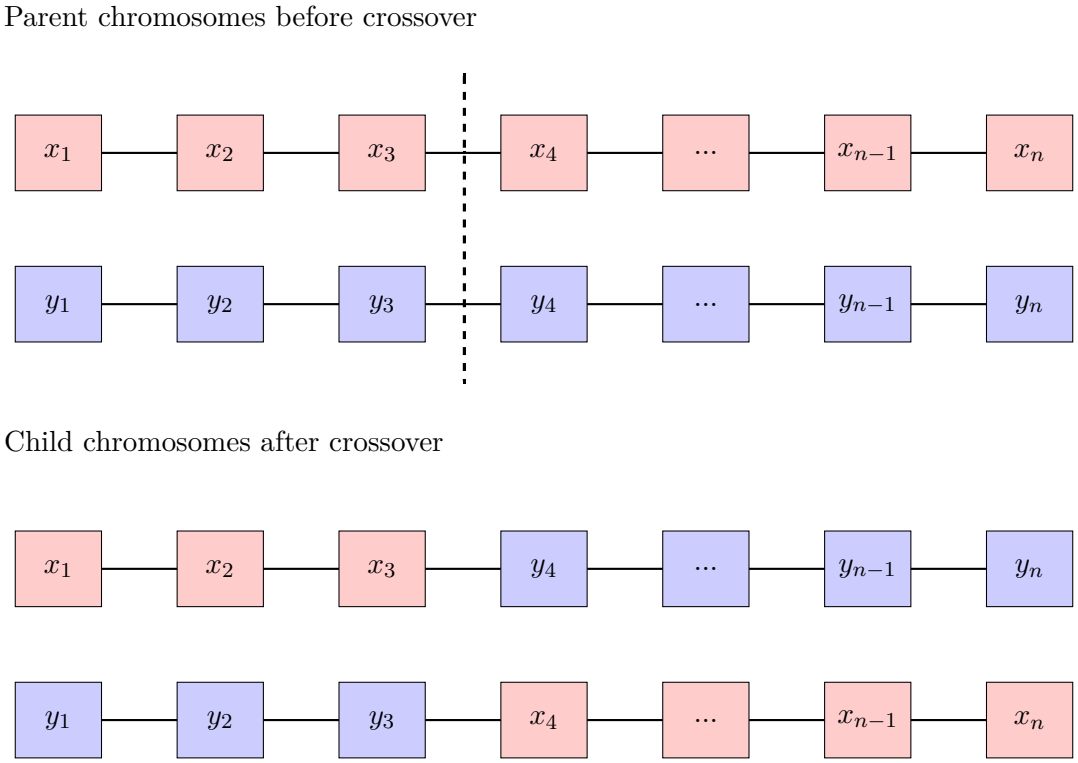

Figure 2.3: Graphical representation of one-point crossover [1].

Uniform crossover is a multi-point crossover technique where two child, new generation solutions, are produced from two initial parent solutions. For every gene of the two child chromosomes, a coin is flipped to determine which child chromosome gets the gene from which parent chromosome [1].

2.2.4.3 Mutation

Mutation is a Genetic Algorithm operator used to introduce diversity into the population and ensure that premature convergence does not occur [19]. Several techniques of mutation are available of which a few are briefly discussed below.

Uniform Mutation

If a randomly selected individual solution is given as $x = (x_1, x_2, x_3, ..., x_{n-1}, x_n)$, then each gene in the selected chromosome has equal chance of undergoing mutation. The resulting child chromosome in the next generation of solutions can then be given as $x_{child} = (x_1, x_2', x_3, ..., x_{n-1}, x_n)$, where x_2' is a randomly generated value between the lower and upper limits of the problem [1].

Boundary Mutation

Boundary mutation is based on the same principle as explained in uniform mutation, with the only difference being that the randomly selected gene from a randomly selected parent

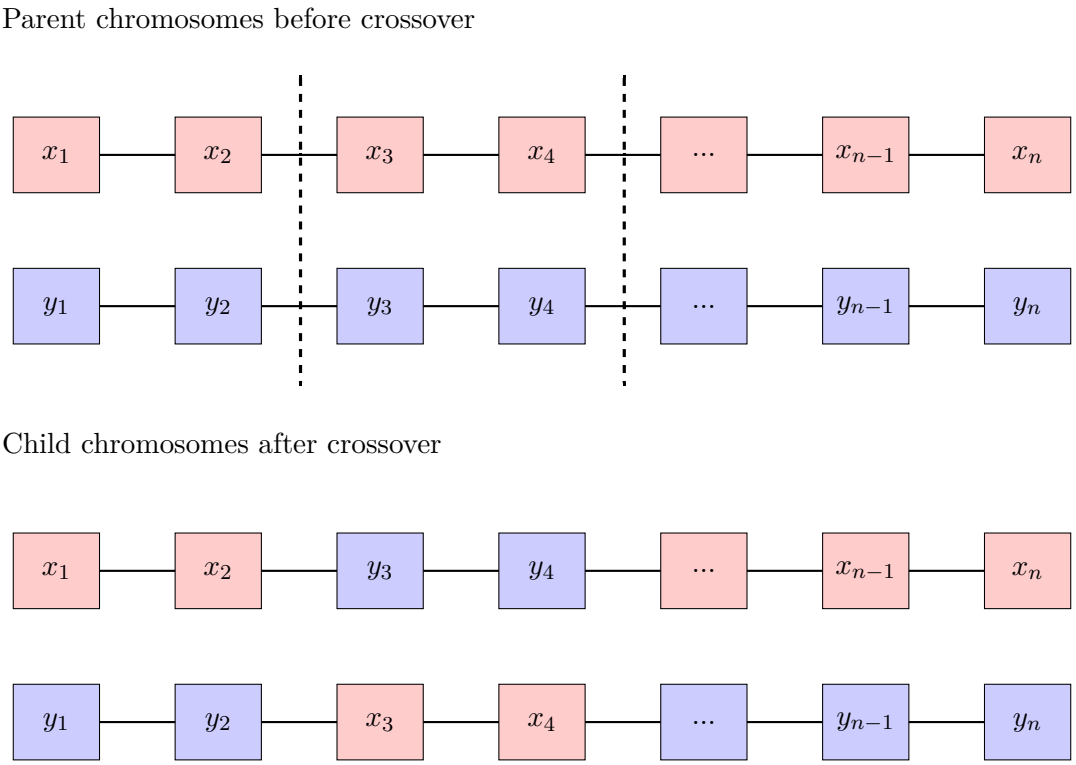

Figure 2.4: Graphical representation of two-point crossover [1].

chromosome undergo mutation by changing the current gene with either the lower or upper limit value of the problem [1].

If an individual solution is given as $x = (x_1,\ x_2,\ x_3,\ ...,\ x_{n-1},\ x_n)$, then the resulting child chromosome in the next generation of solutions is given as $x_{child} = (x_1,\ x'_2,\ x_3,\ ...,\ x_{n-1},\ x_n)$, where x'_2 is either the lower or upper limit value [1].

2.2.5 Replacement

Replacement is a technique used in genetic algorithms where a few of the best performing individual solutions are copied and replaced into the next generation of solutions without undergoing any crossover or mutation. This is done to ensure that the best performing solutions do not get lost or unfavourably mutated during the reproduction processes like crossover and mutation. This process is also known as elitism and significantly increase the effectiveness of the Genetic Algorithm [24].

2.2.6 Fitness Evaluation

The performance of each individual solution from each generation somehow has to be measured and compared to other solutions to establish and determine the optimal or best performing

solutions. In order to measure the performance (fitness) of an individual solution, some objective has to be established. The fitness of each solution is calculated according to the defined objective function, where the lowest fitness value in minimization problems would indicate the solution with the most favourable fitness [19].

With all structural engineering problems, some constraints apply to the structure. If an individual solution does not comply to a specified constraint, the fitness of such a solution has to be altered to make it less favourable. This is done by adding a penalty value to the fitness of such a solution [6]. The concept of penalty values and functions are explained in Section 2.2.7.

2.2.7 Penalty Function

Lagaros, Papadrakakis, and Kokossalakis [23] mentioned that Genetic Algorithms were initially developed to only handle and solve unconstrained optimisation problems, although a lot of research and studies during the last few decades have led to the development of Genetic Algorithms for constrained problems. This is mainly based on the use of penalty functions by adding penalty values to the fitness of a solution not complying to the specified constraints. Two methods of calculating these penalty values are briefly discussed below.

2.2.7.1 Static Penalties

The method of static penalties is a simple method where the objective function is given as in Equation (2.5)

$$F_{new} = F(x) + p.viol(x) \tag{2.5}$$

where $F(x)$ is the initial objective function, p is a static penalty parameter, $viol(x)$ is the sum of the violated constraints and F_{new} is the new objective function.

Even though the use of static penalties are fairly simple, their is no guidance to what the value of the static penalty parameter p should be. A value selected for p too small will cause convergence to an infeasible solution while a large value for p will ensure a feasible solution is obtained, but far from the global optimum solution [23].

2.2.7.2 Dynamic Penalties

Dynamic penalties proposed by Joines and Houck [21], are implemented in constrained optimisation problems by evaluating individual solutions taking into account the generation count.

The method of dynamic penalty values can be described with Equation (2.6)

$$F_{new} = F(x) + (c.g)^{\alpha}(viol(x)) \tag{2.6}$$

where $F(x)$ is the initial objective function, F_{new} the new objective function, $viol(x)$ the number of violated constraints, g the generation counter and c and α are constants. Lagaros, Papadrakakis, and Kokossalakis [23] proposed the following values for the constants c and α: $c = 0.5 \ - \ 2.0$, $\alpha = 1$ or 2.

By taking into account the generation count, a solution violating a constraint at a low generation counter will be slightly penalised, while a solution violating a constraint at a high generation counter being heavily penalised [23]. Figure 2.5 on page 17 is a flow chart of the proposed genetic algorithm programmed in JAVA.

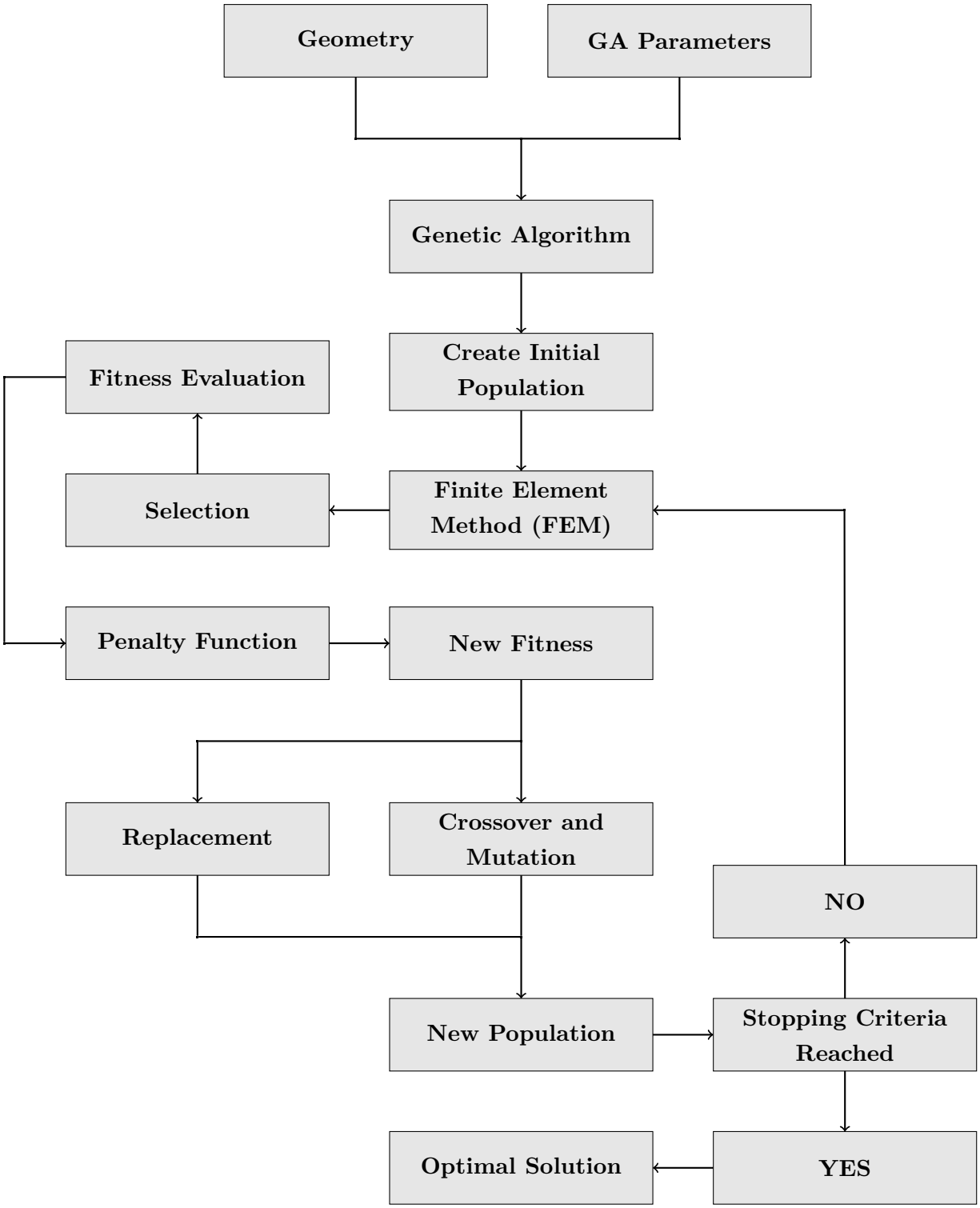

Figure 2.5: Flow chart of proposed genetic algorithm.

2.3 Structural Reliability Theory

2.3.1 Introduction

Following a literature study about the optimisation techniques and Genetic Algorithm required to obtain an optimal portal frame in terms of the column and rafter sizes as well as the haunch length at the eaves and the roof pitch, it is necessary to do a study about the reliability of portal frames and the techniques used to obtain the reliability or safety index of an optimal frame.

In the field of structural reliability analysis there has been several studies as early as the sixties where a large number of researchers contributed to the development of several probability based reliability analysis and design procedures [43].

According to Freudenthal [12], the reliability analysis of a structural system requires specific information in order to obtain a realistic and rational value for the safety and reliability of a structural system which are related to an acceptable probability of failure. The information needed for a reliability analysis include the distribution functions which define the intensity of the applied loads on the structure, the probability of serviceability and failure, and the stress analysis of the structure. The structural failure and serviceability distributions have to be presented in a form which can be extrapolated to high values for the applied load and low values for the serviceability and failure loads.

When thinking about structural reliability and safety, it is important to note and understand that a measure of structural safety is not generally based on a physical property of the structure and that the factors influencing the structural safety of a structure are random variables rather than of deterministic nature. The reliability index is a decision variable that embraces the knowledge about the strength properties of the structure in relation to the actions and loads on the structure. According to ISO 2394, reliability is defined as the ability of a structure to comply with given requirements under specified conditions during the intended lifetime of the structure [17]. It is thus clear that the value of the reliability index is dependent on the amount and quality of information that is available. This theory and philosophy emphasize that the reliability or safety index becomes a design variable during the design phase of a structure [10].

For the reliability analysis of a structural system, there are several approximation methods to obtain the safety or reliability index which are discussed in more detail in Section 2.4. In order to understand the concept of structural reliability, the concepts of reliability index and probability of failure have to be discussed, which are done in Sections 2.3.2 and 2.3.3 respectively.

2.3.2 Probability of Failure

The structural reliability analysis of a component or entire structure is dependent on two random design variables which include the applied load effect (E) and the corresponding resistance (R) respectively. These two design variables are represented by appropriate distribution functions and are used in the calculation of the limit state function G in Equation (2.7).

$$G = R - E \tag{2.7}$$

The applied load and corresponding resistances are both dependent on appropriate parameters, which include the moment parameters $\mu_E, \sigma_E, \alpha_E, \mu_R, \sigma_R$ and α_R. These parameters ensure that the limit state function G is also dependent on moment parameters for example μ_G, σ_G and α_G.

For the defined limit state function G in Equation (2.7), the probability of failure P_f can be defined as the probability that $G \leq 0$ as in Equation (2.8) [43].

$$P_f = P\left(G \leq 0\right) \tag{2.8}$$

Figure 2.6 is a graphical presentation of the probability density functions of the applied load effect and corresponding resistance. The probability of failure P_f is the gray area where the two distributions intersect meaning the applied is greater than its corresponding resistance, therefore causing failure.

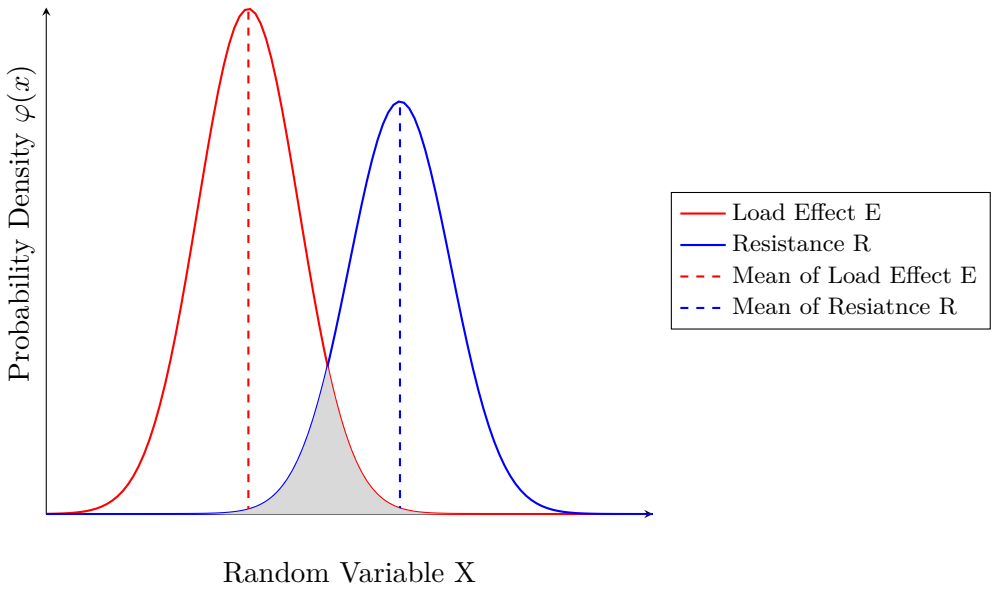

Figure 2.6: The probability density $\varphi_E(x)$ and $\varphi_R(x)$ for load effect E and Resistance R [17].

For the analysis of the structural reliability of a structural system, it is widely accepted that this mathematical probability theory discussed above is an acceptable and rational basis for the

modelling of such problems. According to Ditlevsen and Bjerager [10], the use of this method for the reliability analysis has several problems which are as follows:

1. The identification of physical variables and the mathematical formulation of the limit state function for the given problem.
2. The type of probability density functions for the design variables.
3. A suitable modelling of the uncertainty of the models in 1 and 2.
4. The calculation of the reliability of the models 1 to 3.

Point 1 above is a general deterministic analysis which can be done with knowledge of strength of materials, while point 2 is done by specialized structural engineers with the necessary expert knowledge to obtain a suitable probability density function for the design variables. The aim is to finally obtain a reliability index of a structural system which will be discussed in Section 2.3.3.

In most applications of structural reliability analysis, the probability of failure is generally very small, therefore raising problems for empirical verification. These small failure probabilities cause reliability evaluations to be very sensitive to the probability density functions chosen for the design variables, especially the tail end of the distributions, meaning the lower tail of the resistance distribution and the upper tail of the applied load distribution. These tail ends of the probability distributions are extremely difficult to verify with statistics and data [10].

A lack of sufficient empirical data and the problem of tail uncertainty, as well as the general desire for simplicity caused a huge motivation for the development of methods to calculate the reliability of any structural system. Several methods for the reliability analysis have been developed, for example the Monte Carlo Method, the First-Order Reliability Method (FORM), and the Second-Order Reliability Method (SORM). These methods is briefly discussed in Section 2.4.

2.3.3 Reliability Index

The probability of failure P_f as discussed in Section 2.3.2, is sometimes difficult to interpret in terms of how safe a structure really is, therefore an alternative and more understandable value for the safety of a structure is defined as the reliability index β. The reliability index or safety index is an indication of how safe a component of a structure or the structure as a whole is, and can then be used to calculate the probability of failure of that specific structural component or system.

In order to understand the concept of reliability index, the three fundamental cases for one and two random variables, as explained by Holicky [17], have to be considered.

2.3.3.1 One Random Variable

The first fundamental case is defined by two variables E and R, where the applied load effect E and corresponding resistance R are considered as a deterministic value and a random variable respectively. This can be done when the exact applied load on a structural member is known for a certain problem. The deterministic value of the applied load effect E is for example fixed at a value of $E_0 = 80$, indicated as the vertical line in Figure 2.7.

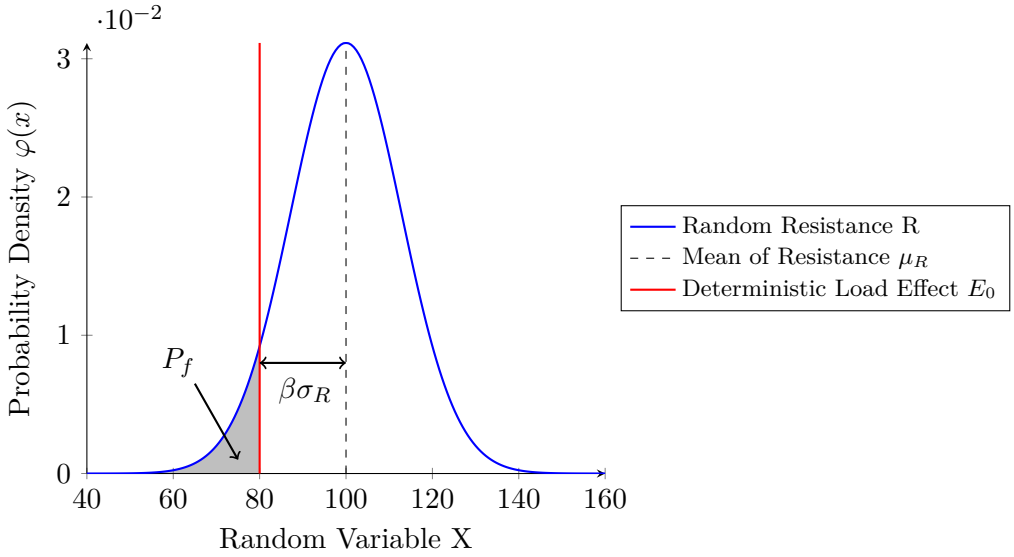

Figure 2.7: The deterministic effect of actions E and random resistance R [17].

Given the problem in Figure 2.7, the probability of failure P_f indicated as the grey area can be determined directly from the distribution function $\Phi_R(x)$. The probability of failure P_f is given as the probability that $R < E_0$ as in equation (2.9)

$$P_f = P(R < E_0) = \Phi_R(E_0) \tag{2.9}$$

where the distribution function $\Phi_R(x)$ is assessed from tables for a standardized random variable U from which the standardised variables U_0 corresponding to E_0 can be determined. The standardised variable U_0 can be calculated with a transformation formula as in Equation (2.10) [17].

$$U_0 = \frac{(E_0 - \mu_x)}{\sigma_x} \tag{2.10}$$

In order to calculate the reliability index β, the value U_0 calculated with Equation (2.10) is defined as the distance between the fixed value E_0 of the applied load effect and the mean of the resistance μ_R. This distance is expressed in units of the standard deviation of the resistance σ_R (Refer to Figure 2.7).

Given that the distribution function of the resistance is defined as a normal distribution, then the value for the reliability index β and probability of failure P_f are calculated using Equations (2.11) and (2.12) respectively.

$$\beta = -U_0 = \frac{(\mu_R - E_0)}{\sigma_R} \tag{2.11}$$

$$P_f = P(R < E_0) = \Phi_U(-\beta) \tag{2.12}$$

When the resistance R is defined by any other distribution function, the reliability index β can be calculated using Equation (2.13) [17].

$$\beta = -\Phi_U^{-1}(P_f) \tag{2.13}$$

2.3.3.2 Two Random Variables with Normal Distributions

The second fundamental case for reliability analysis is when both random variables, namely the applied load effect E and resistance R, are defined by probability distributions. For simplicity and this fundamental case, it will be assumed that both the random variables E and R are defined by normal distributions. With the use of these assumptions the reliability margin G are defined as in Equation (2.7) on page 19.

The reliability margin G is then defined by a normal distribution with parameters for the mean μ_G and standard deviation σ_G defined as

$$\mu_G = \mu_R - \mu_E \tag{2.14}$$

$$\sigma_G^2 = \sigma_R^2 + \sigma_E^2 + 2\rho_{RE}.\sigma_R^2.\sigma_E^2 \tag{2.15}$$

where ρ_{RE} is the coefficient of correlation of the applied load effect and resistance [17].

Often the assumption is made that the two random variables E and R are mutually independent, therefore having a correlation coefficient ρ_{RE} equal to zero. This leads to the probability of failure P_f given as in Equation (2.16), assuming that both variables are defined by normal distributions.

$$P_f = P(R < E) = P(G < 0) = \Phi_G(0) \tag{2.16}$$

For the determination of the distribution function $\Phi_G(0)$, the variable G is transformed to a standardized variable U with the use of Equation (2.10) on page 21. This leads to the calculation of the standardized value U_0 as in Equation (2.17), which correspond with the failure criteria value of $G = 0$ [17].

$$U_0 = \frac{(0 - \mu_G)}{\sigma_G} = -\frac{\mu_G}{\sigma_G} \tag{2.17}$$

The probability of failure P_f and reliability index β can then be given as in Equations (2.18) and (2.19) respectively.

$$P_f = P(R < E) = \Phi_G(0) = \Phi_U(U_0) \tag{2.18}$$

$$\beta = \frac{\mu_G}{\sigma_G} = \frac{\mu_R - \mu_E}{\sqrt{\sigma_R^2 + \sigma_E^2 + 2\rho_{RE}.\sigma_R^2.\sigma_E^2}} \tag{2.19}$$

Figure 2.8 is a graphical presentation of the probability density function $\Phi_G(g)$ of the reliability margin G. The probability of failure P_f is indicated with the grey area

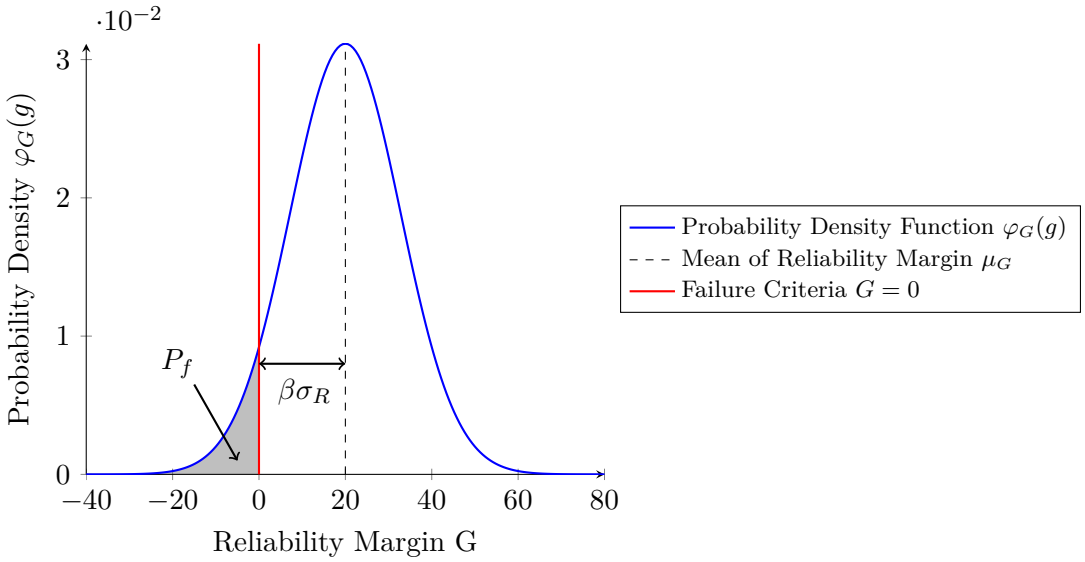

Figure 2.8: Distribution of the reliability margin G [17].

where the reliability index β is measured as the distance between the mean of the reliability margin μ_G from the origin measured in units of the standard deviation σ_G [17].

2.3.3.3 Two Random Variables with General Distributions

For the case of two random variables with general distributions, an exact solution for the probability of failure P_f can be obtained with the use of integration. Given that A denote the occurrence of an applied load effect E in the interval $(x, x + dx)$, and B the occurrence of a resistance R in the interval $(-\infty, x)$, then the probability of event A and event B happening are given by Equations (2.20) and (2.21) respectively. Refer to Figure 2.9.

$$P(A) = P(x < E < x + dx) = \varphi_E(x)dx \tag{2.20}$$

$$P(B) = P(R < x) = \Phi_R(x) \tag{2.21}$$

The incremental probability of failure dP_f corresponding to the occurrence of an applied load effect E in the interval $(x, x + dx)$ as seen in Figure 2.9, can be given as the simultaneous occurrence of both events A and B as in Equation (2.22) [17]

$$dP_f = P(A \cap B) = P(A)P(B) = \varphi_E(x)\Phi_R(x) \tag{2.22}$$

where events A and B are assumed to be mutually independent.

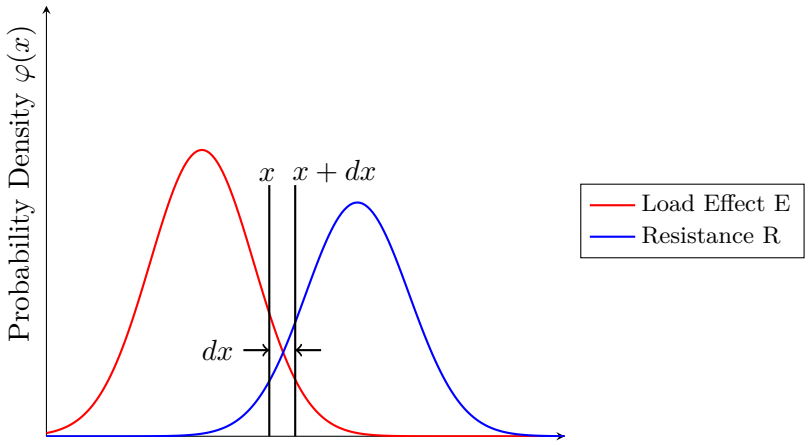

Figure 2.9: Distribution of variables E and R [17].

Following an integration procedure of the incremental probability of failure dP_f as in Equation (2.22) over the interval $(-\infty, \infty)$, the relationship for the probability of failure is given in

Equation (2.23) below.

$$P_f = \int_{-\infty}^{\infty} \varphi_E(x)\Phi_R(x)dx, \tag{2.23}$$

2.3.4 Design Point

Given that the standardized distributions for the load effect E and resistance R are plotted on the x-axis and y-axis respectively as in Figure 2.10, the reliability index β is defined as the shortest distance from the origin (μ_R, μ_E) to the limit state function $G(x)$ given by Equation (2.7) on page 19.

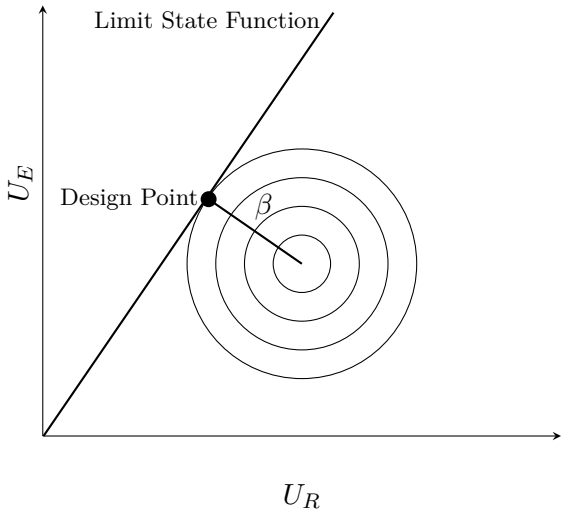

Figure 2.10: Presentation of design point [17].

The location of the design point on the limit state function indicated in Figure 2.10 can be obtained with approximation methods like the first and second order reliability methods.

These concepts and processes used to obtain the optimum design point which will be used for the calculation of the structural reliability index β are discussed in Section 2.4.

2.3.5 Structural Systems

The reliability of a portal frame as determined with the methods discussed in Section 2.4 is based on the calculation of the reliability index of a single member of the portal frame. The reliability index of the entire frame as a whole can be dependent on either a single member or more than one member of the frame. This is known as structural systems used to define failure of a structure and are briefly discussed below [34].

According to Rao [34], structural systems can be classified into two categories, namely the weakest link system (series system) and the fail-safe system (parallel system).

As seen in the literature by Park et al. [27], these two systems can also be combined to form a hybrid system consisting of a combination of series and parallel systems.

2.3.5.1 Series System

A series structural system also known as the weakest link system is where a failure of any one or more members in the system of members will lead to total failure of the entire system, therefore not having any redundancy [17]. A series system is schematically represented in Figure 2.11.

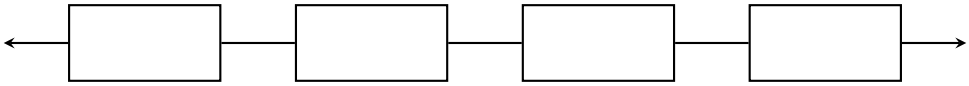

Figure 2.11: Representation of a series system [27].

Given that the failure of component i is denoted by F_i, then the failure of a series system with n components is given by the event F_s as in Equation (2.24) [2].

$$F_s = F_1 \cup F_2 \cup F_3 \cup ... \cup F_n \tag{2.24}$$

Subsequently the safety of the system in which no potential failure modes occur is given by F_s' as in Equation (2.25).

$$F_s' = F_1' \cap F_2' \cap F_3' \cap ... \cap F_n' \tag{2.25}$$

2.3.5.2 Parallel System

A parallel system as in Figure 2.12 consisting of multiple members connected to each other in parallel would only fail completely if all the members in the system fails. A parallel system therefore is a redundant system where the system is still safe if only one member survives [2].

Given that the failure of component i is given by F_i, then the failure of a parallel system with n components is given by F_s as in Equation (2.26).

$$F_s = F_1 \cap F_2 \cap F_3 \cap ... \cap F_n \tag{2.26}$$

The safety of the system is given by F'_s as in Equation (2.27).

$$F'_s = F'_1 \cup F'_2 \cup F'_3 \cup ... \cup F'_n \tag{2.27}$$

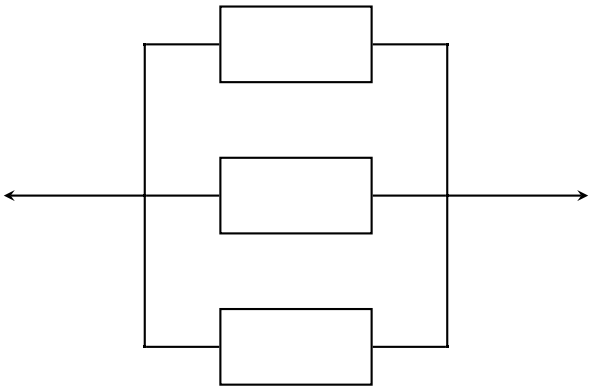

Figure 2.12: Representation of a parallel system [27].

2.3.5.3 Hybrid System

Most engineering systems consist of a combination of series and parallel systems known as hybrid systems as in Figure 2.13. The failure or safety of the substructures consisting of only a series or parallel system are computed with the methods described in series systems and parallel systems respectively [2].

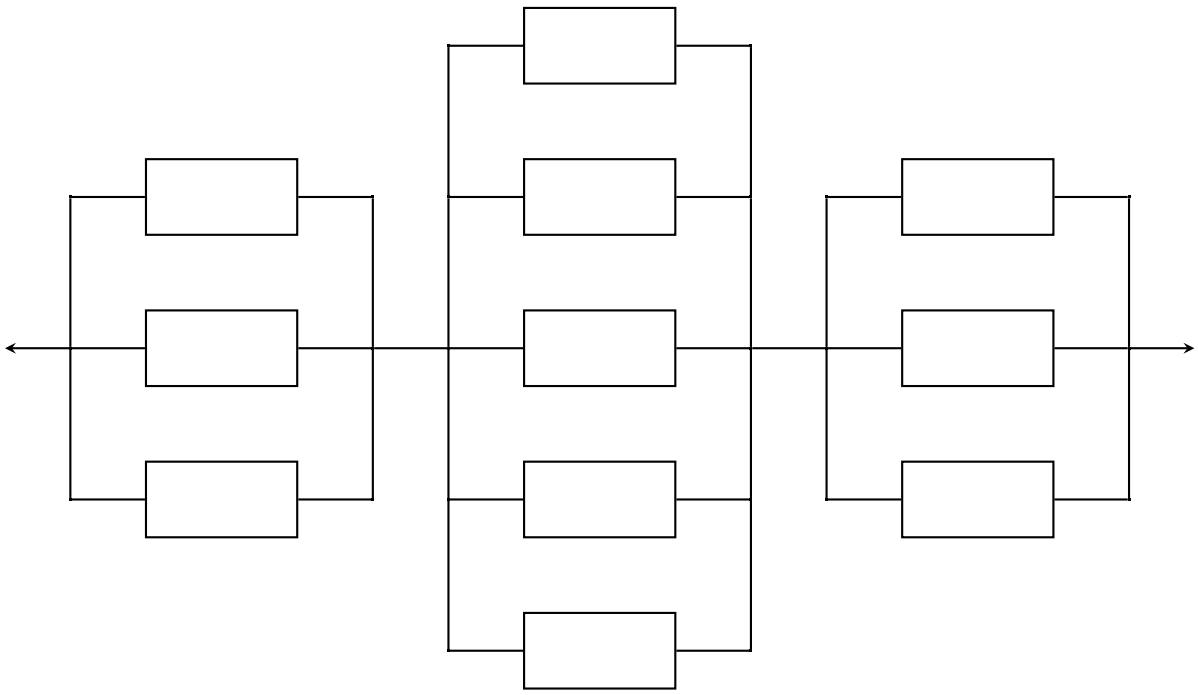

Figure 2.13: Representation of a hybrid system [27].

2.4 Methods for Structural Reliability Analysis

As discussed in Section 2.3, several methods for the analysis of the reliability of a structure have been developed to create simplicity and overcome problems like the lack of sufficient data and tail-end uncertainties. There are a wide variety of methods which can be used for the reliability analysis of portal frames, but for the purpose of this study only a few of these methods will be discussed and studied in order to conclude which method will be the most sufficient.

2.4.1 First-Order Reliability Method (FORM)

In the field of structural reliability, the First Order Reliability Method also known as the Rackwitz-Fiessler method is considered as one of the most reliable and trustworthy computational methods [50]. According to Zhao and Ono [50], these methods for structural reliability are generally only dependent on three parameters which include the curvature radius at the design point, the number of random variables and the first order reliability index β.

In Bjerager [4] it is stated that the general purpose of reliability computational methods like the first and second order reliability methods is to evaluate a multidimensional integral for the probability of failure given in Equation (2.28) which is obtained from Equation (2.8) on page 19.

$$P_f = \int_{G(\mathbf{x})\leq 0} f(\mathbf{x})dx, \tag{2.28}$$

In Equation (2.28), $\mathbf{x}$ is given as $\mathbf{x} = [x_1, x_2, ..., x_n]$, which is a vector containing random variables representing uncertain structural quantities. The joint probability density function of the limit state function $G(\mathbf{x})$ is given by $f(\mathbf{x})$ [50, 4].

The First Order Reliability Method is based on an analytical approximation of the reliability index β which is interpreted as the shortest distance from the origin of a standardized normal space to the surface of the limit state function $G(\mathbf{x})$. The point on the limit state surface closest to the origin is denoted as the design point (failure point) and is represented graphically in Figure 2.10 on page 25. The position of the design point on the linear surface of the limit state function for a situation with uncorrelated variables can be obtained by mathematical programming methods for example the Hasofer-Lind and Rackwitz-Fiessler methods which are discussed below [4].

Considering the following linear limit state function

$$G(x_1, x_2, ..., x_n) = a_0 + a_1x_1 + a_2x_2 + ... + a_nx_n = a_0 + \sum_{i=1}^{n} a_ix_i \tag{2.29}$$

where all the a_i terms are constant values and the x_i terms are uncorrelated random variables,

the reliability index β are defined by Hasofer and Lind [16] as in Equation (2.30).

$$\beta = \frac{a_0 + \sum_{i=1}^{n} a_i \mu_{x_i}}{\sqrt{\sum_{i=1}^{n} a_i \sigma_{x_i}}} \tag{2.30}$$

As seen in Figure 2.10 and discussed previously, the First Order Reliability Method makes use of a linear limit state function. When a limit state function for a specific problem is strongly non-linear, accuracy problems occur with the use of a linear approximation for the limit state function $G(\mathbf{x})$. This lead to the development of the Second Order Reliability Method (SORM) in an attempt to improve the First Order Reliability Method [50, 11]. A brief discription of the Second Order Reliability Method is given in Section 2.4.2.

2.4.1.1 Hasofer-Lind Reliability Index

As discussed above, the reliability index can be obtained with the use of the Hasofer-Lind procedure where the reliability index is defined as the shortest distance from the origin of the standardized normal space to the limit state function $G(\mathbf{x}) = 0$. The Hasofer-Lind procedure uses the mean and standard deviation of the random variables to obtain the reliability index β. The limit state function is not known a-priori, therefore an iteration method is needed for the calculation of the reliability index [25].

Considering the limit state function $G(x_1, x_2, ..., x_n)$ consisting of uncorrelated random variables x_i, the limit state function can be rewritten in terms of the standard form of the variables with the use of Equation (2.31).

$$z_i = \frac{x_i - \mu_{x_i}}{\sigma_{x_i}} \tag{2.31}$$

Given that the limit state function is non-linear, iteration is required to obtain the design point $\mathbf{z}^* = (z_1^*, z_2^*, ..., z_n^*)$, corresponding to the shortest distance from the origin to the limit state function [25]. This concept is illustrated in Figure 2.14.

The Hasofer-Lind reliability index has two procedures which can be used to perform the iterative process [16, 25]. These two procedures are called the simultaneous equation procedure and the matrix procedure respectively and are described below.

Simultaneous Equation Procedure

1. Define the limit state function for the problem as well as the parameters of all the random variables involved.

2. Express the limit state function in terms of the standardized normal space with reduced variables z_i.

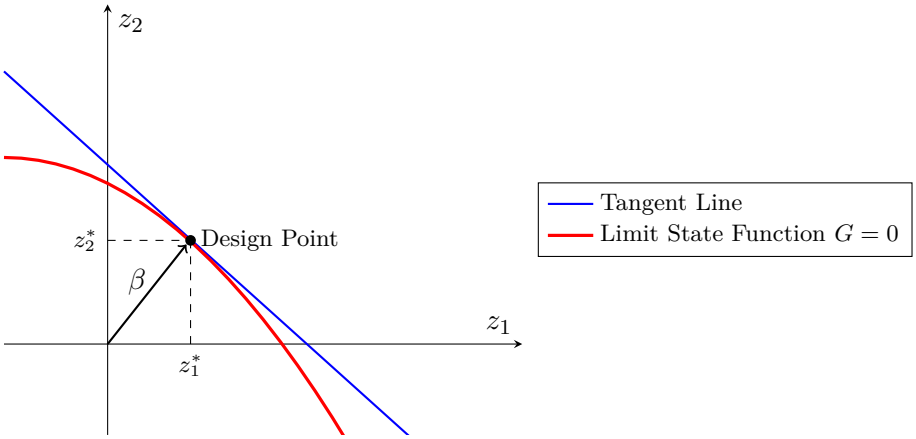

Figure 2.14: Hasofer-Lind reliability index for two design variables [25].

3. Express the limit state function $G(x)$ in terms of α and β with the use of Equation (2.32).

$$z_i^* = \beta\alpha_i \tag{2.32}$$

4. Calculate all the values for α_i with the use of Equation (2.33) and use Equation (2.32) to express each α_i value in terms of all the α_i and β values

$$\alpha_i = \frac{-\frac{\partial g}{\partial z_i}\Big|_{evaluated\ at\ design\ point}}{\sqrt{\sum_{k=1}^{n}\left(\frac{\partial g}{\partial z_k}\Big|_{evaluated\ at\ design\ point}\right)^2}} \tag{2.33}$$

where $\frac{\partial g}{\partial z_i}$ is given as:

$$\frac{\partial g}{\partial z_i} = \frac{\partial g}{\partial x_i}\frac{\partial x_i}{\partial z_i} = \frac{\partial g}{\partial x_i}\sigma_{x_i} \tag{2.34}$$

5. Start the first cycle and assume numerical values for all α_i and β values with all α_i values satisfying Equation (2.35).

$$\sum_{i=1}^{n}(a_i)^2 = 1 \tag{2.35}$$

6. Use the values obtained for α_i and β from Equation (2.32) in steps 3 and 4.

7. Solve each of the $(n+1)$ simultaneous equations from step 6 for α_i and β.

8. Repeat steps 6 to 8 until the values for α_i and β converge.

Matrix Procedure

1. Define the limit state function for the problem as well as all appropriate parameters for the random variables x_i involved.

2. Assume values for $(n-1)$ of the random variables x_i in order to obtain an initial design

point $\mathbf{x}^*$ (the mean values are often a good initial assumption for the random variables). For the remaining random variable, the limit state equation $G = 0$ is solved ensuring that the design point is on the limit state function.

3. With the use of Equation (2.36), determine the reduced variates z_i^* corresponding to the design point x_i^*.

$$z_i^* = \frac{x_i^* - \mu_{x_i}}{\sigma_{x_i}} \tag{2.36}$$

4. Define a column vector **dG** as in Equation (2.37) consisting of the partial derivatives of the limit state function with respect to the reduced variates z_i^* multiplied by -1

$$\mathbf{dG} = \begin{Bmatrix} dG_1 \\ dG_2 \\ \vdots \\ dG_n \end{Bmatrix} \tag{2.37}$$

where G_i is calculated as in Equation (2.38) evaluated at each design point.

$$dG_i = -\frac{\partial g}{\partial z_i} = -\frac{\partial g}{\partial x_i}\frac{\partial x_i}{\partial z_i} = -\frac{\partial g}{\partial x_i}\sigma_{x_i} \tag{2.38}$$

5. The partial derivatives of the limit state function obtained in step 4 are then used to calculate an estimate value for β in Equation (2.39)

$$\beta = \frac{\{dG\}^T\{z^*\}}{\sqrt{\{dG\}^T\{dG\}}} \tag{2.39}$$

where $\mathbf{z}^*$ is given as:

$$\mathbf{z}^* = \begin{Bmatrix} z_1^* \\ z_2^* \\ \vdots \\ z_n^* \end{Bmatrix} \tag{2.40}$$

For a linear limit state function, Equation (2.39) reduce to Equation (2.30) on page 29.

6. A column vector consisting of all the sensitivity factors are calculated using Equation (2.41).

$$\alpha = \frac{\{dG\}}{\sqrt{\{dG\}^T\{dG\}}} \tag{2.41}$$

7. A new design point in terms of the reduced variates z_i^* for $(n-1)$ random variables are determined using Equation (2.42).

$$z_i^* = \alpha_i\beta \tag{2.42}$$

8. Use the values obtained in step 7 in order to determine the corresponding original coordinates x_i^* of the new design point using Equation (2.43).

$$x_i^* = \mu_{x_i} + z_i^* \sigma_{x_i} \tag{2.43}$$

9. Determine the remaining random variable with the use of the limit state function $G = 0$.

10. Repeat steps 3 to 9 until the values for β and the design point $\mathbf{x}^*$ converge.

Reliability Analysis for Correlated Variables

The first and second order reliability methods assume that all random variables are uncorrelated, however in several practical situations some of the random variables might be correlated which might have a great influence on the reliability index [25, 15]. Given that the random variables x_i are correlated with mean values μ_{x_i} and standard deviation σ_{x_i}, then the covariance matrix are given as in Equation (2.44).

$$[C] = \begin{bmatrix} \sigma_{x_i}^2 & COV(x_1, x_2) & \dots & COV(x_1, x_n) \\ COV(x_2, x_1) & \sigma_{x_2}^2 & \dots & COV(x_2, x_n) \\ \vdots & \vdots & \vdots & \\ COV(x_n, x_1) & COV(x_n, x_2) & \dots & \sigma_{x_n}^2 \end{bmatrix} \tag{2.44}$$

Given that the standardized variables z_i are defined as in Equation (2.31), then the correlation matrix $[C_z]$ of the standardized variables can be given as

$$[C_z] = \begin{bmatrix} 1 & \rho_{x_1,x_2} & \dots & \rho_{x_1,x_n} \\ \rho_{x_2,x_1} & 1 & \dots & \rho_{x_2,x_n} \\ \vdots & \vdots & \vdots & \\ \rho_{x_n,x_1} & \rho_{x_n,x_2} & \dots & 1 \end{bmatrix} \tag{2.45}$$

where ρ_{x_i,x_j} as in Equation (2.46) is defined as the correlation coefficient of the random variables x_i and x_j [15].

$$\rho_{x_i,x_j} = \frac{COV(x_i, x_j)}{\sigma_{x_i}\sigma_{x_j}} \tag{2.46}$$

For correlated random variables, the matrix procedure can be used with the incorporation of the correlation matrix $[C_z]$ in Equation (2.45) [15, 25].

According to Nowak and Collins [25], the steps for the correlated variables procedure are the same as the steps discussed for the matrix procedure. The only difference is the modification of Equations (2.39) and (2.41). The modified equations for the reliability index and sensitivity

factors for correlated variables are given as in Equations (2.47) and (2.48) respectively.

$$\beta = \frac{\{G\}^T\{z^*\}}{\sqrt{\{G\}^T[C_z]\{G\}}} \tag{2.47}$$

$$\alpha = \frac{[C_z]\{G\}}{\sqrt{\{G\}^T[C_z]\{G\}}} \tag{2.48}$$

2.4.1.2 Rackwitz-Fiessler Method

The Hasofer-Lind reliability index method described above use the mean and standard deviations of all the random variables to determine the reliability index β. For the Hasofer-Lind method, no detailed information about the probability distribution of the random variables were needed. When information about the type of distribution of all the random variables are available, a more accurate procedure can be used for the calculation of the reliability index. This method proposed by Rackwitz and Fiessler [31], is based on the idea of calculating normal values for the mean and standard deviation of each non-normal random variable [25].

The normal mean μ_x and standard deviation σ_x of a particular random variable x of each non-normal random variable can be obtained with the use of the cumulative distribution function (CDF) $F(x)$ and probability density function (PDF) $f(x)$. The normal mean and standard deviation are obtained by assuming that the CDF and PDF of the actual function are equal to the normal CDF and normal PDF at a value x^* on the failure boundary of the problem prescribed by the limit state function $G = 0$ [25]. This can be expressed with the use of Equations (2.49) and (2.50) respectively

$$F_x(\mathbf{x}^*) = \Phi\left(\frac{\mathbf{x}^* - \mu_x}{\sigma_x}\right) \tag{2.49}$$

$$f_x(\mathbf{x}^*) = \frac{1}{\sigma_x}\phi\left(\frac{\mathbf{x}^* - \mu_x}{\sigma_x}\right) \tag{2.50}$$

where Φ and ϕ are prescribed as the CDF and PDF of the standard normal distribution.

By manipulating Equations (2.49) and (2.50), expressions for the equivalent normal mean μ_x and standard deviations σ_x can be obtained. This is given by Equations (2.51) and (2.52) [25, 31].

$$\mu_x = \mathbf{x}^* - \sigma_x\left[\Phi^{-1}\left(F_x(\mathbf{x}^*)\right)\right] \tag{2.51}$$

$$\sigma_x = \frac{1}{f_x(\mathbf{x}^*)}\phi\left(\frac{\mathbf{x}^* - \mu_x}{\sigma_x}\right) = \frac{1}{f_x(\mathbf{x}^*)}\phi\left[\Phi^{-1}\left(F_x(\mathbf{x}^*)\right)\right] \tag{2.52}$$

The steps for the implementation of the Rackwitz-Fiessler method are the same than the steps followed by the matrix procedure except that a step has to be added for the calculation of the equivalent normal mean and standard deviation of all the non-normal random variables. The following step has to be added between steps 2 and 3 of the matrix procedure:

- Determine the equivalent standard mean and standard deviation for each of the design point values $\mathbf{x}^*$ with a non-normal distribution. For the design point values corresponding to a normal distribution, the equivalent normal mean and standard deviation are just the actual values.

From the procedures discussed above, it was noted that the Hasofer-Lind reliability index method as well as the Rackwitz-Fiessler method require that the limit state function needs to be evaluated and solved in order to obtain a new design point. For practical problems and strongly non-linear limit state functions, the evaluation of the limit state function G is often very difficult or even impossible. In order to solve this problem, an alternative method has to be used like the Newton-Raphson type recursive algorithm. This is discussed below [15].

2.4.1.3 Newton-Raphson Recursive Method

The Newton-Raphson recursive algorithm suggested by Rackwitz and Fiessler [31] make use of the same principle than the Hasofer-Lind reliability index and the Rackwitz-Fiessler methods in the sense that the performance function is linearised at each iteration point. The only difference is that the Newton-Raphson make use of derivatives in order to find the new design point instead of solving the limit state function G explicitly for the reliability index β. This method will be explained for a linear and non-linear performance function.

Linear Limit State Function

When a linear performance function is considered as in Figure 2.15, the limit state function may not be clearly defined, hence the initial design point $\mathbf{z}_0^*$ may not be on the limit state function $G(z_1, z_2) = 0$, but rather on a parallel line to the performance function $G(z_1, z_2) = k$ [15].

As seen from Figure 2.15, the algorithm starts from an initial design point $\mathbf{z}_0^*$ which is not on the limit state function, and then converge to the point $\mathbf{z}^*$ where the distance from the origin to the limit state function is a minimum. For a linear limit state function as in this case, the limit state function can be expressed as in Equation (2.53) [15]

$$Gz = b + \mathbf{a}^T\mathbf{z} = b + a_1 z_1 + a_2 z_2 \tag{2.53}$$

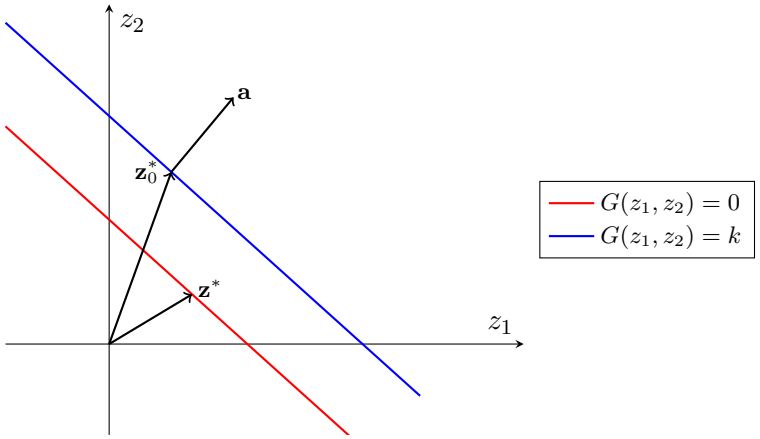

Figure 2.15: Newton-Raphson recursive method for a linear limit state function [15].

where $\mathbf{a}^T = (a_1, a_2)$, which is the transpose of the gradient vector of the limit state function. From geometry in Figure 2.15, the design point $\mathbf{z}^*$ can be expressed in terms of the initial design point $\mathbf{z}_0^*$ as in Equation (2.54).

$$\mathbf{z}^* = \frac{\mathbf{a}}{|\mathbf{a}|^2}\left[\mathbf{a}^T\mathbf{z}_0^* - g(\mathbf{z}_0^*)\right] \tag{2.54}$$

Non-Linear Limit State Function

When a linear limit state function is considered as in Figure 2.15, the gradient is constant. For a non-linear limit state function like in Figure 2.16, Equation (2.54) for the design point can be generalized as in Equation (2.55) [15]

$$\mathbf{z}_{k+1}^* = \frac{1}{|\nabla g(\mathbf{z}_k^*)|^2}\left[\nabla g(\mathbf{z}_k^*)^T\mathbf{z}_k^* - g(\mathbf{z}_k^*)\right]\nabla g(\mathbf{z}_k^*) \tag{2.55}$$

where $\nabla g(\mathbf{z}_k^*)$ is the gradient vector at the k^{th} iteration point $\mathbf{z}_k^*$ (Equation (2.56))

$$\mathbf{z}_k^* = \begin{Bmatrix} z_{1k}^* \\ z_{2k}^* \\ \vdots \\ z_{nk}^* \end{Bmatrix} \tag{2.56}$$

and n is the number of random variables and k the iteration number.

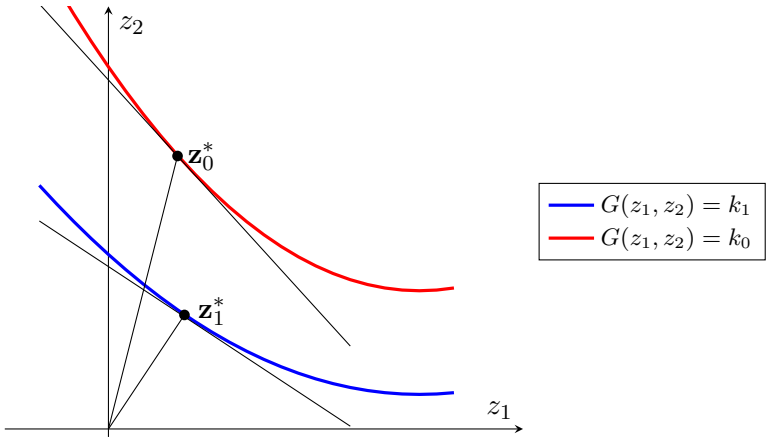

Figure 2.16: Newton-Raphson recursive method for a non-linear limit state function [15].

As mentioned, the gradient of a non-linear limit state function is not constant, therefore the recursive formula in Equation (2.55) has to be used. The recursive formula will be repeated until convergence of the design point and the gradient of the tangent at the design point. The convergence is generally reached when the difference in the design point and gradient of the tangent are less than or equal to 0.001 [15].

When convergence occur and the final design point $\mathbf{z}^*$ is obtained, the reliability index can be determined with the use of Equation (2.57).

$$\beta = \sqrt{\sum_{i=1}^{n} (z_i^*)^2} \tag{2.57}$$

With the use of the obtained design point $\mathbf{z}^*$ in the standardized normal space, the coordinates of the design point in the actual space can be determined with the use of Equation (2.58).

$$x_i^* = \mu_{x_i} + \sigma_{x_i} z_i^* \tag{2.58}$$

The steps discussed by Haldar and Mahadevan [15] for the Newton-Raphson method is as follows:

1. Define the limit state function for the specific problem at hand.
2. Assume values for all the random variables x_i in order to obtain an initial design point $\mathbf{x}^*$ (The mean values are often a good initial assumption for the random variables).
3. Substitute the assumed values for the initial design point into the limit state function in order to obtain the value of the limit state function.
4. Calculate the equivalent mean and standard deviations of all the non-normal random variables with the use of equations (2.51) and (2.52) respectively.

5. Rewrite all the design point values in standardized form (z_i^*) with the use of Equation (2.31).
6. Calculate the derivatives of the limit state function with respect to all the standardized design point values with the use of Equation (2.34).
7. The new design point can then be calculated with the use of Equation (2.55).
8. Using the new design point, the reliability index are obtained with Equation (2.57).
9. Calculate the design point in terms of actual values with Equation (2.58).
10. Repeat steps 2 to 9 until convergence of the design point and reliability index are reached.

According to Haldar and Mahadevan [15], with the Newton-Raphson algorithm each new iteration point is computed with a single recursive formula which means that the only information needed is the value of the previous design point and the gradient of the tangent at that point. Because of the above mentioned reason, fast convergence occur as well as minimal storage space is needed which make the algorithm optimal for computer analysis [15].

2.4.2 Second-Order Reliability Method (SORM)

As mentioned before, a strongly non-linear limit state function might cause accuracy and convergence problems with the use of the First Order Reliability Method. According to Haldar and Mahadevan [15], the FORM method is fairly accurate when the probability density function (PDF) of the random variables decay rapidly as the iteration point moves away from the optimal design point. When the PDF decays slowly and the limit state function is highly non-linear, a higher order approximation is necessary for the computation of the reliability index and probability of failure. This lead to the development and use of the Second Order Reliability Method (SORM) which takes into account additional information about the curvature of the limit state function.

2.4.3 Monte Carlo Simulation

The First Order Reliability Methods are fairly accurate for the computation of the reliability index and probability of failure when an explicit limit state function can be defined, for example the limit state function in Equation (2.7) on page 19. However, the Newton-Raphson method makes use of the concept of reliability evaluation when the limit state function is implicit. The use of any First Order Reliability Methods require a good background and knowledge about probability and statistics. With the use of simulation methods like for example the Monte Carlo simulation method, the probability of failure of any explicit or implicit limit state function can be determined with only little background and knowledge about probability and statistics [15].

The Monte Carlo simulation method, first developed and used by von Neumann during World War II, is a very effective tool used by engineers with only the basic knowledge about probability and statistics to determine the reliability and probability of failure of complex engineering systems and structures [15].

The Monte Carlo simulation involves the repetition of a simulation process where a value for each random variable is generated with the use of the corresponding probability distributions. The set or sample of values for the random variables generated in each simulation is similar to a sample of experimental observations. The results and observations obtained from a Monte Carlo simulation can therefore be treated as statistical data [2].

The Monte Carlo technique is also a sampling technique which is subjected to sampling problems and errors. Therefore the use of the Monte Carlo simulation is not an exact solution, however, uncertainties and errors can be minimized for a large number of simulations. Due to the large number of simulations needed in order to minimize sampling problems, the Monte Carlo simulation is ineffective and costly for large and complex systems [15, 2].

2.5 Motivation for This Study

Following a thorough literature study about the techniques and algorithms necessary to obtain an optimal portal frame and the reliability thereof given that the size of the columns and rafters as well as the haunch length and roof pitch are used as design variables, Sections 2.5.1 to 2.5.3 will motivate why the reliability of optimal portal frames has to be studied and investigated.

2.5.1 Design of Optimal Portal Frames

As mentioned in Section 2.1.3, the design variables that will be used to find an optimal portal frame will consist of the column and rafter sizes as well as the haunch length at the eaves and the roof pitch. For the purpose of this study, an optimal portal frame is defined as the lightest possible structure of given span and height dimensions conforming to both ultimate and serviceability limit state criteria. Saka [39] proved that the use of haunched rafters have a significant effect on the weight of portal frame structures and therefore it was decided that the haunch length will be used as a design variable. The main reason for the roof pitch of a portal frame also being a design variable is to investigate what roof pitch would be optimal in terms of the weight of the frame.

In order to obtain and design an optimal portal frame, meaning the lightest possible design for a specified span and height, each frame has to comply with ultimate and serviceability limit state criteria. The procedures and techniques used to design an optimal portal frame in terms of ultimate and serviceability limit states as well as the applied loading are discussed in Chapter 3.

During the structural design of a portal frame, the structural dimensions and proportions are determined according to the ultimate limit state design criteria. With the use of the structure conforming to the ultimate limit states, the deflections of the structure due to statically applied live load as well as wind loads are compared with deflection limits. The conformance of the obtained deflections with the deflection limits are viewed as an assurance of service performance of the structure during its intended lifetime. It is therefore necessary to design buildings for ultimate limit state as well as serviceability limit state [13].

According to Galambos and Ellingwood [13], the simple act of limiting the deflections of the structure to allowable limits protect the structure against complicated serviceability demands. There are however two problems with this approach which include a very costly remedial procedure if failure occur as well as the irrational decision of static deflection limits controlling unacceptable vibrations.

Common serviceability problems include the following:

- Damage to non-structural elements e.g. partitions, ceilings, windows, cladding.
- Large deflections would cause distress to occupants.
- Visual acceptability of the structure.
- Water tightness are influenced when large deflections occur.
- Physical discomfort of occupants due to large lateral deflections and vibrations.
- Distortion of friction grip connections.

Given the wide variety of serviceability problems mentioned above, it is clear that all of these problems can not be dealt with by limiting the stiffness of the structure. Each serviceability criterion has to be considered separately by the engineer in order to ensure that all the performance requirements of the structure are met [13]. The main questions that arise in order for the engineer to design a structure with confidence in terms of the serviceability limit state are as follows:

1. What is an appropriate deflection limit for the specified structure?
2. What is the magnitude of the serviceability loads applied on the structure?

Galambos and Ellingwood [13] mentioned that the origin of customary deflection limits used in design codes can not be clearly documented and are mainly based on experience. Accurate serviceability limits for the use in structures are impossible to determine during the design phase of a project and are dependent on several factors that are difficult to define. Unserviceability of a structure is dependent on the type of structure and the perception of occupants in the building. Large deflections might cause visible cracks in walls, floors and non-structural components and cause general public to see these cracks as imminent danger [13].

According to Galambos and Ellingwood [13], little basis exist for changing existing deflection limits until a worldwide research project is conducted in order to obtain more accurate and better limiting criteria for deflections. Even though the current limits seems acceptable for design purposes, these limits influence the optimal weight and reliability of steel structures and directly influence the cost of these structures.

Woolcock and Kitipornchai [48] did a survey in Australia through the Australian Institute of Steel Construction among engineers in the country to obtain deflection limits used in practise for industrial buildings. They mentioned that the lack of information on deflection limits is due to the fact that there is no rational basis for calculating deflection limits and that the performance of excessively flexible frames is unlikely to be reported.

The lack of published guidance in terms of deflection limits and the responsibility of practising engineers to use their designers' judgement are heavily counter productive in engineering offices. Especially young graduate engineers with little or no experience need good guidance in order to decide on realistic deflection limits [48].

The survey prepared by Woolcock and Kitipornchai [48] was published in the August 1986 edition of Steel Construction and 90 credible responses from practising engineers were received and compared. Even though the conditions in terms of wind loadings and design codes differ from country to country, these results indicated that there are quite a wide variety of deflection limits used in Australia. This again prove that it is important to investigate what effect these limits has on industrial buildings in terms of weight and reliability.

For lateral deflection of a duo-pitched roof portal frame, the following questions were asked:

Which of the following criteria should be used to control lateral deflections?

1. A fraction of column height h and/or
2. A fraction of frame spacing b and/or
3. An absolute deflection value.

Table 2.1 contain the results obtained from this question in the survey.

As a second and third question, the survey asked to choose a lateral and vertical deflection limit as a fraction of the column height and span length of the structure respectively. Figure 2.17 and 2.18 indicate the results obtained from the survey for these two questions.

Following the study done by Woolcock and Kitipornchai [48] in terms of deflection limits used in Australia, it is evident that these deflection limits are based on experience. The effect of the deflection limits on the optimal weight and reliability of portal frame structures are therefore of great importance.

Table 2.1: Criteria for limiting lateral deflection [48].

Criteria	**Number**	**%**
Fraction of column height only	32	35.6
Fraction of column height and frame spacing	31	34.4
Fraction of column height and an absolute deflection	6	6.7
Fraction of frame spacing only	6	6.7
Fraction of frame spacing and an absolute deflection	1	1.1
An absolute deflection only	2	2.2
Fraction of column height, frame spacing and an absolute deflection	8	8.9
Unsure	4	4.4
	90	**100.0**

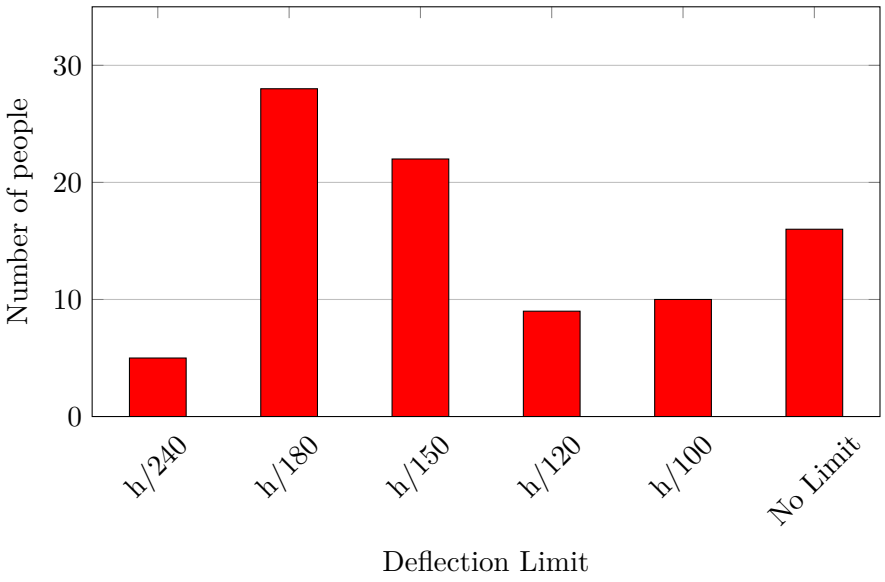

Figure 2.17: A histogram indicating the lateral deflection limit as a fraction of the column height used by practising engineers in Australia [48].

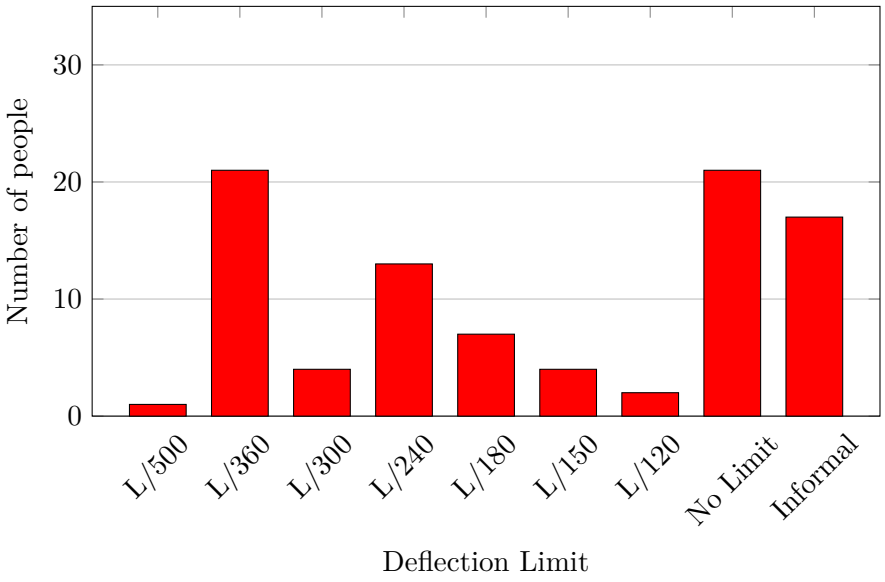

Figure 2.18: A histogram indicating the vertical deflection limit as a fraction of the span length under a live load used by practising engineers in Australia [48].

Even though the origin of deflection limits is unknown, the decision was made to use the horizontal and vertical deflection limits of height/200 and span/180 in accordance with SANS 10160-1:2011. This was done to ensure that the reliability index values obtained from the First Order Reliability Method can be evaluated and compared to target reliability index values adopted in SANS 10162-1:2011.

For the reliability analysis of an optimal portal frame governed by the serviceability limit state,a probabilistic description of deflections that would result in damage (i.e. exceeding the irreversible SLS as per SANS 10160-1:2011) are obtained from a study done by Ter Haar, Retief, and Dunaiski [45] about the probabilistic models for the serviceability limit state design of industrial steel buildings. These damage deflection probabilistic models for horizontal and vertical deflections are given in Table 3.1 on page 57.

2.5.2 Why the use of Genetic Algorithms

Following the literature study regarding structural optimisation and the use of Genetic Algorithms as a searching mechanism to obtain an optimal solution from a large population of possible solutions, it is necessary to highlight and summarize why the use of genetic algorithms are preferred rather than more traditional searching methods.

The main advantage of the use of Genetic Algorithms is the effectiveness and more importantly the robustness that it provides in terms of calculation time and obtaining a global optimal solution. For this reason it is fairly important to question and investigate if more conventional optimisation and search methods meet the robustness requirements needed for structural engineering problems.

According to Goldberg [14], the literature identified three main conventional search methods: calculus-based, enumerative, and random. These techniques are briefly discussed below as well as a brief overview of Genetic Algorithms compared to these conventional methods.

2.5.2.1 Calculus-Based Search Method

The calculus-based search methods are subdivided into two types: direct and indirect. For the indirect search method, a set of non-linear equations have to be solved by setting the gradient of the specified objective function equal to zero. This will result in finding a local maximum of minimum value given the objective function is a smooth and unconstrained function. By restricting the search domain to all points with zero gradients in all directions, the global optimum value of the problem is obtained [14]. This is a generalization of the calculus technique known as extremal points in multiple dimensions as is illustrated with Figure 2.19 where several local maximum and minimum points are present.

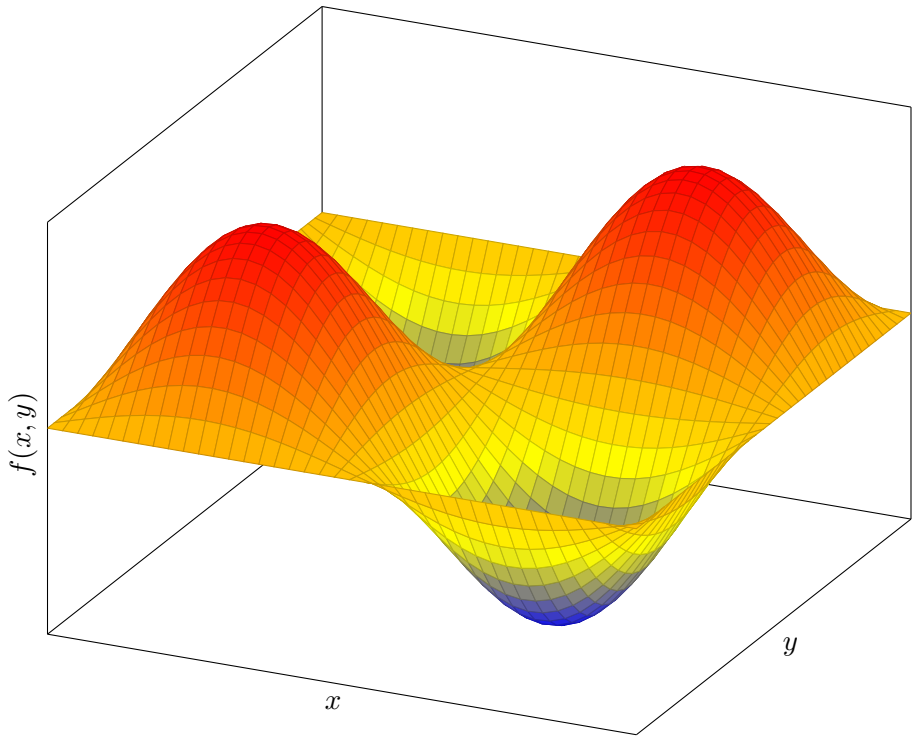

Figure 2.19: Multi peak mathematical function solved with indirect calculus-based search method [14].

The direct calculus-based search method is based on the principle of "hill climbing". Hill climbing is a technique where the local minimum or maximum value is obtained by climbing the objective function in the steepest permissible direction [14].

Even though the use of calculus-based searching methods have been studied and improved, there are clear reasons showing their lack in terms of robustness. The first and most important

shortcoming of calculus-based searching methods are the fact that they are local in scope, meaning that the optimal value obtained is only the optimum in the neighbourhood of the current point. Secondly, calculus-based functions rely on smooth, unconstrained objective functions with the existence of derivatives. This is almost never the case in real life structural engineering problems which means that the use of calculus-based searching methods are unsuitable for almost all engineering problems [14].

2.5.2.2 Enumerative Search Methods

Enumerative searching methods are based on the simple idea of looking at the objective function at each point individually in the finite search space. These types of search methods are very human like and attractive due to its simplicity, however it has very weak robustness characteristics due to its lack in efficiency. Search spaces related to real life engineering problems are simply too large to inspect each single point in the search space separately [14].

2.5.2.3 Random Search Methods

With the shortcomings and ineffective use of calculus-based and enumerative searching methods, the use of random searching methods have achieved an increase in popularity. The use of random search methods also have shortcomings in terms of efficiency and might not perform better than enumerative techniques when the search space is very large. Random searching methods have to be separated from randomized searching techniques like Genetic Algorithms, as Genetic Algorithms are based on random choices which are highly effective and efficient [14].

2.5.2.4 Genetic Algorithms

According to Goldberg [14], the reason why Genetic Algorithms are more efficient in terms of robustness when compared to the more conventional searching methods explained above is because of the following four fundamental reasons:

1. Genetic algorithms make use of a set of parameters during the coding process instead of working with the parameters themselves.
2. Genetic algorithms search through a population of possible solutions instead of a single solution.
3. Genetic algorithms make use of an objective function for the evaluation of solutions, not derivatives.
4. Genetic algorithms make use of probabilistic rules during transition instead of deterministic rules.

As mentioned before, conventional optimisation techniques make use of a point-to-point searching technique where the possibility of locating false lower peaks in a multi-peak problem are high. In contrast, the Genetic Algorithm works with an entire population of solutions simultaneously, climbing many peaks at the same time, therefore increasing the probability of finding the optimal peak instead of a local, lower peak value as in Figure 2.19 [14].

Goldberg [14] mentioned that conventional searching methods require auxiliary information, for example, derivatives are needed for gradient based techniques, where genetic algorithms require no such information to perform its optimisation and searching techniques.

Taking all the above mentioned advantages of Genetic Algorithms over more conventional searching methods in terms of robustness and efficiency into account, it is evident that the use of Genetic Algorithms are more useful for the optimisation of steel portal frames when a huge number of possible solutions exist.

Given the advantages of Genetic Algorithms listed above, it is also important to mention the disadvantages of using Genetic Algorithms to obtain an optimal solution from a large population of possible solutions. Some disadvantages of Genetic Algorithms include the following:

1. As with most searching algorithms like Genetic Algorithms, there is always a possibility that the algorithm will find a local optimal solution instead of the global optimum due multiple peaks as was explained in Section 2.5.2.1. Genetic Algorithm operators are implemented to decrease the possibility of obtaining local optimal values [14].

2. A time of 1.67 hours were needed to obtain an optimal portal frame structure with only four design variables. An increase in design variables will cause an exponential increase in possible solutions and therefore can become computationally expensive.

3. To ensure that an optimal or near optimal solution is obtained, the correct mutation rate and penalty function constants have to be selected and calibrated.

For the purpose of this study and the fact that the same algorithm techniques were used by Saka [39] and Phan et al. [29] for the optimisation of steel portal frames with haunched rafters, it was decided to use Genetic Algorithms as a searching method to obtain an optimal portal frame for the reliability calculation of a weight optimized portal frames.

Other extensive research has been done on the use of Genetic Algorithms for structural optimisation which can be found in [28, 33, 20, 5, 32]

Given the 62 available sizes from the South African Steel Construction Handbook, a roof pitch in the range of 0 - 25 degrees and a haunch length being selected in 10 mm intervals with a maximum length of 10 % of the span length, a massive $62 \times 62 \times 25 \times 300 = 28.83 \times 10^6$ number of solutions are possible for a frame with a span length of 30 m. With the use of the Genetic Algorithm, an optimal or near optimal solution from this large population of possible solutions were obtained in 1.67 hours with the use of a computer with a 3.3 GHz processor and an available

16 GB of memory of which 8 GB could be utilized for the Genetic Algorithm.

To put the time of 1.67 hours it took to obtain an optimal solution into perspective, the rafters of the frame being optimized with a span of 30 m were subdivided into 48 smaller frame sections to simulate the effect of haunched rafters. This meant that a 30 m span frame consists of atleast 98 members, resulting in a stiffness matrix for the deflection calculations within the linear finite element analysis of more or less 300×300 in size. It took the computer with a possible 8 GB of memory 0.07 seconds to complete an entire analysis of one single solution which means that if all of the 28.83×10^6 possible solutions had to be analysed separately, it would take approximately 560 hours to complete. This clearly indicate that the use of Genetic Algorithms are very effective and time efficient for the purpose of finding an optimal solution from a large populations of possible solutions.

2.5.3 Reliability of an Optimal Portal Frame

With the use of structural optimisation and a Genetic Algorithm, an optimal portal frame in terms of column and rafter size, haunch length and roof pitch for a given span and height was obtained. Given this optimal portal frame, the reliability index can be calculated with the use of a First Order Reliability Method as explained in Section 2.3.

From the theory of reliability and the methods used to determine a reliability index studied in Sections 2.3 and 2.4 respectively, a decision was made to make use of the non-linear Newton-Raphson Recursive method due to the fact that this method does not require the calculation of derivatives of the limit state function. The limit state functions used for the definition of failure for the ultimate limit state given later in Equations (3.14) to (3.10) on page 58 are strongly non-linear, therefore making the calculation of partial derivatives extremely difficult.

In Section 2.4.3 it was mentioned that the Monte Carlo method for the calculation of a reliability index irrespective of the limit state function being highly non-linear or explicit is very accurate. Even though the use of a Monte Carlo method for the calculation of the reliability index of an optimal portal frame would yield sufficiently accurate results if a large enough number of repetitions were used in the analysis without the need of statistical knowledge, the conclusion was made that it would not be inefficient to use. This is due to the fact that a very large number of repetitions are necessary to determine the final design value for each design variable. A large number of analyses had to be done to compare the reliability index for frames of different span to height ratios and therefore the First Order Reliability Method was deemed more sufficient in terms of the time it needed to compute the reliability index.

It is important to note that the use of structural optimisation and Genetic Algorithms are necessary to obtain a solution for a portal frame that is at its extreme limit either in terms of ultimate or serviceability limit state. The only way to compare a reliability index of a portal frame obtained from the First Order Reliability Method with prescribed target reliability values

in SANS 10160-1:2011 is by ensuring that the frame has no extra capacity either in terms of ultimate or serviceability depending on which limit state function governs the design. This is achieved with the use of the Genetic Algorithm where the haunch length of the rafters are incremented in 10 mm intervals and a solution is obtained where for example a frame governed by the serviceability limit state has a deflection of at least 99 % of its deflection limit.

The obtained reliability index of an optimal frame at its extreme limit are used to determine if current deflection limits and partial factors are sufficient to obtain a target reliability of $\beta = 3.0$ and $\beta = 2.0$ for ultimate and irreversible serviceability limit states respectively as accepted in SANS 10160-1:2011. The need for this is due to the fact that the origin of current deflection limits are unknown. These results can then be used to evaluate the sensitivity of several design variables like material properties and peak wind pressure on the structural reliability of an optimal portal frame.

Chapter 3

Method and Analysis

3.1 Introduction

For the purpose of this study, the decision was made to write a program in JAVA to obtain the optimal weight of any portal frame structure with given loading and boundary conditions and subsequently determine the reliability of the structure.

The JAVA program contains several sub-modules which are used to obtain an optimal solution and calculate the reliability index of the frame. These subcategories include a Genetic Algorithm, a linear Finite Element Method (FEM), a design module as well as a First Order Reliability Method (FORM).

3.2 Genetic Algorithm

To obtain the optimal design of a portal frame structure, a Genetic Algorithm which is part of the evolutionary algorithm family was programmed in JAVA. Following a thorough literature study and the studies specifically performed by Saka [39] and Phan et al. [29], a decision was made to use the following design variables due to the large population of possible solutions it provides.

- The **column size** of the portal frame chosen from the list of I and H-section profiles in the South African Steel Construction Handbook 2013 [38].
- The **rafter size** of the portal frames chosen from the list of I and H-section profiles in the South African Steel Construction Handbook 2013 [38].
- The **haunch length** used in the portal frame as a continuous variable with 10 mm intervals between 0 and span/10.

- The **roof pitch** of the portal frame as a continuous variable with one degree intervals between 0 and 25 degrees.

Figure 3.1 is a graphical presentation of a typical portal frame structure being optimised with the use of the Genetic Algorithm.

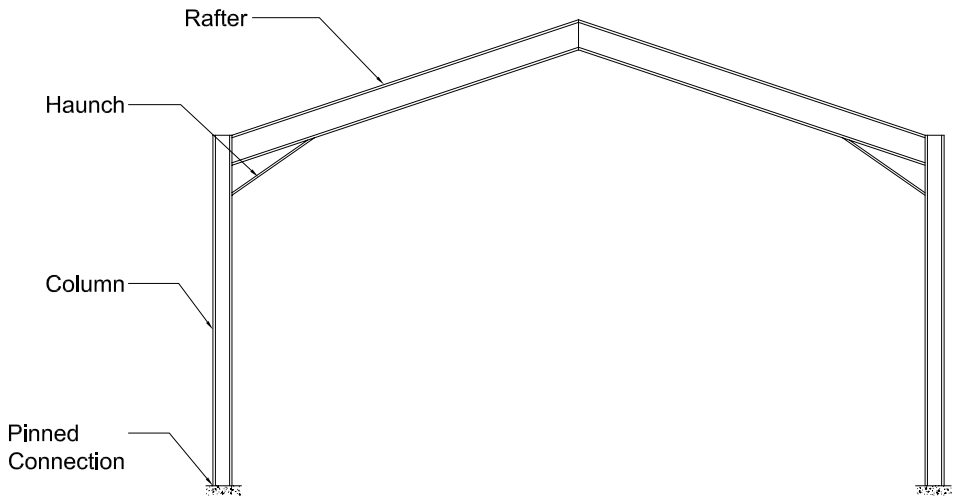

Figure 3.1: Presentation of typical portal frame being optimised.

As discussed in Section 2.2, Genetic Algorithms make use of the biological phenomenon known as survival-of-the-fittest to obtain a near optimal solution from a very large population of possible solutions. With the use of Genetic Algorithm operators like crossover and mutation, diversity in the population is ensured.

For each iteration in the Genetic Algorithm, the forces acting on each structure resulting from wind pressures have to be determined in accordance with SANS 10160-3:2011 [36]. The process and techniques used in the JAVA program to obtain the wind loads as distributed loads on each possible portal frame depending on the height and roof pitch of each frame are discussed in Section 3.3.

To obtain the fitness (weight) of each solution, each member of the structure have to be checked for failure as well as deflection limits. For this purpose a finite element method is used to find the reaction forces and moments in each member of the structure as well as deflections resulting from the applied loading. The finite element analysis and processes used to obtain these resulting deflections, reaction forces and moments in the JAVA program are discussed in Section 3.4.

Following the finite element analysis, each structure has to be designed in accordance with SANS 10162-1:2011 [37]. For the Genetic Algorithm to evaluate the fitness of each possible solution, penalty functions have to be applied to frames that do not comply with the limiting resistances and deflection limits of members in order to make these solutions less favourable. These penalty values discussed in Section 2.2.7 are calculated with the use of resistance checks during the design phase of each structure. The design procedure for portal frames used in the JAVA program is discussed in Section 3.5.

With the Genetic Algorithm program completed and an optimal solution obtained, the reliability of this frame is determined with the use of a First Order Reliability Method (FORM) programmed in JAVA. The methods and procedures used in the programming of the First Order Reliability Method are discussed in Section 3.6

3.3 Loading

Wind actions and loads are determined in accordance with SANS 10160-3:2011 which gives guidance to the calculation of natural wind actions on structures, parts of structures or elements attached to structures for structural design purposes of buildings and industrial structures [36].

In order to obtain wind forces on a portal frame, the peak wind pressure at the location of the structure as well as external and internal pressure coefficients have to be determined. These methods and calculations exclude wind loading effects due to high intensity wind conditions like tornadoes and micro-bursts [36].

According to SANS 10160-3:2011, wind forces act directly as external pressure forces on closed structures as well as internal pressure forces on open structures. The pressure forces acting on the structure result in forces being applied in a direction perpendicular to the structure or cladding elements. When wind is blowing along a large surface area, frictional forces also develop that have to be considered [36].

In order to obtain the wind pressure on a surface, a pressure coefficient is used to transform free flow pressure to account for bluff body effects. External pressure coefficients c_{pe} are used for determining the wind pressure on external surfaces of the structure while internal pressure coefficients c_{pi} are used for internal surfaces.

The external and internal pressure coefficients for this study are only determined for duo-pitch roof structures and flat roof structures. The internal and external wind pressures on a surface of the structure are determined with Equations (3.1) and (3.2) respectively [36].

$$w_i = q_p(z_i) \times c_{pi} \tag{3.1}$$

$$w_e = q_p(z_e) \times c_{pe} \tag{3.2}$$

where

- w_i is the wind pressure acting on internal surfaces,
- w_e is the wind pressure acting on external surfaces,
- z_i and z_e are the reference height relevant to the internal and external pressures respectively,
- c_{pi} is the internal pressure coefficient,
- c_{pe} is the external pressure coefficient,
- $q_p(z_i)$ is the peak wind pressure at a height z_i, and
- $q_p(z_e)$ is the peak wind pressure at a height z_e.

The net pressure acting on a surface is determined with the summation of internal and external pressures on the surface taking into account the direction of the pressures. A pressure onto the surface is taken as a positive pressure while a suction away from the surface is a negative pressure. Figure 3.2 on page 51 from SANS 10160-3:2011 is a graphical representation of the net effect caused by internal and external pressures on a surface.

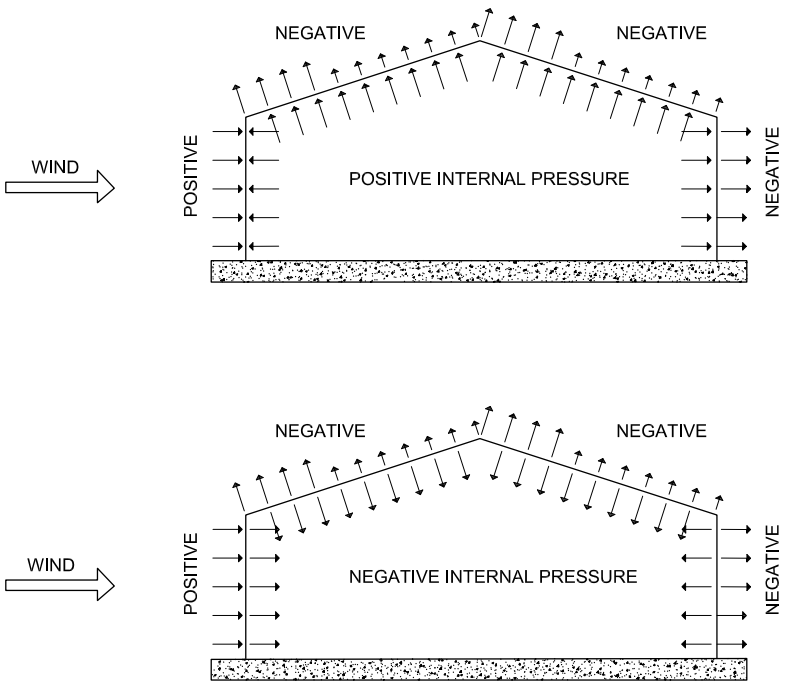

Figure 3.2: Representation of internal and external pressures on surface [36].

Given a peak wind pressure and all the pressure coefficients for internal and external surfaces, the wind forces on each surface are obtained with Equations (3.3), (3.4) and (3.5) which represent the internal, external and frictional forces on a surface respectively [36].

$$F_{w,i} = w_i \times A_{ref} \tag{3.3}$$

$$F_{w,e} = c_s \times c_d \times w_e \times A_{ref} \tag{3.4}$$

$$F_{fr} = c_{fr} \times q_p(z_e) \times A_{fr} \tag{3.5}$$

where

- $F_{w,i}$ is the wind force on an internal surface,
- $F_{w,e}$ is the wind force on an external surface,
- $c_s c_d$ is a structural factor taken as 1.0,
- c_{fr} is a frictional coefficient obtained from SANS 10160-3:2011 §8,
- A_{ref} is the reference area of the surface on which the pressure act, and
- A_{fr} is the exposed area of a surface parallel to the wind direction.

The wind force calculations as explained above are programmed in JAVA so that the applied loading for all possible wind combinations including internal and external pressure coefficients are calculated automatically for a given roof pitch. These distributed loads are then applied to the portal frame given specified wind conditions during the finite element analysis to obtain resulting deflections, reaction forces and moments for wind load combination.

Most structures including portal frames are usually subjected to multiple load cases and it would therefore be useful to analyse each portal frame for each possible load case. To achieve an optimal portal frame for multiple load cases, each member of the structure is analysed for all possible load cases to ensure that each member of the structure has sufficient capacity for both ultimate and serviceability limit state criteria for all the load cases.

For simplicity of the Genetic Algorithm it was decided to analyse each portal frame structure for only one single load case to focus the scope of this study on obtaining an optimal portal frame with the use of the Genetic Algorithm and calculating the reliability index of each optimal frame to compare with target reliability values in SANS 10160-1:2011. Due to the limitation of only one load case for simplicity and scope of this study, the results might be biased towards lateral deflection due to lateral wind load. Even though this simplification will limit the results,

these optimal portal frames are still sufficient to investigate the reliability index of frames at its limit either in terms of the ultimate or serviceability limit state.

3.4 Finite Element Method

Reaction forces and moments are obtained from a first-order elastic finite element analysis programmed in JAVA and implemented as part of the Genetic Algorithm program by using input values and wind loading results and computing forces, bending moments and deflections for each member of the structure. The results for each member are then used to identify critical members in the structure for design purposes.

For the design of steel structures like portal frames, it has long been recognised by engineers that there is a need to take into account second order effects and inelastic material behaviour due to a change in geometry of the structure. With the use of a first-order elastic design procedure, these effects are only accounted for through specifying certain provisions during member design. The use of a first-order elastic analysis for the calculation of forces and moments provide safe and serviceable structures, however with the development and advances of high speed computers and design software, it is possible to use sophisticated analysis procedures that take into account second-order effects and material behaviour that provide more realistic and rational results. These procedures known as plastic design methods therefore provide more economical and cost effective structures.

Due to the large number of iterations and finite element analyses necessary to obtain an optimal portal frame and the reliability thereof, a basic first-order elastic analysis was used due to the fact that the use of a sophisticated second-order finite element computer software program would not be time and cost efficient. The direct-stiffness method for the calculation of deflections and reactions forces were therefore programmed and used as explained in Cook [8].

3.5 Portal Frame Design

For the structural design of each portal frame structure in each GA iteration, the results obtained from the finite element analysis are used to determine if the portal frame has sufficient capacity to carry the applied loads given ultimate limit state loading conditions and compare obtained deflections with maximum deflection limits for serviceability limit state loading conditions.

Each portal frame structure is analysed for ultimate and serviceability limit states which means that two finite element analyses are done with the respective limit state load and partial factors for each limit state.

The capacity of each member of the portal frame structure is calculated for a beam-column in combined axial force and bending in accordance with SANS 10162-1:2011 §13.8.2 and §13.8.3.

Lateral torsional buckling is not taken into account and it is therefore assumed that lateral support to both flanges are provided at each purlin position along the length of each beam-column with the use of knee braces. Even though this is not standard construction practice, it is sometimes used for portal frames or fairly large span lengths and is assumed for this study for simplicity reasons as was done in Saka [39] and Phan et al. [29].

This assumption is used to simplify the calculation of bending resistance due to flexural torsional buckling to ensure that the effective length of each member is the distance between purlins. The complex situation where the compression flange of the member will be on either the outside or inside of the member at different positions along the length of the member was the main reason for this simplification. This will thus ensure the members are not prone to flexural torsional buckling. From Equation 3.6 below it is clear that a member with a small effective length factor $K.L$ will result in a large bending resistance and therefore not being critical in terms of torsional flexural buckling.

$$M_{cr} = \frac{\omega_2.\pi}{K.L}\sqrt{E.I_y.G.J + \left(\frac{\pi.E}{K.L}\right)^2.I_y.C_w} \tag{3.6}$$

Due to the simplicity constraints of not taking into account lateral torsional buckling as well as only analysing each portal frame for one single load case being lateral wind load as mentioned in Section 3.3, there is a clear limitation on results in terms of the optimal portal frame. However, these constraints do not limit the reliability calculations of an optimal portal frame and therefore the limitations of lateral torsional buckling and a single load case are deemed acceptable.

Following the procedure in SANS 10162-1:2011 §13.8.2 and §13.8.3 for the capacity check of each member in the portal frame structure under ultimate limit state loading conditions, Equations (3.7) to (3.10) are evaluated to determine if each beam-column has sufficient capacity to sustain the loads and moments applied to it.

$$\frac{C_u}{C_r} + \frac{0.85U_1M_u}{M_r} \leq 1.0 \tag{3.7}$$

$$\frac{M_u}{M_r} \leq 1.0 \tag{3.8}$$

$$\frac{T_u}{T_r} + \frac{M_u}{M_r} \leq 1.0 \tag{3.9}$$

$$\frac{M_u}{M_r} + \frac{T_u.Z}{M_r.A} \leq 1.0 \tag{3.10}$$

where

- T_u, C_u and M_u are the applied tension force, compression force and bending moment on the member respectively,
- T_r, C_r and M_r are the tensile, compressive and bending resistances of the member respectively,
- U_1 defined as in SANS 10162-1:2011 taking into effect second order effects,
- Z is the section modulus dependent on the class of member, and
- A is the cross sectional area of the member.

The maximum value from Equations (3.7) to (3.10) is then used to calculate a penalty value with the use of the dynamic penalty method discussed in Section 2.2.7. This penalty value is then added to the fitness (weight) of the structure to make this structure less favourable if the capacity of any member is not sufficient.

Under serviceability limit state loading conditions, the horizontal and vertical deflections of the portal frame structure are evaluated and compared to the maximum allowed deflection limits. Equation (3.11) is used to determine if the obtained deflections from the finite element analysis are acceptable and subsequently compute a penalty value to be added to the fitness if the deflections are not acceptable.

$$\frac{\Delta}{\Delta_{MAX}} \leq 1.0 \tag{3.11}$$

Rafters with haunches were analysed by using small beam elements along the length of the rafter with the calculated area and moment of inertia of each beam element based on the length and the depth of the haunch. The depth of the haunch was linearly decreased along the length of the haunch with the maximum depth being the depth of the rafter section. All haunches are assumed to be cut from the same cross-sectional size I or H-section as the rafter of the portal frame being analysed. Accuracy will improve depending on the length of the beam elements selected along the length of the rafter as the cross-sectional area of the haunch section will decrease more linearly when using smaller elements.

For the design aspects of the rafter beams with haunches, each small beam element was designed separately based on the axial forces and bending moments in that element and evaluated in accordance with SANS 10162-1:2011 with the use of Equations (3.7) to (3.10).

Figure 3.3 is a typical cross-section of a haunched rafter beam where the value of D_h represents the depth of the haunch along the length of the rafter which will decrease linearly.

The neutral axis of the haunched-rafter is dependent on the depth D_h and was determined as in Equations (3.12) and (3.13) for haunched-rafters where the NA falls within the middle flange of the beam and within the web of the beam respectively. The assumption was made that the NA will lie within the middle flange of the beam where the haunch is welded to the rafter which

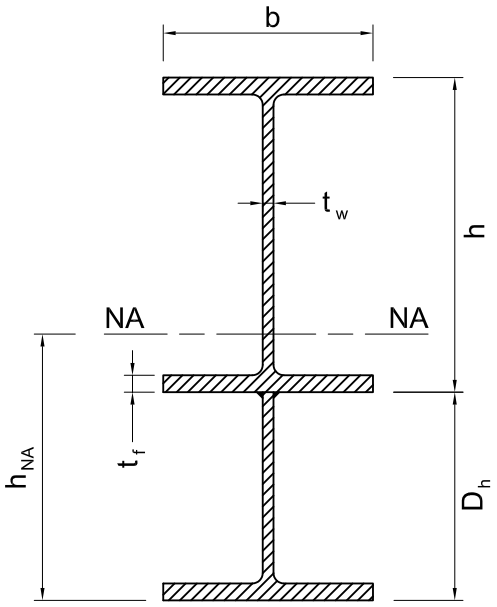

Figure 3.3: Representation of a rafter beam with a haunch

occurs mostly for H-section profiles, therefore calculating the NA with Equation (3.12). This assumption is then evaluated and recalculated with Equation (3.13) if the first assumption was false.

$$h_{NA} = \frac{h.t_w - t_f.t_w + b.t_f + D_h.b - D_h.t_w + D_h.b}{2.b} \tag{3.12}$$

$$h_{NA} = \frac{-b.t_f + t_f.t_w + h.t_w + D_h.t_w}{2.t_w} \tag{3.13}$$

The neutral axis obtained is used to calculate the plastic section modulus of the haunch-rafter at the specific cross-section for the resisting moment calculations as in SANS 10162-1:2011 [37].

3.6 Reliability

The reliability and probability of failure of an optimal solution obtained from the Genetic Algorithm are calculated using a First Order Reliability Method (FORM). As mentioned in Section 2.4, several methods exist to calculate the First Order Reliability of a portal frame. For the purpose of this study, the second order Newton-Raphson recursive method was used due to the non-linearity of the limit state functions and the short calculation time it requires.

For each optimal portal frame obtained from the Genetic Algorithm, the reliability of the entire frame will depend on the governing limit state function. This limit state function can either be one of the members of the frame not having sufficient capacity to carry the applied loads or an unacceptable horizontal or vertical deflection. This gives clear indication that a series system for system reliability was assumed as discussed in Section 2.3.5, meaning that the reliability of the whole portal frame is dependent on its weakest member.

For the reliability analysis of an optimal portal frame structure, the following design variables, model uncertainty factors and probability distributions were used from Holicky [17]. A probabilistic model for vertical and horizontal deflection that will result in damage for industrial structures were obtained from Ter Haar, Retief, and Dunaiski [45]:

1. Specified minimum yield stress f_y of structural steel with a Log-Normal distribution,
2. Peak wind pressure on the structure q_p with a Gumbel distribution,
3. Model uncertainty factor for axial force in a frame C_{uK} with a Log-Normal distribution,
4. Model uncertainty factor for moments in a frame M_{uK} with a Log-Normal distribution,
5. Model uncertainty factor for column resistance C_{rK} with a Log-Normal distribution,
6. Model uncertainty factor for beam bending moment resistance M_{rK} with a Log-Normal distribution,
7. Model uncertainty factor for deflections in a frame Δ_K with a Log-Normal distribution,
8. Vertical damage deflection in a frame $V\Delta_{damage}$ with a Log-Normal distribution, and
9. Horizontal damage deflection in a frame $H\Delta_{damage}$ with a Log-Normal distribution.

Table 3.1 contains the probabilistic models and information of all the basic design variables used in the reliability analysis.

Table 3.1: Probabilistic models of basic design variables [17, 45].

Design Variable	Distribution	Dimension	Mean μ_X	St.dev σ_X	Reference
f_y	LN	kN/m^2	$f_{yk} + 2\sigma_X$	$0.08\mu_X$	[17]
q_p	GU	kN/m^2	$0.7q_{pk}$	$0.35\mu_X$	[17]
C_{uK}	LN	-	1.0	0.05	[17]
M_{uK}	LN	-	1.0	0.1	[17]
C_{rK}	LN	-	1.2	0.12	[17]
M_{rK}	LN	-	1.0	0.05	[17]
Δ_K	LN	-	1.0	0.07	[17]
$V\Delta_{damage}$	LN	m	$L/125$	0.45	[45]
$H\Delta_{damage}$	LN	m	$H/125$	0.45	[45]

During the reliability analysis of an optimal frame at either 99 % of its ultimate capacity in terms of the ultimate limit state or a deflection of at least 99 % of its deflection limit, the limit state function is obtained by removing partial factors (which introduced conservative bias) from the design equations and including model factors to account for the uncertainty of capacity prediction inherent to these design equations. Model uncertainty factors are also described by probabilistic distributions as provided in Table 3.1. The limit state functions, with the inclusion of model uncertainty factors, used during the reliability analysis are given in Equations (3.14) to (3.18) respectively.

$$\frac{C_u \times C_{uK}}{C_r \times C_{rK}} + \frac{0.85U_1 M_u \times M_{uK}}{M_r \times M_{rK}} \leq 1.0 \tag{3.14}$$

$$\frac{M_u \times M_{uK}}{M_r \times M_{rK}} \leq 1.0 \tag{3.15}$$

$$\frac{T_u \times C_{uK}}{T_r \times C_{rK}} + \frac{M_u \times M_{uK}}{M_r \times M_{rK}} \leq 1.0 \tag{3.16}$$

$$\frac{M_u \times M_{uK}}{M_r \times M_{rK}} - \frac{T_u \times C_{uK}.Z}{M_r \times M_{rK}.A} \tag{3.17}$$

$$\frac{\Delta \times \Delta_K}{\Delta_{damage}} \leq 1.0 \tag{3.18}$$

With the use of the First Order Reliability Method and the above mentioned equations, the reliability index of an optimal portal frame are calculated and subsequently compared to the target reliability values in SANS 10160-1:2011 of $\beta = 3.0$ and $\beta = 2.0$ for frames governed by the ultimate and irreversible serviceability limit state respectively. From the results for reliability indexes, sensitivity values and final design point values obtained from the FORM analysis, conclusions can be drawn about current deflection limits and partial factors adopted in current design codes. The results of optimal portal frames obtained from the Genetic Algorithm as well as the reliability results of optimal portal frames are discussed in Chapter 4.

Chapter 4

Results and Discussions

4.1 Genetic Algorithm Accuracy and Effectiveness

In order to test the accuracy and convergence of the Genetic Algorithm, a standard span to height ratio frame was selected and evaluated with an increase in the number of generations. This test was done for a frame with and without haunches in order to ensure that convergence is obtained for both cases.

Figure 4.1 contains the results for the accuracy test of the Genetic Algorithm. Each point on the graph indicate a single Genetic Algorithm analysis. From this graph it is evident that convergence of both the frames with and without haunches are obtained at more or less thirty five generations and therefore it was concluded that sixty generations should be sufficient for all remaining tests to ensure convergence.

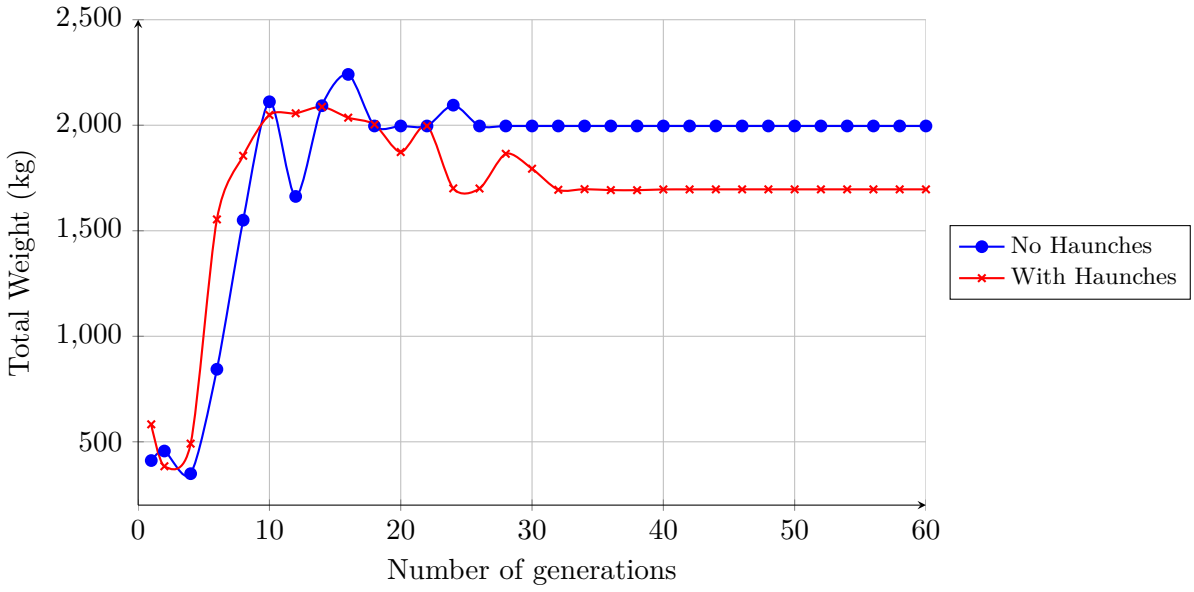

Figure 4.1: Accuracy of genetic algorithm with an increase in the number of generations

4.2 Haunched Rafters

For portal frame structures, haunched rafters are widely used due to the positive effect it has on a frame in terms of decreasing deflections. This is due to increased stiffness and moment capacity at the position of maximum moment due to the larger cross sectional area and moment of inertia. Even though it is clear that these haunches decrease deflections, the question that arise is what length these haunches should be for an optimal effect on the weight of the structure. For this reason, the haunch length was selected as a continuous variable in the Genetic Algorithm ensuring that an optimal haunch length for a portal frame of specified dimensions can be obtained.

Several analyses were done for portal frames of fixed heights with and without haunched rafters to determine the optimal haunch length and investigate how significant the effect of haunched rafters is on the optimal weight of portal frames. The results of these analyses were obtained for a range of heights of 4 m to 8 m and are represented in Figures 4.2 to 4.6 respectively. For each portal frame height, the span length were incrementally increased to investigate what effect the haunched rafters have on the weight of the frame depending of the span to height ratio.

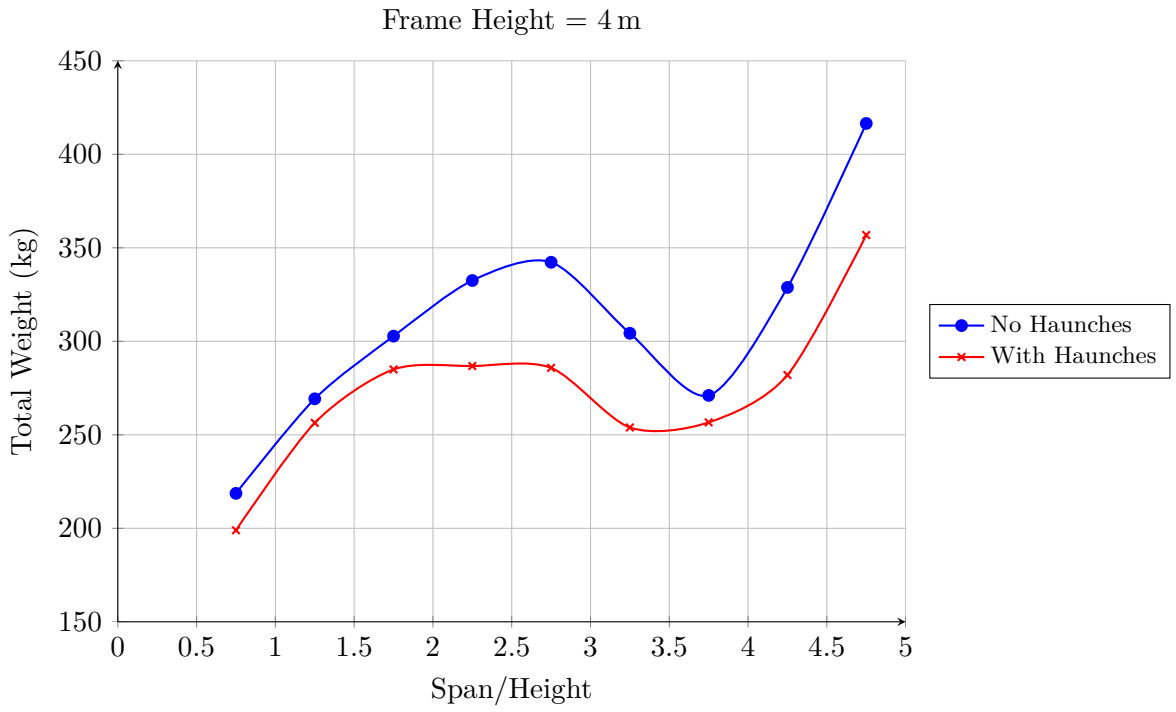

Figure 4.2: Representation of the effect of haunched-rafters on optimal weight of a portal frame with a fixed height of 4 m.

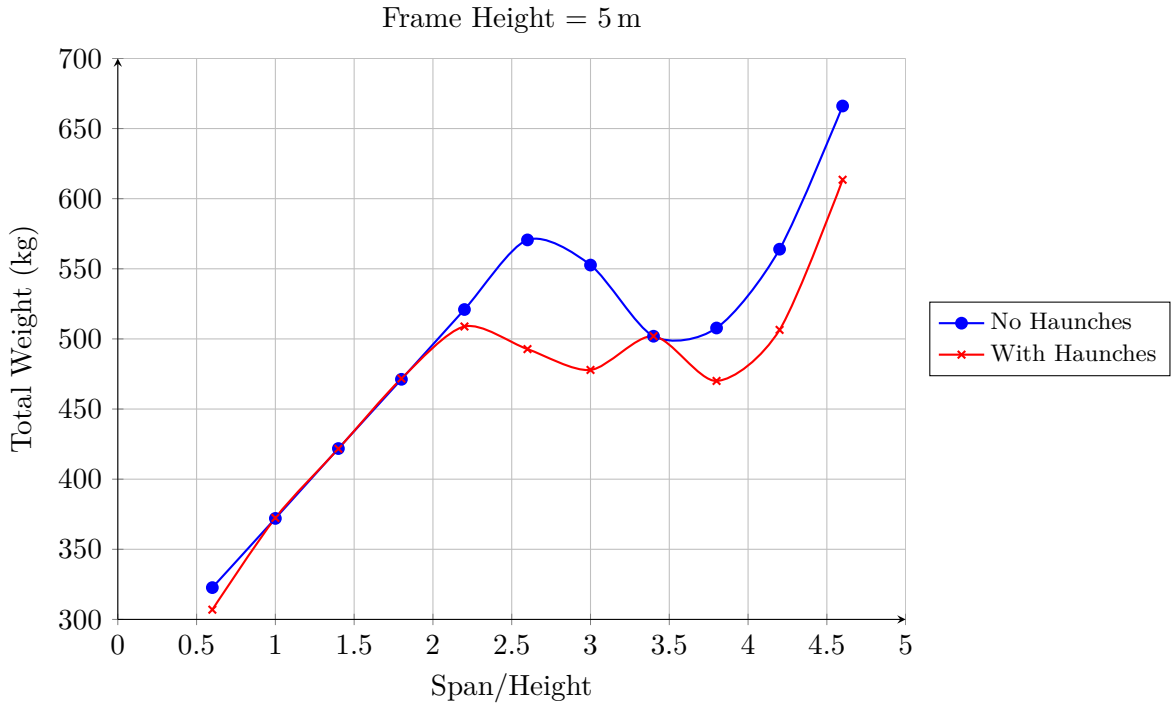

Figure 4.3: Representation of the effect of haunched-rafters on optimal weight of a portal frame with a fixed height of 5 m.

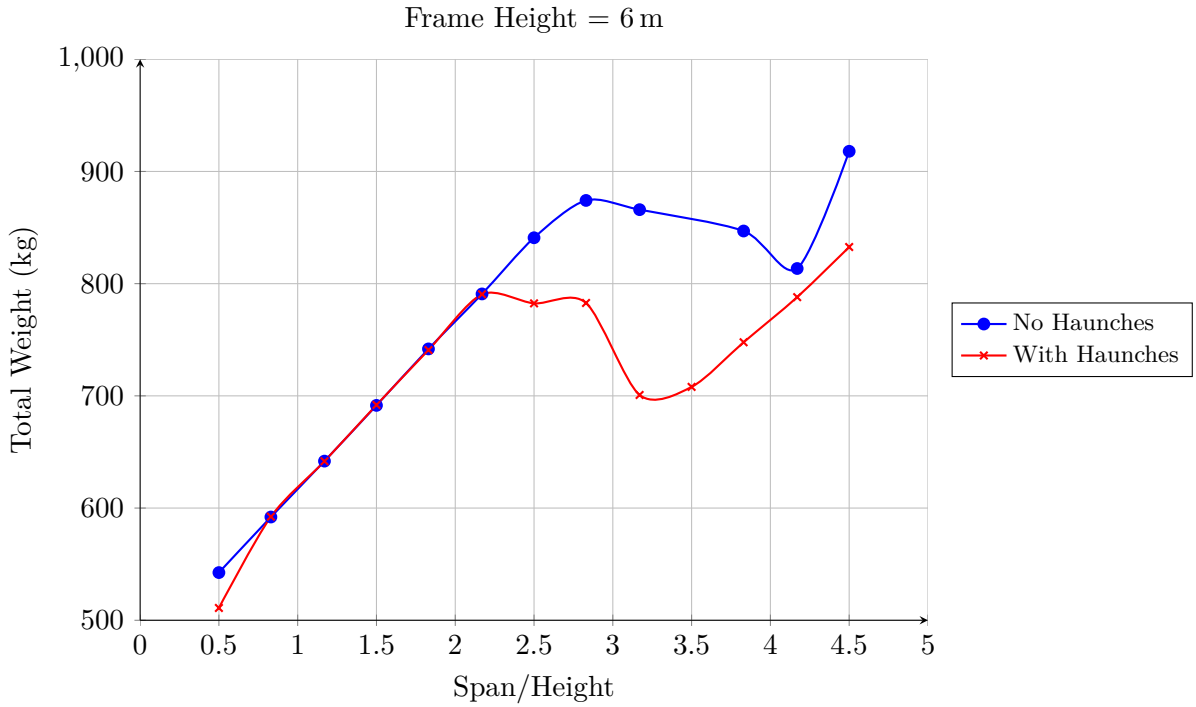

Figure 4.4: Representation of the effect of haunched-rafters on optimal weight of a portal frame with a fixed height of 6 m.

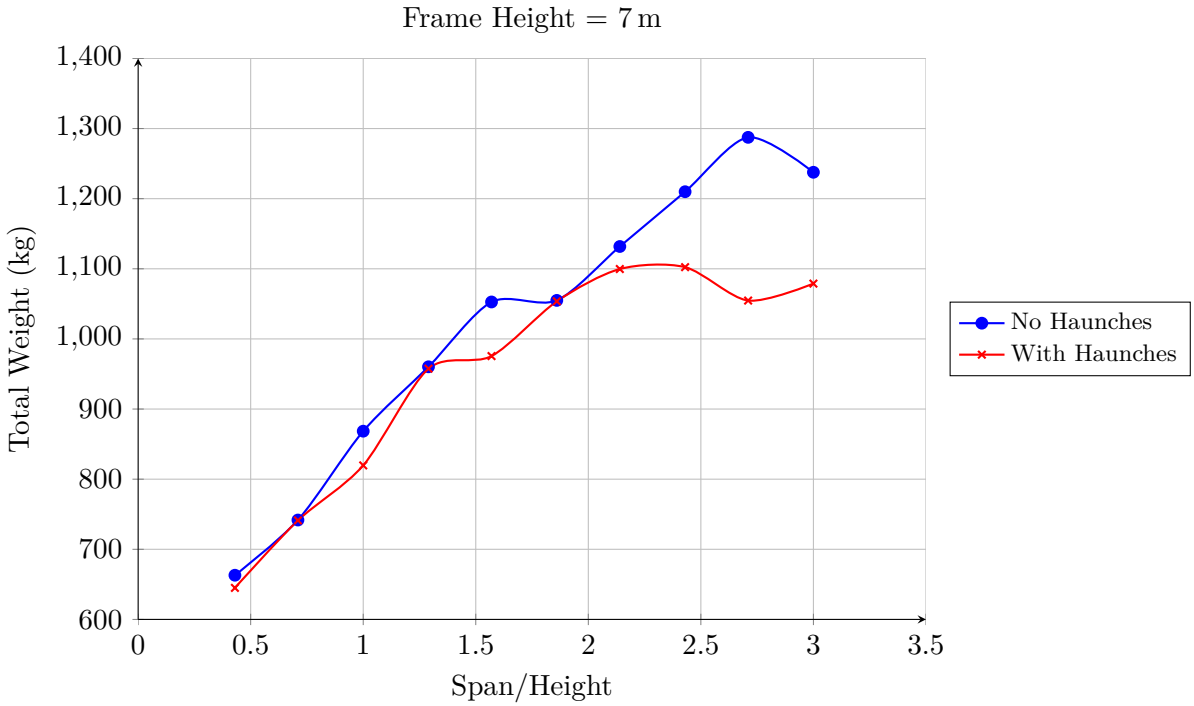

Figure 4.5: Representation of the effect of haunched-rafters on optimal weight of a portal frame with a fixed height of 7 m.

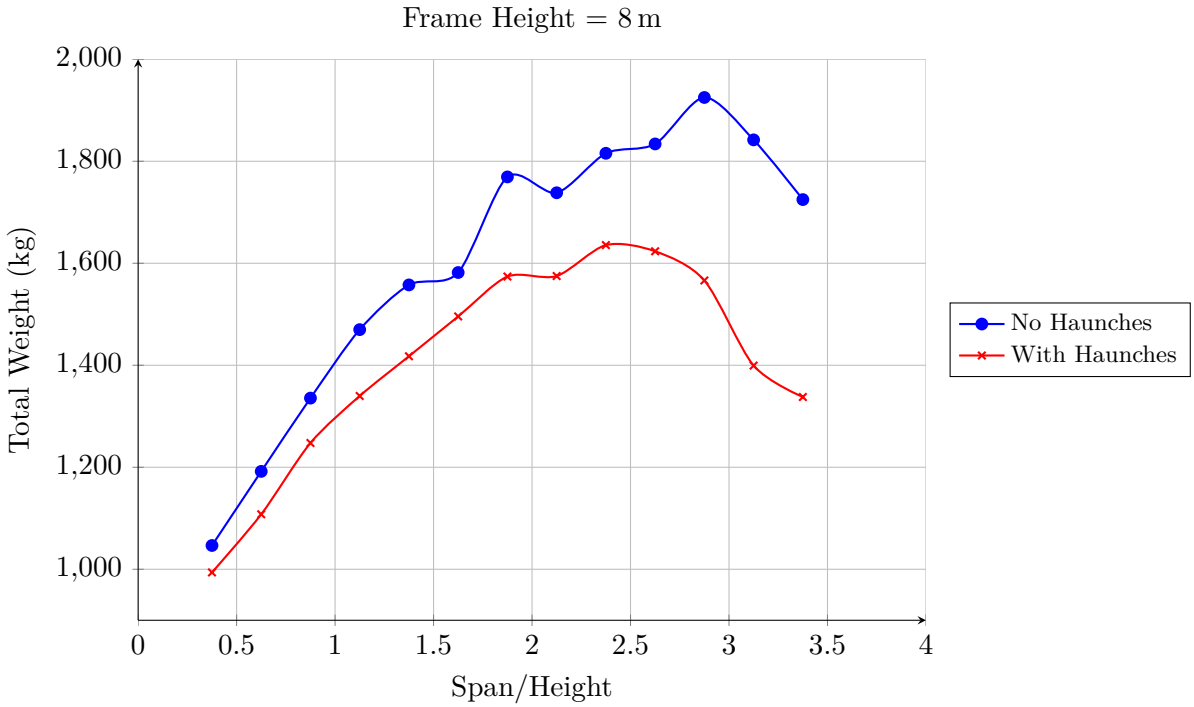

Figure 4.6: Representation of the effect of haunched-rafters on optimal weight of a portal frame with a fixed height of 8 m.

The results in Figures 4.2 to 4.6 indicate that the use of haunched rafters only have a significant effect on the optimal weight of a portal frame of span to height ratios larger than two. An overall average decrease in total weight of 9 % were obtained when haunched rafters were used while a 12 % average decrease in total weight are obtained for frames with a span to height ratio larger than two. This indicates that the use of haunched rafters may have a significant effect on weight, cost and economy of portal frame structures.

In terms of the optimal haunch length for a portal frame structure, it was not possible to establish a clear trend between the span and height of the portal frame and the optimal haunch length as the optimal length vary depending on the specific frame and can be anything from 0 - 10 percent of the span length for any frame. Even though a clear trend could not be established, it is worth mentioning that in some cases for larger span to height ratio frames, it was more economical in terms of frame weight to have a larger haunch and a smaller column size. This is discussed in more detail in Section 4.5. In order to obtain the optimal haunch length of a specific frame, a program similar to the Genetic Algorithm for this study has to be used.

4.3 Effect of Roof Pitch on Optimal Weight

During Genetic Algorithm simulations of different span to height ratio portal frames, it was observed that the roof pitch of a portal frame might have a significant influence on the optimal weight of the structure. It was decided that the Genetic Algorithm has to be altered in a way to specify the roof pitch of the portal frame instead of the roof pitch being a design variable being selected at random by the Genetic Algorithm as mentioned in Section 3.2.

With this functionality added to the Genetic Algorithm, a portal frame with a specified span and height could be analysed for a range of roof pitches. Table 4.1 contains the span and height values as well as figure references of four portal frames analysed for a range of roof pitches to evaluate the effect of the roof pitch on the optimal weight of portal frame structures.

Table 4.1: Effect of roof pitch on optimal weight analyses.

Analysis	**Span** (m)	**Height** (m)	**Span/Height**	**Figure Reference**
1	6	6	1.0	4.7
2	12	6	2.0	4.8
3	20	5	4.0	4.9
4	35	8	4.4	4.10

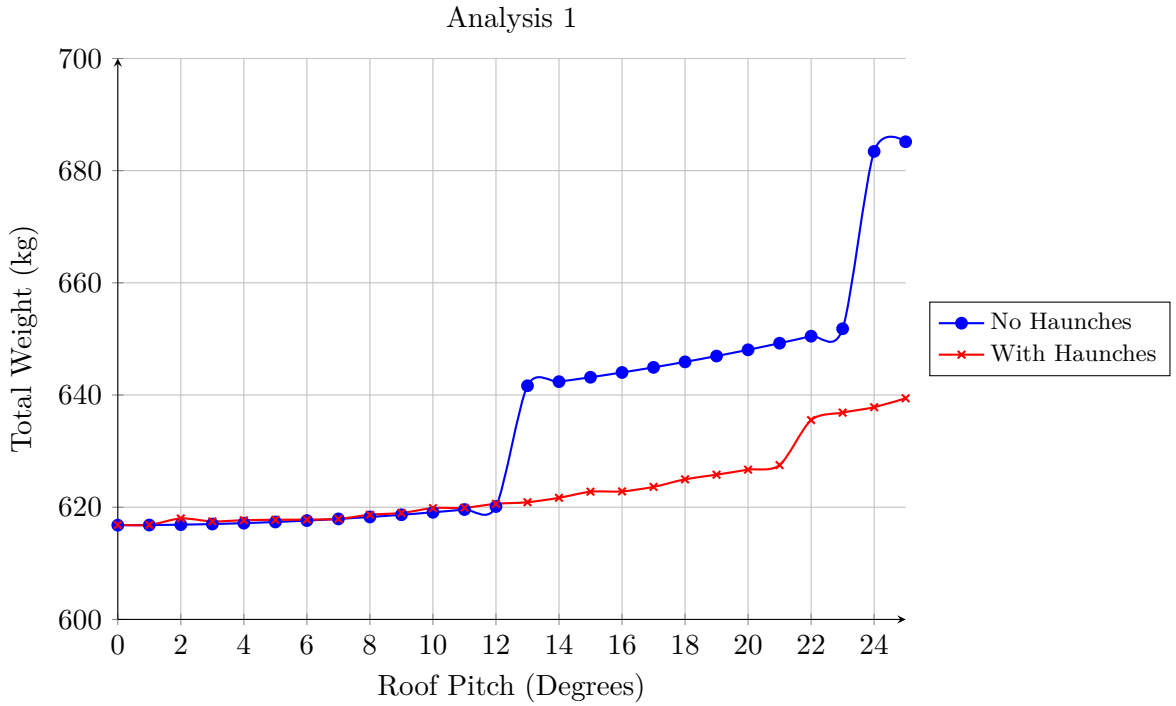

Figure 4.7: Effect of roof pitch on the optimal weight of a portal frame with a span of 6 m and a height of 6 m.

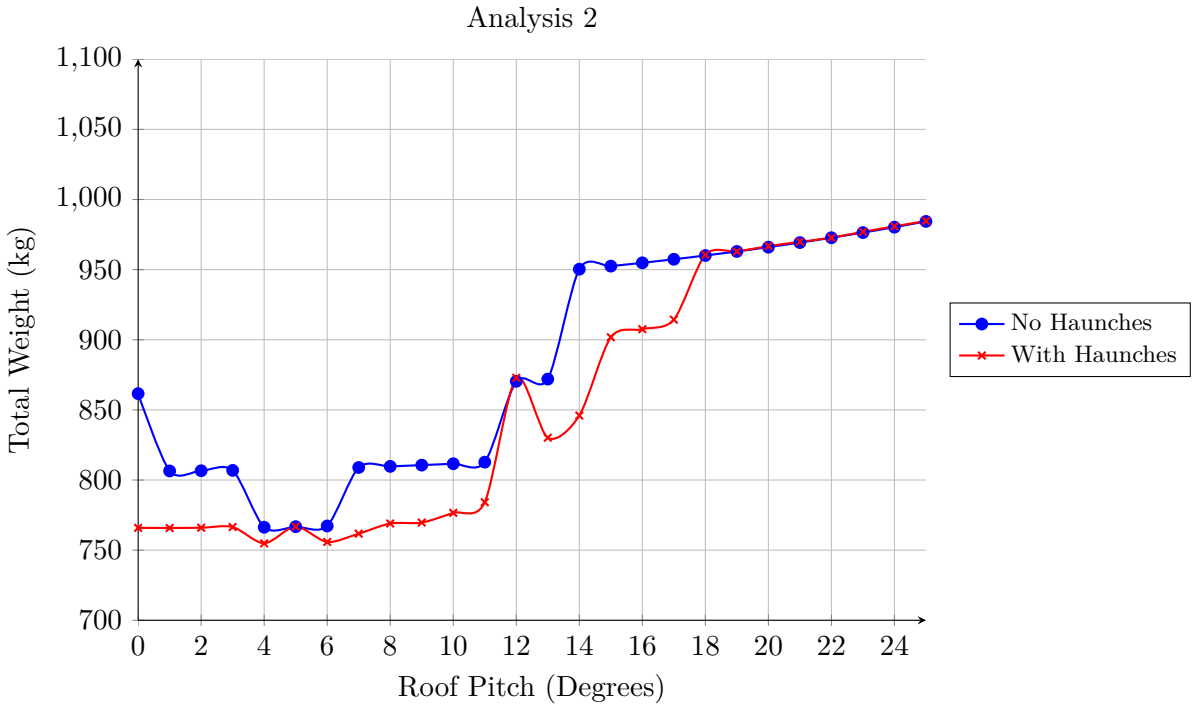

Figure 4.8: Effect of roof pitch on the optimal weight of a portal frame with a span of 12 m and a height of 6 m.

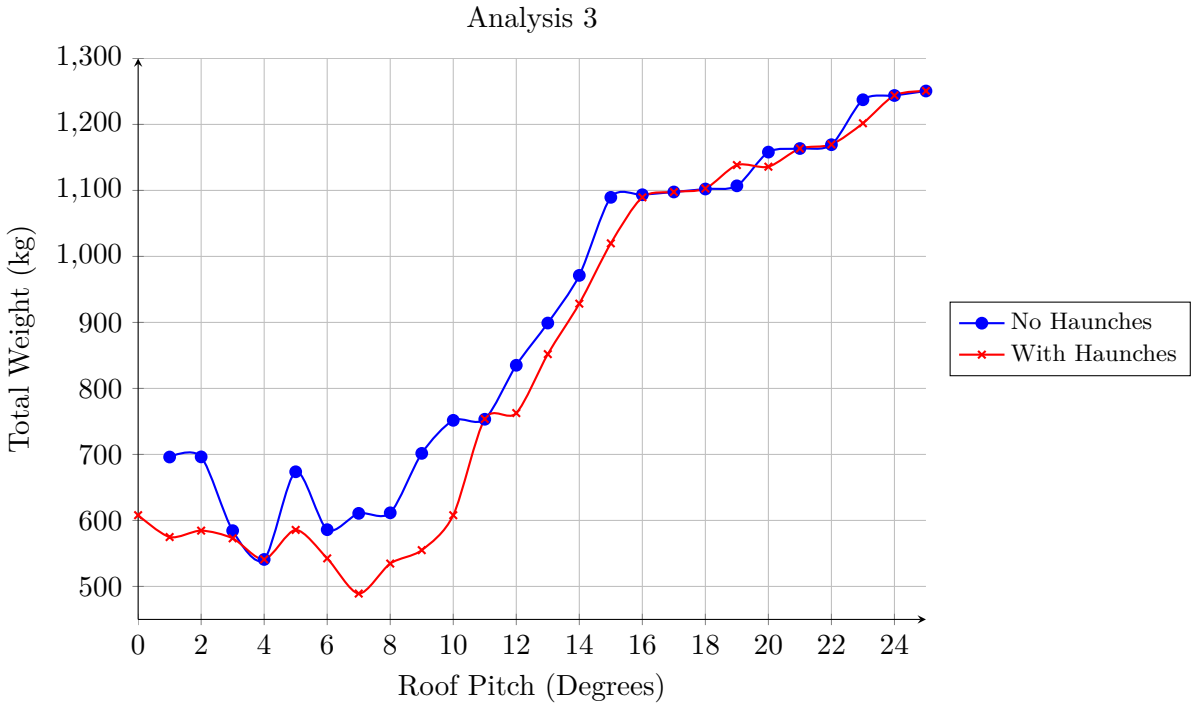

Figure 4.9: Effect of roof pitch on the optimal weight of a portal frame with a span of 20 m and a height of 5 m.

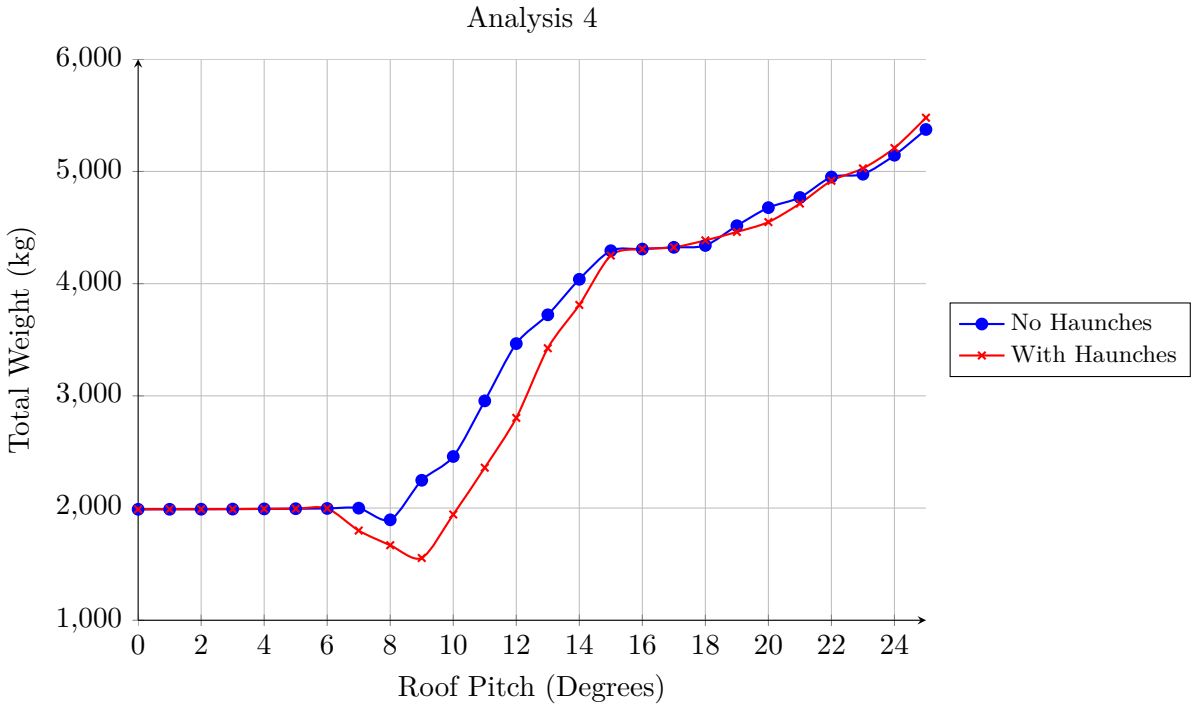

Figure 4.10: Effect of roof pitch on the optimal weight of a portal frame with a span of 35 m and a height of 8 m.

As expected due to the previous results, the roof pitch of a portal frame does indeed have a significant effect on the optimal weight. As seen from Figures 4.7 and 4.8, the roof pitch does not have a large influence for frames of a span to height ratio smaller than two. For larger span to height ratio frames as in Figures 4.9 and 4.10, the roof pitch has such a significant influence on the optimal weight that a 110% increase in weight occurs with a 6 degree increase in roof pitch from 8 degrees to 14 degrees in Figure 4.10.

All four analyses indicated that the roof pitch of portal frames has a negligible influence on the optimal weight for any roof pitch smaller than 8 degrees, with a sudden and drastic increase in weight as the roof pitch becomes larger than 8 degrees. This is of great importance during the design phase of a portal frame as the percentage increase in frame weight due to roof pitch drastically increases with larger span to height ratio frames.

4.4 Governing Limit State Function

From the results given in Section 4.2, an important observation was made about the governing limit state function during the design of portal frames. As the literature and general knowledge of structural design indicate, a portal frame is designed in accordance with the ultimate limit state and then evaluated to ensure compliance with the deflection limits of the serviceability limit state.

From a total of 119 portal frames of different span and height dimensions tested, a very large percentage of 87 % of the portal frames were governed by the serviceability limit state. 82 % of the tests conducted were governed by the horizontal deflection limit of height/200 which indicates that for the current deflection limits, it would be more appropriate to design a portal frame in accordance with the serviceability limit state and then evaluate the obtained frame for the ultimate limit state.

For a portal frame governed by ultimate limit state, the weakest member will be at its limit in terms of capacity. For the 87 % of frames governed by the serviceability limit state, there is an average of 51 % capacity in the weakest member still available for the ultimate limit state. This indicates that the deflections dominate the design of a portal frame at its optimal capacity in terms of ultimate and serviceability limit states. Table 4.2 contains the results of the governing limit state function for the 119 tests done.

Table 4.2: Governing limit state function

Height [m]	**Span** [m]	**ULS**	**SLS Vertical**	**SLS Horizontal**	**Total**	**% ULS**	**% SLS**
4	3 - 21	1	0	18	19	5.26	94.74
5	3 - 24	2	4	16	22	9.09	90.91
6	3 - 28	9	0	17	26	34.62	65.38
7	3 - 28	2	2	22	26	7.69	92.31
8	3 - 28	2	0	24	26	7.69	92.31
					119	**12.87**	**87.13**

4.5 Optimality of Portal Frames from Genetic Algorithm

For the purpose of calculating the reliability index of optimal portal frames, only frames at 99 % or more of its ultimate capacity either in terms of ultimate or serviceability limit state were deemed satisfying. The results obtained from the Genetic Algorithm for optimal portal frames proved that it was not always possible to find a frame at its ultimate capacity, therefore yielding a higher reliability due to reserve capacity and not being able to compare such a frame's reliability with a frame at its limit. In order to indicate and prove that the Genetic Algorithm obtains optimal frames when possible, a few results for the optimality calculations are given in Table 4.3 for a range of heights. All the results for all the frames analysed with the Genetic Algorithm are given in Appendix A.

From the results in Appendix A, an important observation was made about the column size of large span to height ratio portal frames. The results of frames ranging in heights of 4 m to 8 m as in Tables A1 to A5 respectively, clearly indicate that the design column size decrease slightly with an increase in the span length. Even though this is counter intuitive due to the fact that logical thinking would suggest that larger members would be used for larger frames, the following explains this occurrence.

From Table 4.3 it can be seen that the horizontal deflection is the governing limit state function for small span to height ratio frames while the vertical deflection or the ultimate limit state is generally the governing limit state function for larger span to height ratio frames. This trend caused the column size to be smaller when the horizontal deflection limit was not the governing limit state function due to extra capacity still available in terms of horizontal deflection. A smaller column can therefore be selected which could have significant cost advantages in terms of the entire structure.

Table 4.3: Optimal portal frame results from genetic algorithm

Span	**Height**	**S/H**	**Capacity Checks**					
[m]	[m]		**Column 1**	**Column 2**	**Rafter 1**	**Rafter 2**	VΔ	HΔ
4	4	1.00	0.235	0.322	0.204	0.252	0.037	0.999
5	4	1.25	0.214	0.324	0.146	0.196	0.030	0.993
12	4	3.00	0.035	0.543	0.174	0.546	0.275	0.999
13	4	3.25	0.093	0.581	0.304	0.801	0.595	0.992
20	4	5.00	0.402	0.773	0.469	0.757	0.628	0.996
21	4	5.25	0.465	0.819	0.611	0.866	0.808	0.995
4	5	0.80	0.256	0.319	0.334	0.378	0.049	0.997
6	5	1.20	0.184	0.242	0.292	0.339	0.056	0.999
10	5	2.00	0.104	0.252	0.210	0.446	0.076	0.999
19	5	3.80	0.288	0.914	0.420	0.905	1.000	0.641
20	5	4.00	0.396	0.931	0.495	0.949	0.995	0.903
21	5	4.20	0.419	0.934	0.530	0.952	0.999	0.954
4	6	0.67	0.262	0.384	0.144	0.194	0.018	0.990
18	6	3.00	0.023	0.434	0.245	0.913	0.391	0.999
19	6	3.17	0.059	0.531	0.290	0.948	0.521	0.993
20	6	3.33	0.089	0.551	0.344	0.999	0.694	0.990
24	6	4.00	0.290	0.746	0.454	0.990	0.811	0.716
25	6	4.17	0.346	0.786	0.537	0.998	0.916	0.665
7	7	1.00	0.255	0.350	0.210	0.259	0.034	0.996
8	7	1.14	0.238	0.334	0.196	0.254	0.035	0.989
9	7	1.29	0.180	0.258	0.272	0.357	0.052	0.999
22	7	3.14	0.050	0.443	0.314	0.990	0.584	0.823
24	7	3.43	0.176	0.842	0.404	0.994	0.909	0.903
28	7	4.00	0.305	0.983	0.446	0.907	0.986	0.797
6	8	0.75	0.245	0.326	0.237	0.288	0.036	1.000
7	8	0.88	0.219	0.278	0.301	0.346	0.045	0.997
17	8	2.13	0.118	0.314	0.142	0.348	0.056	0.999
18	8	2.25	0.103	0.322	0.124	0.354	0.067	0.999
27	8	3.38	0.117	0.644	0.344	0.992	0.622	0.782
28	8	3.50	0.149	0.666	0.376	0.997	0.717	0.581

The optimal haunch length for each portal frame could also have a significant effect on the column size. For larger span to height ratio frames, the results indicate that it would be more economical in terms of weight to make use of a larger haunch and a smaller column. A larger haunch length would increase stiffness at points of maximum moment and subsequently decrease frame deflections. Due to smaller obtained deflections, specifically horizontal deflections at the eaves, it might be possible to design the portal frame with a smaller column. This observation will have significant cost advantages when a portal frame is designed at its ultimate capacity where a smaller column could be used for large span to height ratio frames with haunched rafters.

In order to evaluate the correctness of the results obtained from the Genetic Algorithm, two frames governed by the ultimate and serviceability limit states respectively were selected and analysed with the use of a commercial finite element package called Prokon and hand calculations. These results were then compared to the results from the Genetic Algorithm. Table 4.4 indicate the dimensions and results from the Genetic Algorithm of the two frames selected.

Table 4.4: Portal frames dimensions for hand calculations

Span [m]	**Height** [m]	**S/H**	**Capacity Checks**					
			Column 1	**Column 2**	**Rafter 1**	**Rafter 2**	VΔ	HΔ
20	7	2.86	0.01	0.40	0.18	0.65	0.23	**1.00**
26	6	4.33	0.33	**0.93**	0.39	0.70	0.81	0.45

The first frame with a span to height ratio of 2.86 were governed by the serviceability limit state as can be seen from Table 4.4. This frame with the exact same loads as in the Genetic Algorithm was then analysed in Prokon to compare the deflections, reaction forces and moments obtained from Prokon with those calculated with the use of a linear finite element method in the Genetic Algorithm. The results for the Genetic Algorithm and Prokon analyses are given in Table 4.5.

Table 4.5: Deflection and reaction results from Genetic Algorithm and Prokon

		Prokon	
	GA	**Linear**	**Second Order**
VΔ [mm]	25.66	25.26	25.52
HΔ [mm]	34.97	34.77	35.48
$R1_x$ [kN]	20.98	20.98	21.09
$R1_y$ [kN]	3.24	3.24	3.35
$R2_x$ [kN]	9.15	9.15	9.03
$R2_y$ [kN]	30.45	30.45	30.57
M_{max} [kNm]	91.41	91.34	93.02

The results in Table 4.5 for deflections, reaction forces and maximum moments obtained from the linear finite element method programmed as part of the Genetic Algorithm is verified through

the comparison with the results obtained from Prokon. An important observation from the Prokon results is that there is no significant change in any of the results, given that a linear or second order finite element analysis were used. It was therefore concluded that a linear analysis is sufficient for the optimisation of portal frame structures with the use of the Genetic Algorithm.

The second frame mentioned in Table 4.4 had a span to height ratio of 4.33 and were governed by the ultimate limit state. The leeward column was the governing member during the design with a capacity check of 0.93. A hand calculation was done in accordance with SANS 10162-1:2011 to compare the results obtained from the Genetic Algorithm with the results from hand calculations.

A comparative value for Equations (3.7) and (3.8) of 0.934 obtained from hand calculations for the critical column is used to verify that the design calculations done during the Genetic Algorithm analysis are correct. The complete hand calculations for the critical column are given in Appendix B.

4.6 Reliability

With the Genetic Algorithm providing a portal frame of given dimensions at its optimal weight, the reliability indexes of each frame are calculated with the use of a First Order Reliability Method as discussed in Chapter 3.

For each optimal portal frame in Appendix A optimized with the use of the Genetic Algorithm, the reliability was calculated with respect to either the ultimate limit state or serviceability limit state depending on which limit state governed the design calculations. For frames governed by the ultimate limit state, a reliability index of $\beta = 3.0$ is acceptable in accordance with SANS 10160-1:2011 while a reliability index of $\beta = 2.0$ is acceptable for frames governed by the irreversible serviceability limit state.

4.6.1 Ultimate Limit State

Table 4.2 shows that only 13 % of the 119 frames optimized were governed by the ultimate limit state. For the calculation of the reliability index for frames governed by the ultimate limit state, it was mentioned that a series system is used by evaluating the reliability of the weakest member in the entire portal frame i.e. the member closest to its ultimate capacity. The weakest member from the analysis is obtained by selecting the member with its ultimate failure check from Equations (3.7) to (3.10) on page 54 closest to 1.00. The reliability of the entire frame is then given with respect to this weakest member.

On average a reliability index $\beta = 3.3$ was obtained for all the frames governed by the ultimate limit state at 99 % or more of its capacity which is higher than the required reliability index

of $\beta = 3.0$ in accordance with SANS 10160-1:2011 and therefore acceptable. It is important to note that the reliability index of all frames governed by the ultimate limit state were greater than the allowable $\beta = 3.0$.

In order to investigate the sensitivity of the different design variables on the reliability calculations with the First Order Reliability Method for the ultimate limit state, 7 optimal frames governed by the ultimate limit state for a range of heights were selected. Table 4.6 contains the span and height dimensions of the 7 selected frames.

Table 4.6: Span and height dimensions for ULS reliability investigation

Height = 6 m			Height = 7 m			Height = 8 m		
Analysis	Span [m]	S/H	**Analysis**	Span [m]	S/H	**Analysis**	Span [m]	S/H
1	20	3.33	**4**	22	3.14	**6**	27	3.38
2	22	3.67	**5**	24	3.43	**7**	28	3.50
3	24	4.00						

Tables 4.7, 4.8 and 4.9 contain the results for the sensitivity factors (α-values), final design point values in the standard space and standard normal space for all the design variables respectively.

Table 4.7 indicates that only the specified minimum yield stress f_y, the peak wind pressure q_p, and both the model uncertainty factors for moments in a frame M_{uK} and the beam bending moment capacity M_{rK} have an influence on the reliability of portal frames governed by the ultimate limit state. An important observation from the sensitivity factors in Table 4.7 is the fact that the peak wind pressure q_p dominates with a sensitivity factor of around 0.9 irrespective of the span or height of the portal frame.

As expected from initial results for the optimisation of portal frames, the α-values for both the model uncertainty factors of axial force in a frame and the column resistance are zero. This clearly indicates that the axial forces for portal frames due to wind forces is so small that it has no effect on the design or reliability of a portal frame structure. The reliability index values for each of the 7 frames tested, governed by the ultimate limit state, are given in Table 4.9.

Table 4.7: Sensitivity factors for design variables from ULS FORM analyses

Analysis	α_{f_y}	α_{q_p}	$\alpha_{C_{uK}}$	$\alpha_{M_{uK}}$	$\alpha_{C_{rK}}$	$\alpha_{M_{rK}}$	α_{Δ_K}	$\alpha_{V\Delta_{damage}}$	$\alpha_{H\Delta_{damage}}$
1	0.221	-0.916	0	-0.304	0	0.139	0	0	0
2	0.232	-0.908	0	-0.318	0	0.145	0	0	0
3	0.244	-0.897	0	-0.335	0	0.153	0	0	0
4	0.219	-0.918	0	-0.301	0	0.137	0	0	0
5	0.225	-0.913	0	-0.309	0	0.141	0	0	0
6	0.222	-0.915	0	-0.306	0	0.139	0	0	0
7	0.226	-0.913	0	-0.310	0	0.141	0	0	0

Table 4.8: Final design point values in standard space from ULS FORM analyses

Analysis	f_y [MPa]	q_p [kPa]	C_{uK}	M_{uK}	C_{rK}	M_{rK}	Δ_K	$V\Delta_{damage}$ [m]	$H\Delta_{damage}$ [m]
1	398.530	0.965	0.999	1.094	1.194	0.977	0.998	0.146	0.000
2	396.017	1.020	0.999	1.106	1.194	0.975	0.998	0.160	0.000
3	394.344	1.022	0.999	1.114	1.194	0.973	0.998	0.175	0.000
4	398.699	1.041	0.999	1.094	1.194	0.977	0.998	0.160	0.051
5	397.321	1.072	0.999	1.100	1.194	0.976	0.998	0.175	0.051
6	397.753	1.124	0.999	1.098	1.194	0.977	0.998	0.197	0.058
7	397.018	1.140	0.999	1.102	1.194	0.976	0.998	0.204	0.058

Table 4.9: Final design point values in standard **normal** space from ULS FORM analyses

Analysis	Z_{f_y}	Z_{q_p}	$Z_{C_{uK}}$	$Z_{M_{uK}}$	$Z_{C_{rK}}$	$Z_{M_{rK}}$	Z_{Δ_K}	$Z_{V\Delta_{damage}}$	$Z_{H\Delta_{damage}}$	β
1	-0.695	2.875	0	0.955	0	-0.435	0	0	0	3.138
2	-0.774	3.034	0	1.063	0	-0.484	0	0	0	3.342
3	-0.827	3.040	0	1.136	0	-0.517	0	0	0	3.389
4	-0.690	2.893	0	0.947	0	-0.431	0	0	0	3.151
5	-0.733	2.977	0	1.007	0	-0.458	0	0	0	3.260
6	-0.719	2.960	0	0.988	0	-0.450	0	0	0	3.234
7	-0.742	3.000	0	1.020	0	-0.464	0	0	0	3.288

4.6.2 Serviceability Limit State

The results of the reliability index for frames ranging from heights of 4 m to 8 m governed by horizontal deflection limits are graphically presented in Figures 4.11 to 4.15 respectively. The values in Figures 4.11 to 4.15 only represent the reliability index for frames with a horizontal deflection at 99% or more of the horizontal limit as it was not possible to optimize all possible frames to 99% of its limit due to the discrete nature of the section sizes available. The reliability analysis for each frame was done with a range of coefficient of variation values for the distribution of the horizontal damage deflection to indicate the effect of the coefficient of variation on the reliability index. A coefficient of variation of 0.45 was suggested by Ter Haar, Retief, and Dunaiski [45].

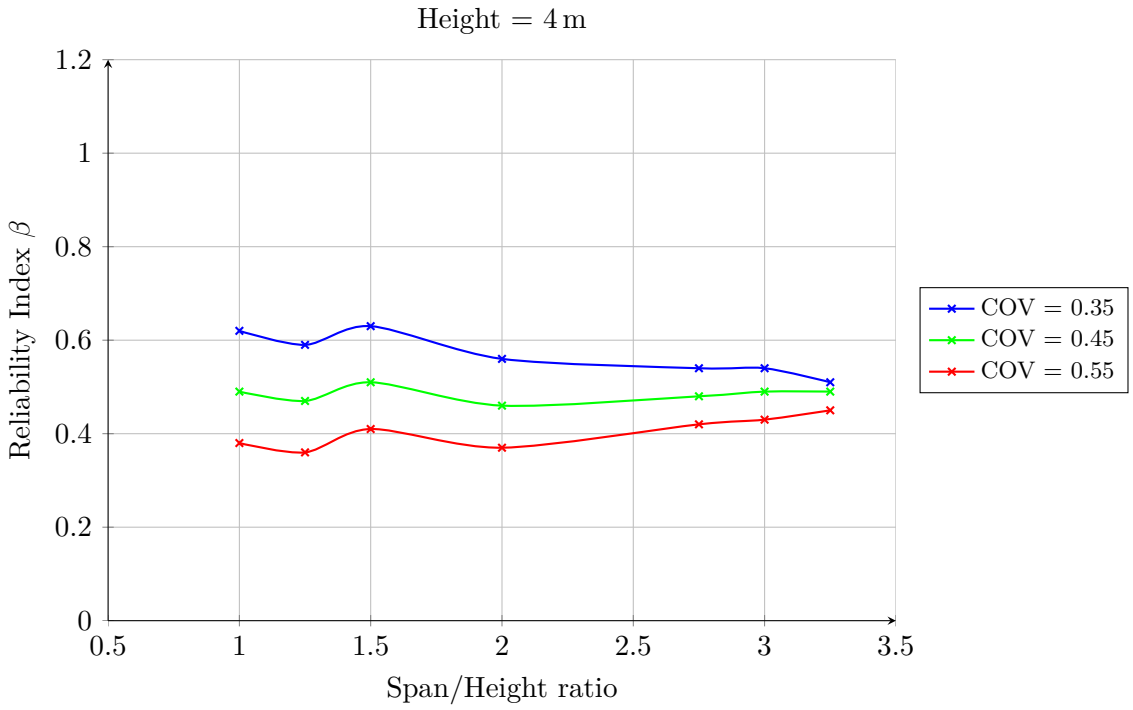

Figure 4.11: Reliability index β for frames with a height of 4 m governed by the horizontal deflection limit.

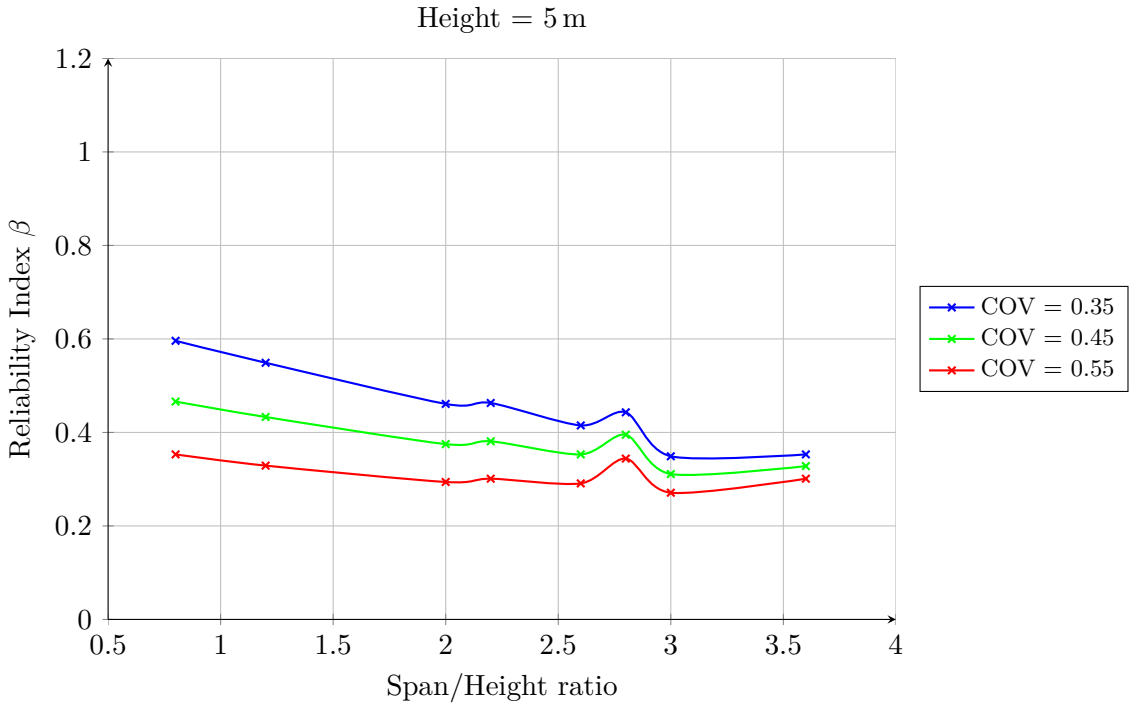

Figure 4.12: Reliability index β for frames with a height of 5 m governed by the horizontal deflection limit.

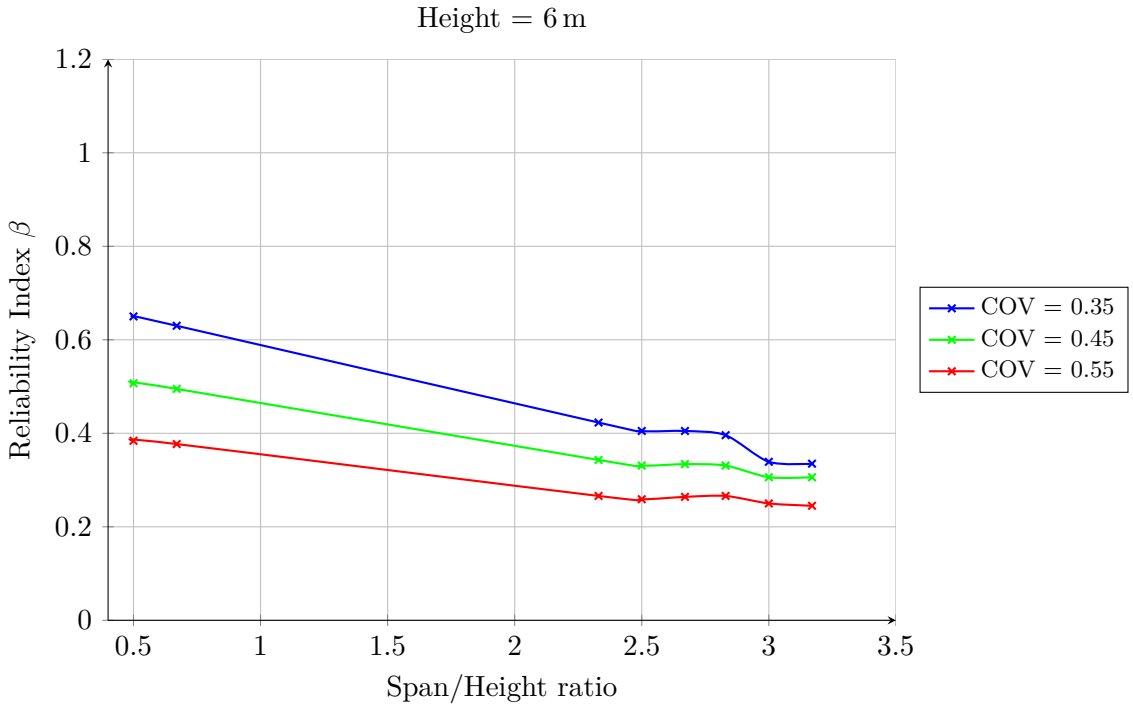

Figure 4.13: Reliability index β for frames with a height of 6 m governed by the horizontal deflection limit.

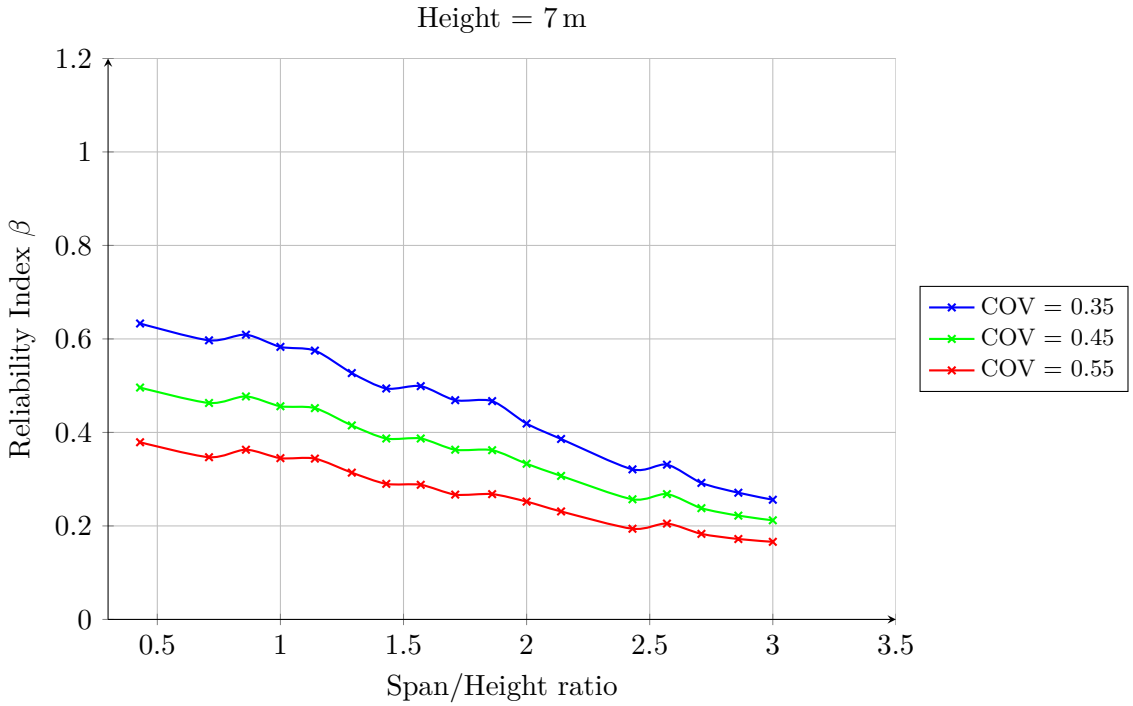

Figure 4.14: Reliability index β for frames with a height of 7 m governed by the horizontal deflection limit.

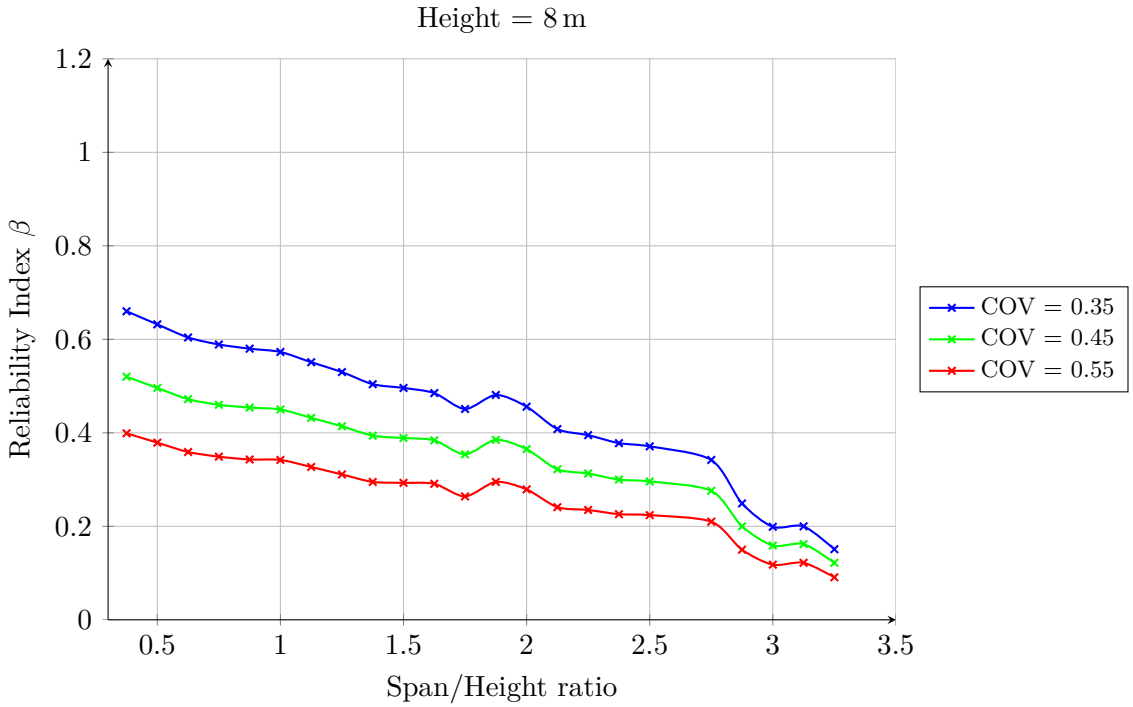

Figure 4.15: Reliability index β for frames with a height of 8 m governed by the horizontal deflection limit.

Figures 4.11 to 4.15 indicate a clear decline in reliability with an increase in span to height ratio

with some reliability index values for large span to height ratio frames being as low as 0.1 which are unacceptable. It is also evident that on average the reliability index of all the frames is far less than the allowable limit from SANS 10160-1:2011 of $\beta = 2$.

The representation of the reliability index for various frames of different heights indicate that for any height, the reliability index is fairly constant for a specific span to height ratio and the gradient of decline in reliability index with an increase in span to height ratio is more or less the same for any height. Some perturbations exist in Figures 4.11 to 4.15 which is caused by the fact that some frames governed by the serviceability limit state are at 99% of the allowable deflection limit while some are at 100% of the limit which has an influence on the reliability index.

This gave reason for investigating why there is a constant decrease in reliability index with an increase in span to height ratio of portal frames independent of the height of the frame.

4.6.2.1 Effect of span to height ratio on reliability

Following the observation about the similar decrease in reliability of portal frames of the same span to height ratios independent of the height of the frame, 8 frames were selected in order to investigate the sensitivity factors and final design points obtained from the First Order Reliability Method for each design variable. For the 8 frames selected, it was ensured that all 8 frames were at 99 % or more of its deflection limit to ensure accurate results and reliability index values to compare. It was mentioned above that not all frames could be optimized to 99 % of its limit due to the discrete nature of section sizes available. For this reason only frames of 7 m and 8 m heights were selected to ensure that a comparison of the reliability results can be made for frames with the same span to height for different heights. Table 4.10 contains the span and height dimensions of the 8 frames used.

Table 4.10: Span and height dimensions for SLS reliability investigation

Height = 7 m			Height = 8 m		
Analysis	Span [m]	S/H	**Analysis**	Span [m]	S/H
1	3	0.43	**5**	4	0.50
2	7	1.00	**6**	8	1.00
3	14	2.00	**7**	16	2.00
4	21	3.00	**8**	24	3.00

For each of the 8 analyses, the final sensitivity factors obtained from the First Order Reliability Method for the 9 design variables defined in Table 3.1 on page 57 are given in Table 4.11. The final design point values for the 9 design variables in the standard and standard normal space are tabulated in Tables 4.12 and 4.13 respectively.

From the results in Table 4.11, it is evident that the peak wind pressure q_p is dominating the design point calculation for larger span to height ratio frames. This dominating sensitivity factor indicates that the reliability index is greatly affected by any change in the peak wind pressure.

From Table 4.13, the design point value for damage deflections is approximately 0.37 standard deviations from the mean and this decreases rapidly for larger span to height ratio frames. This indicates that the only design variable that still has a significant effect on the reliability index for large span to height ratio frames is the peak wind pressure as was seen from the sensitivity factors in Table 4.11.

The design point values for each design variable in the standard normal space in Table 4.13 are used for the calculation of the reliability index β with the use of Equation (2.57) on page 36.

Table 4.11: Sensitivity factors for design variables from SLS FORM analyses

Analysis	α_{f_y}	α_{q_p}	$\alpha_{C_{uK}}$	$\alpha_{M_{uK}}$	$\alpha_{C_{rK}}$	$\alpha_{M_{rK}}$	α_{Δ_K}	$\alpha_{V\Delta_{damage}}$	$\alpha_{H\Delta_{damage}}$
1	0	-0.659	0	0	0	0	-0.133	0	0.740
2	0	-0.676	0	0	0	0	-0.130	0	0.726
3	0	-0.788	0	0	0	0	-0.109	0	0.606
4	0	-0.915	0	0	0	0	-0.071	0	0.396
5	0	-0.662	0	0	0	0	-0.132	0	0.738
6	0	-0.688	0	0	0	0	-0.128	0	0.714
7	0	-0.776	0	0	0	0	-0.111	0	0.621
8	0	-0.924	0	0	0	0	-0.067	0	0.375

Table 4.12: Final design point values in standard space from SLS FORM analyses

Analysis	f_y [MPa]	q_p [kPa]	C_{uK}	M_{uK}	C_{rK}	M_{rK}	Δ_K	$V\Delta_{damage}$ [m]	$H\Delta_{damage}$ [m]
1	421.273	0.430	0.999	0.995	1.194	0.999	1.002	0.022	0.044
2	421.273	0.428	0.999	0.995	1.194	0.999	1.002	0.051	0.044
3	421.273	0.421	0.999	0.995	1.194	0.999	1.000	0.102	0.047
4	421.273	0.411	0.999	0.995	1.194	0.999	0.999	0.153	0.049
5	421.273	0.454	0.999	0.995	1.194	0.999	1.002	0.029	0.050
6	421.273	0.452	0.999	0.995	1.194	0.999	1.002	0.058	0.051
7	421.273	0.447	0.999	0.995	1.194	0.999	1.000	0.117	0.053
8	421.273	0.427	0.999	0.995	1.194	0.999	0.998	0.175	0.057

Table 4.13: Final design point values in standard **normal** space from SLS FORM analyses

Analysis	Z_{f_y}	Z_{q_p}	$Z_{C_{uK}}$	$Z_{M_{uK}}$	$Z_{C_{rK}}$	$Z_{M_{rK}}$	Z_{Δ_K}	$Z_{V\Delta_{damage}}$	$Z_{H\Delta_{damage}}$	β
1	0	0.327	0	0	0	0	0.066	0	-0.368	0.496
2	0	0.308	0	0	0	0	0.059	0	-0.331	0.456
3	0	0.262	0	0	0	0	0.036	0	-0.202	0.333
4	0	0.194	0	0	0	0	0.015	0	-0.084	0.212
5	0	0.329	0	0	0	0	0.066	0	-0.366	0.496
6	0	0.310	0	0	0	0	0.058	0	-0.321	0.450
7	0	0.283	0	0	0	0	0.041	0	-0.226	0.365
8	0	0.147	0	0	0	0	0.011	0	-0.060	0.159

4.6.2.2 Sensitivity of deflection due to peak wind pressure

As mentioned in the previous section, the reliability index of a portal frame governed by the horizontal deflection limit is totally dominated by the peak wind pressure for large span to height ratio frames. It was clearly indicated in Table 4.11 that for span to height ratios larger than 3, the sensitivity factor for the peak wind pressure is greater than 0.9. This caused all other design variables to have little to no effect on the reliability. For this reason, it is important to establish why the deflection is so sensitive to the peak wind pressure.

For a fixed end cantilever column as in Figure 4.16 which is used as a simplistic model with a distributed load applied to it, the maximum deflection of the column is given as in Equation (4.1)

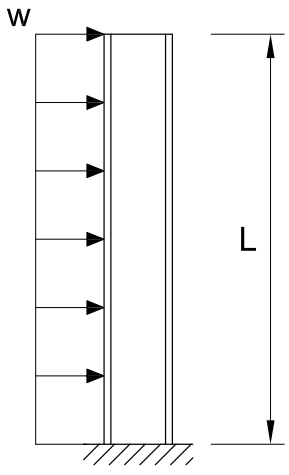

Figure 4.16: Representation of a cantilever column used as a simplistic model

$$\delta_{max} = \frac{\omega L^3}{8EI} \tag{4.1}$$

where

- δ_{max} is the maximum deflection,
- ω is the applied distributed load,
- L is the length of the beam,
- E is the modulus of elasticity, and
- I is the second moment of inertia.

From the deflection equation for a cantilever column, it is clear the the length of the beam has a great influence of the deflection as the length of the column is to the power of three. The applied distributed load ω is dependent on the peak wind pressure q_p and the internal and external pressure coefficients as in Equations (3.1) and (3.2) as per SANS 10160-3:2011. An increase in height would therefore result in an greater peak wind pressure and subsequently a greater applied distributed load. With an increase in the applied distributed load and length of the column, it is therefore evident that larger deflections are obtained for higher frames subjected to the same wind speed. Even though the use of a simplistic cantilever column is far from the more complex configuration of a portal frame with several degrees of freedom, it is evident that for a portal frame structure, the height of the structure will have a great influence on the deflection of that frame. For this reason the large sensitivity factor of the peak wind pressure may explain the decrease in the reliability index for larger span to height ratio frames.

From a logical point of view it is also very likely that a larger span to height ratio frame has a larger surface area on which the peak wind pressure act. Hence will this result in a larger total load on the structure and a greater possibility of the frame deflection being greater than the damage deflection. This will therefore result in a larger probability of failure and lower reliability index β.

Even though this explains why the reliability index for portal frames decrease with an increase in span to height ratio, the magnitude of the reliability index values for all span to height ratio portal frames, governed by the serviceability limit state and more specifically the horizontal deflection, is much lower than the target reliability index of $\beta = 1.0$ specified in SANS 10160-1:2011 [35].

Chapter 5

Conclusions and Recommendations

The main objective of this study was to investigate the reliability index of optimal portal frames and compare the obtained reliability index values with target reliability values accepted in SANS 10160:1-2011 [35].

A Genetic Algorithm was used to obtain an optimal portal frame and therefore the efficiency of using a Genetic Algorithm was investigated. This Genetic Algorithm was also programmed in such a manner that the effect of haunched rafters and roof pitch on the optimal weight of a portal frame could be investigated. The conclusions made from the results obtained in this study are given below.

5.1 Genetic Algorithms

In Section 2.5.2 it was shown that there is 28.83×10^6 number of possible solutions for a single portal frame with a span of 30 m given that the member sizes, haunch length and roof pitch are design variables. If every single solution from this population of possible solutions were to be analysed separately with the same linear finite element method and design section used in the Genetic Algorithm, it would take approximately 560 hours to find the optimal solution. With the use of the Genetic Algorithm programmed in JAVA for this study, it took only 1.67 hours to find the optimal solution for exactly the same portal frame with the same number of elements. It is therefore concluded that the use of Genetic Algorithms or some other similar searching method is the only realistic possible way of finding an optimal solution.

Even though only four design variables were used to characterise an optimal portal frame in this study, there are still a significant number of solutions and this number of design variables would rapidly increase for multi-storey buildings and result in a much larger population of possible solutions.

5.2 Optimal Portal Frames

The Genetic Algorithm was also used to investigate the effect of haunched rafters and roof pitch on the optimal weight of a portal frame. The conclusions made for the use of haunched rafters and the optimal roof pitch of a portal frame are given below.

5.2.1 Haunched Rafters

In Section 4.2 it was mentioned that haunched rafters don't have a significant effect on the weight of portal frames with a span to height ratio smaller than two. For frames with a span to height ratio larger than two, an average of 12 % decrease in total weight were obtained which indicates that the correct selection of the haunch length for a specific frame could have significant weight and financial advantages. Even though these haunched rafters had a significant effect on the optimal weight of the frames, it was not possible to establish a clear trend between the haunch length and the span and height of optimal frames as this length varied depending on the frame being analysed. However, in some cases the for large span to height ratio frames, it was more economical in terms of weight to make use of a larger haunch length which would result in a smaller column size due to increased stiffness at points of maximum moment and subsequently smaller horizontal deflections. This is clearly seen from the results for all the tests documented in Appendix A.

5.2.2 Roof Pitch

Section 4.3 presents the data on the effect of roof pitch on the optimal weight of portal frames. From Figure 4.7 to 4.10 it is clear that a roof pitch of less than eight degrees for steel portal frames does not have a significant effect on the optimal weight of the frame. The data clearly indicates that a significant and drastic increase in frame weight can occur when a roof pitch of more than eight degrees is used.

These results also indicate that the roof pitch has a much greater effect on the optimal weight of a portal frame for larger spans. Even though most portal frames have a small roof pitch in practise, it is evident that attention has to be given when a larger roof pitch is necessary.

5.2.3 Governing Limit State Function

From the 119 analyses of different span to height ratio frames, a significant 87 % of frames were governed by the serviceability limit state. In Section 2.5.1 it was mentioned that the structural dimensions and proportions of a portal frame are determined according to the ultimate limit state design criteria followed by a comparison of obtained deflections to maximum deflection limits due to statically applied live load and wind loads [13].

This indicates that the general method of designing a portal frame with respect to the ultimate limit state and then evaluating serviceability limits is inaccurate and it would be more appropriate to firstly design a portal frame in accordance with the serviceability limit state and then check for ultimate limit state criteria. From these 119 analyses, 82 % of the frames were more specifically governed by the horizontal deflection serviceability limit state. This indicate that these deflection limits which have no clear origin and are mainly based on experience, should be thoroughly investigated.

5.3 Reliability

Following the results obtained from the Genetic Algorithm for frames of a wide range of span and height dimensions, those frames for which it was possible to obtain a solution at more than 99 % of its ultimate capacity either in terms of ultimate or serviceability limit states could be analysed with a non-linear Newton Raphson First Order Reliability Method in order to obtain the reliability of optimal frames.

5.3.1 Ultimate Limit State

Frames governed by the ultimate limit state had an average reliability index of $\beta = 3.3$ as obtained in Chapter 4. According to SANS 10160-1:2011, an ultimate limit state reliability index of $\beta = 3.0$ is acceptable and therefore the conclusion can be made that the reliability index for frames governed by the ultimate limit state is within the acceptable limit. This also indicates that model uncertainty factors and loading partial factors for the ultimate limit state are accurate in terms of reliability.

5.3.2 Serviceability Limit State

The serviceability limit state and more specifically the horizontal deflection limit was the governing limit state function for 82 % of the 119 frames of different span and height ratios tested. Of these 82 % of frames, only the frames at more than 99 % of its deflection limit were selected and analysed with the First Order Reliability Method to obtain the reliability index for optimal frames governed by the serviceability limit state. Following the results in Chapter 4 for the reliability of portal frames, it is concluded that the obtained reliability for steel portal frames governed by the horizontal deflection limit are far less than the allowable reliability index for irreversible deflections in SANS 10160-1:2011 of $\beta = 2.0$.

Figures 4.11 to 4.15 proved that there is a constant decline in reliability index with an increase in span to height ratio of portal frames. Following an investigation into the cause of this constant decline, it is concluded that the peak wind pressure is dominating the reliability calculations

and increases in dominance with a larger span to height ratio due to the sensitivity of deflection with respect to span length as was mentioned in Section 4.6.2.

The conclusion is therefore that the only way to increase the reliability index for optimal portal frames governed by the horizontal serviceability limit state is by increasing the partial factor for wind loads due to the extreme dominance of the peak wind pressure. Another possibility is to decrease the design horizontal deflection limit of height/200 to lower the possibility of an optimal frame reaching the damage deflection of height/230 as determined by Ter Haar, Retief, and Dunaiski [45].

5.4 Recommendations for Further Studies

With the use of a non-linear Newton Raphson First Order Reliability Method, the reliability of portal frames governed by the ultimate limit state was determined with respect to a series system i.e. for system reliability where the reliability of the entire frame is dependent on the reliability of the weakest member. It is recommended for further studies to investigate the effect of using a parallel system or even a hybrid system on the reliability of optimal portal frames.

For the calculation of deflections, reaction forces and member forces, an elastic linear finite element analysis was programmed in JAVA as part of the Genetic Algorithm. It is strongly recommended to investigate what the difference in results in terms of optimal design and reliability of portal frames are when a more advanced plastic analysis is used for the calculation of deflections and reaction forces.

The use of Genetic Algorithms proved very useful in terms of reducing calculation time to obtain an optimal solution for portal frame structures. A further study can be done to extend this Genetic Algorithm with its built-in finite element analysis, wind loading calculations, First Order Reliability Method and design calculations for the analysis of multi-storey buildings or other frame structures. It is also recommended to improve on the simplification of using a single load case to limit the scope of this study by optimizing steel portal frames for multiple load cases.

A full and thorough investigation has to be done to determine what changes have to be made in terms of wind loading partial factors and model uncertainty factors to ensure a reliability index higher than the target SANS 10160-1:2011 limit of $\beta = 2.0$ is obtained for an optimal portal frame governed by the irreversible serviceability limit state. By changing either the horizontal deflection limits or the wind load partial factor $\gamma = 0.6$ for irreversible serviceability loads, the reliability index for frames governed by serviceability should be improved to attain the target $\beta = 2.0$.

References

[1] AA Adewuya. "New methods in genetic search with real-valued chromosomes". PhD thesis. Massachusetts Institute of Technology, 1996.

[2] AHS Ang and WH Tang. *Probability concepts in engineering planning and design*. Wiley, 2007.

[3] NA Barricelli. "Numerical testing of evolution theories". In: *Acta Biotheoretica* 16.1-2 (1962), pp. 69–98.

[4] P Bjerager. "On Computation Methods for Structural Reliability Analysis". In: *Structural Safety* 9 (1990), pp. 76–96.

[5] Charles Camp, Shahram Pezeshk, and Guozhong Cao. "Optimized design of two-dimensional structures using a genetic algorithm". In: *Journal of structural engineering* 124.5 (1998), pp. 551–559.

[6] L Castro, L Chong, and PW Partridge. "Minimum weight design of framed structures using a genetic algorithm considering dynamic analiysis". In: *Latin American Journal of Solids and Structures* 3.2 (2006), pp. 107–123.

[7] DA Coley. *An introduction to genetic algorithms for scientists and engineers*. Vol. 31. World scientific Singapore, 1999.

[8] RD Cook. *Concepts and applications of finite element analysis*. John Wiley & Sons, 2007.

[9] ES Croce et al. "A genetic algorithm for structural optimization of steel truss roofs". In: *XXV CILAMCE, 25th Iberian Latin-American Congress on Computational Methods in Engineering, UFPE, Recife, PE, Brasil*. 2004.

[10] O Ditlevsen and P Bjerager. "Methods of structural system reliability". In: *Structural Safety* 3(3) (1986), pp. 195–229.

[11] B Fiessler, R Rackwitz, and HJ Neumann. "Quadratic limit states in structural reliability". In: *Journal of the Engineering Mechanics Division* 105 (1979), pp. 661–676.

[12] AM Freudenthal. "Safety and the Probability of Structural Failure". In: *American Society of Civil Engineers Transactions* (1983).

[13] TV Galambos and B Ellingwood. "Serviceability limit states: deflection". In: *Journal of Structural Engineering* 112.1 (1986), pp. 67–84.

[14] DE Goldberg. "Genetic algorithms in search, optimization, and machine learning". In: *Addion wesley* 1989 (1989).

[15] A Haldar and S Mahadevan. *Reliability assessment using stochastic finite element analysis*. John Wiley & Sons, 2000.

[16] AM Hasofer and NC Lind. "Exact and invariant second-moment code format". In: *Journal of the Engineering Mechanics Division* 100.1 (1974), pp. 111–121.

[17] M Holicky. "Reliability Analysis for Structural Design". In: *SUN Media, Stellenbosch* 1 (1986).

[18] JH Holland. "Genetic algorithms". In: *Scientific american* 267.1 (1992), pp. 66–72.

[19] M. Hultman. "Weight optimization of steel trusses by a genetic algorithm." In: *Department of Structural Engineering. Lund University* (2010).

[20] WM Jenkins. "Towards structural optimization via the genetic algorithm". In: *Computers & Structures* 40.5 (1991), pp. 1321–1327.

[21] J.A. Joines and C.R. Houck. "On the use of non-stationary penalty functions to solve nonlinear constrained optimization problems with GA's." In: *Evolutionary Computation, 1994. IEEE World Congress on Computational Intelligence., Proceedings of the First IEEE Conference on*. IEEE. 1994, pp. 579–584.

[22] Anders Klarbring. *An introduction to structural optimization*. Vol. 153. Springer, 2008.

[23] N.D. Lagaros, M. Papadrakakis, and G. Kokossalakis. "Structural optimization using evolutionary algorithms." In: *Computers & structures* 80.7 (2002), pp. 571–589.

[24] M. Mitchell. *An introduction to genetic algorithms*. MIT press, 1998.

[25] A.S. Nowak and K.R. Collins. *Reliability of structures*. CRC Press, 2012.

[26] Manolis Papadrakakis, Nikos D Lagaros, and Yiannis Tsompanakis. "Structural optimization using evolution strategies and neural networks". In: *Computer methods in applied mechanics and engineering* 156.1 (1998), pp. 309–333.

[27] S. Park et al. "Efficient method for calculation of system reliability of a complex structure". In: *International journal of Solids and Structures* 41.18 (2004), pp. 5035–5050.

[28] S Pezeshk, CV Camp, and D Chen. "Design of nonlinear framed structures using genetic optimization". In: *Journal of Structural Engineering* 126.3 (2000), pp. 382–388.

[29] D.T. Phan et al. "Effect of serviceability limits on optimal design of steel portal frames." In: *Journal of Constructional Steel Research* 86 (2013), pp. 74–84.

[30] W Prager and JE Taylor. "Problems of optimal structural design". In: *Journal of Applied Mechanics* 35.1 (1968), pp. 102–106.

[31] R. Rackwitz and B. Fiessler. "Structural reliability under combined random load sequence.s". In: *Computers & Structures* 9.5 (1978), pp. 489–494.

[32] H Rahami, A Kaveh, and Y Gholipour. "Sizing, geometry and topology optimization of trusses via force method and genetic algorithm". In: *Engineering Structures* 30.9 (2008), pp. 2360–2369.

[33] S Rajeev and CS Krishnamoorthy. "Discrete optimization of structures using genetic algorithms". In: *Journal of structural engineering* (1992).

[34] S.S. Rao. *Reliability-based design*. McGraw-Hill Companies, 1992.

[35] SABS. "Basis of structural design and actions for buildings and industrial structures, Part 1:Basis of structural design." In: *SANS 10160* 1 (2011).

[36] SABS. "Basis of structural design and actions for buildings and industrial structures, Part 3:Wind actions." In: *SANS 10160* 3 (2011).

[37] SABS. "The structural use of steel, Part 1: Limit-states design of hot-rolled steelwork." In: *SANS 10162* 1 (2011).

[38] SAICE. *South African Steel Construction Handbook*. SAICE, 2013.

[39] M.P. Saka. "Optimum design of pitched roof steel frames with haunched rafters by genetic algorithm." In: *Computers & structures* 81.18 (2003), pp. 1967–1978.

[40] LA Schmit and M Hirokazu. "Approximation concepts for efficient structural synthesis". In: (1976).

[41] Lucien A Schmit. "Structural design by systematic synthesis". In: *Proc. of the Second ASCE Conference on Electronic Computation*. 1960, pp. 105–122.

[42] AJG Schoofs. "Structural optimization history and state-of-the-art". In: *Topics in Applied Mechanics*. Springer, 1993, pp. 339–345.

[43] M. Shinozuka. "Basic analysis of structural safety." In: *Journal of Structural Engineering* 109(3) (1983), pp. 721–740.

[44] J Sobieszczanski and D Loendorf. "A mixed optimization method for automated design of fuselage structures". In: *Journal of Aircraft* 9.12 (1972), pp. 805–811.

[45] TR Ter Haar, JV Retief, and PE Dunaiski. "Towards a more rational approach of the serviceability limit states design of industrial steel structures". In: *2end World conference on steel in construction*. 1998.

[46] Garret N Vanderplaats. "Thirty years of modern structural optimization". In: *Advances in Engineering Software* 16.2 (1993), pp. 81–88.

[47] VB Venkayya, NS Khot, and VS Reddy. *Optimization of structures based on the study of energy distribution*. Tech. rep. DTIC Document, 1968.

[48] S.T. Woolcock and S. Kitipornchai. "Survey of deflection limits for portal frames in Australia." In: *Journal of Constructional Steel Research* 7.6 (1987), pp. 399–417.

[49] A.H. Wright. "Genetic algorithms for real parameter optimization." In: *FOGA*. Citeseer. 1990, pp. 205–218.

[50] Y.G. Zhao and T. Ono. "A General Procedure for First/Second-Order Reliability Method (FORM/SORM)." In: *Structural Safety* 21 (1999), pp. 95–112.

Appendices

Appendix A

Optimization Results from Genetic Algorithm

Tables A1 to A5 include all the results obtained from the Genetic Algorithm for a range of portal frames. These results indicate the span and height of each portal frame as well as the four design variables and total weight of a single optimal frame with pinned bases. The design variables indicate which column size, rafter size, haunch length and roof pitch are to be used for each frame to ensure that the frame is at its ultimate capacity depending on the governing limit state function. These frames were then used to obtain a first order reliability index for each optimal portal frame.

Table A1: Results from genetic algorithm for frames with height of 4 m

Span [m]	**Height** [m]	**S/H**	**Column**	**Rafter**	**Haunch Length** [mm]	**Pitch** [deg]	**Total Weight** [kg]
3	4	0.75	$IPE_{AA}200$	$IPE_{AA}200$	40	6	198.945
4	4	1.00	$IPE_{AA}200$	$IPE_{AA}200$	360	6	222.859
5	4	1.25	$IPE_{AA}200$	$IPE200$	20	3	256.400
6	4	1.50	$IPE_{AA}200$	$IPE_{AA}200$	0	7	252.829
7	4	1.75	$305 \times 102 \times 25$	$IPE_{AA}160$	30	3	284.963
8	4	2.00	$IPE_{AA}200$	$IPE_{AA}180$	710	4	273.951
9	4	2.25	$IPE_{AA}200$	$IPE_{AA}180$	540	6	286.780
10	4	2.50	$IPE_{AA}200$	$IPE_{AA}180$	30	5	293.912
11	4	2.75	$IPE_{AA}200$	$IPE_{AA}160$	510	4	285.793
12	4	3.00	$IPE_{AA}180$	$IPE_{AA}160$	1050	4	279.977
13	4	3.25	$IPE_{AA}180$	$IPE_{AA}140$	310	4	253.921
14	4	3.50	$IPE_{AA}160$	$IPE_{AA}140$	380	4	243.963
15	4	3.75	$IPE_{AA}160$	$IPE_{AA}140$	560	7	256.643
16	4	4.00	$IPE_{AA}160$	$IPE_{AA}140$	610	8	267.678
17	4	4.25	$IPE_{AA}160$	$IPE_{AA}140$	970	9	281.997
18	4	4.50	$IPE_{AA}160$	$IPE_{AA}160$	330	9	326.520
19	4	4.75	$IPE_{AA}180$	$IPE_{AA}160$	30	10	356.837
20	4	5.00	$IPE_{AA}180$	$IPE_{AA}160$	1560	11	388.931
21	4	5.25	$IPE_{AA}180$	$IPE_{AA}160$	900	11	393.331

Table A2: Results from genetic algorithm for frames with height of 5 m

Span [m]	**Height** [m]	**S/H**	**Column**	**Rafter**	**Haunch Length** [mm]	**Pitch** [deg]	**Total Weight** [kg]
3	5	0.60	$305 \times 102 \times 25$	$IPE_{AA}200$	280	2	306.947
4	5	0.80	$305 \times 102 \times 25$	$IPE200$	390	2	346.234
5	5	1.00	$305 \times 102 \times 25$	$305 \times 102 \times 25$	20	1	372.366
6	5	1.20	$305 \times 102 \times 28$	$IPE200$	0	4	416.751
7	5	1.40	$305 \times 102 \times 25$	$305 \times 102 \times 25$	0	1	421.676
8	5	1.60	$305 \times 102 \times 25$	$305 \times 102 \times 25$	20	1	446.777
9	5	1.80	$305 \times 102 \times 25$	$305 \times 102 \times 25$	30	0	471.746
10	5	2.00	$305 \times 102 \times 28$	$IPE_{AA}200$	850	4	477.668
11	5	2.20	$305 \times 102 \times 25$	$IPE200$	620	4	508.867
12	5	2.40	$305 \times 102 \times 25$	$305 \times 102 \times 25$	0	1	545.745
13	5	2.60	$305 \times 102 \times 25$	$IPE_{AA}200$	560	4	492.741
14	5	2.80	$305 \times 102 \times 25$	$IPE_{AA}180$	1240	5	475.798
15	5	3.00	$305 \times 102 \times 25$	$IPE_{AA}180$	400	4	477.887
16	5	3.20	$305 \times 102 \times 25$	$IPE_{AA}180$	0	4	486.997
17	5	3.40	$305 \times 102 \times 25$	$IPE_{AA}180$	0	4	501.978
18	5	3.60	$IPE_{AA}200$	$IPE_{AA}180$	600	4	457.750
19	5	3.80	$IPE_{AA}200$	$IPE_{AA}180$	420	4	470.049
20	5	4.00	$IPE_{AA}200$	$IPE_{AA}180$	640	7	489.759
21	5	4.20	$IPE_{AA}200$	$IPE_{AA}180$	710	8	506.450
22	5	4.40	$IPE200$	$IPE_{AA}200$	23	7	623.370
23	5	4.60	$IPE_{AA}200$	$IPE_{AA}200$	800	9	613.489
24	5	4.80	$IPE200$	$IPE_{AA}180$	1670	10	611.955

Table A3: Results from genetic algorithm for frames with height of 6 m

Span [m]	**Height** [m]	**S/H**	**Column**	**Rafter**	**Haunch Length** [mm]	**Pitch** [deg]	**Total Weight** [kg]
3	6	0.50	$305 \times 102 \times 33$	$406 \times 140 \times 39$	0	4	510.964
4	6	0.67	$305 \times 102 \times 33$	$406 \times 140 \times 39$	0	2	549.890
5	6	0.83	$406 \times 140 \times 39$	$305 \times 102 \times 25$	20	2	592.348
6	6	1.00	$406 \times 140 \times 39$	$305 \times 102 \times 25$	0	2	616.965
7	6	1.17	$406 \times 140 \times 39$	$305 \times 102 \times 25$	0	0	641.724
8	6	1.33	$406 \times 140 \times 39$	$305 \times 102 \times 25$	0	3	666.672
9	6	1.50	$406 \times 140 \times 39$	$305 \times 102 \times 25$	0	4	691.894
10	6	1.67	$406 \times 140 \times 39$	$305 \times 102 \times 25$	30	3	716.985
11	6	1.83	$406 \times 140 \times 39$	$305 \times 102 \times 25$	0	0	740.850
12	6	2.00	$406 \times 140 \times 39$	$305 \times 102 \times 25$	20	0	765.873
13	6	2.17	$406 \times 140 \times 39$	$305 \times 102 \times 25$	0	1	790.524
14	6	2.33	$305 \times 102 \times 33$	$305 \times 102 \times 25$	1000	4	766.448
15	6	2.50	$305 \times 102 \times 33$	$305 \times 102 \times 25$	650	4	782.430
16	6	2.67	$305 \times 102 \times 28$	$305 \times 102 \times 25$	1430	4	771.435
17	6	2.83	$305 \times 102 \times 28$	$305 \times 102 \times 25$	880	4	782.779
18	6	3.00	$305 \times 102 \times 33$	$IPE_{AA}200$	1520	4	745.715
19	6	3.17	$305 \times 102 \times 28$	$IPE_{AA}200$	1090	4	700.801
20	6	3.33	$305 \times 102 \times 28$	$IPE_{AA}200$	430	4	706.965
21	6	3.50	$305 \times 102 \times 25$	$IPE_{AA}200$	1770	3	707.979
22	6	3.67	$305 \times 102 \times 25$	$IPE_{AA}200$	1860	4	727.885
23	6	3.83	$305 \times 102 \times 25$	$IPE_{AA}200$	1790	8	747.763
24	6	4.00	$305 \times 102 \times 25$	$IPE_{AA}200$	1780	8	765.760
25	6	4.17	$305 \times 102 \times 25$	$IPE_{AA}200$	2000	8	787.986
26	6	4.33	$305 \times 102 \times 25$	$305 \times 102 \times 25$	0	2	942.967
27	6	4.50	$305 \times 102 \times 25$	$IPE_{AA}200$	2400	9	832.660
28	6	4.67	$305 \times 102 \times 25$	$305 \times 102 \times 25$	0	3	992.978
29	6	4.83	$305 \times 102 \times 25$	$305 \times 102 \times 25$	0	8	1023.992

Table A4: Results from genetic algorithm for frames with height of 7 m

Span [m]	**Height** [m]	**S/H**	**Column**	**Rafter**	**Haunch Length** [mm]	**Pitch** [deg]	**Total Weight** [kg]
3	7	0.43	406 × 140 × 39	305 × 102 × 33	0	6	644.975
4	7	0.57	406 × 140 × 39	406 × 140 × 39	30	2	702.992
5	7	0.71	406 × 140 × 39	406 × 140 × 39	0	0	741.195
6	7	0.86	406 × 140 × 39	406 × 140 × 39	20	2	780.767
7	7	1.00	406 × 140 × 39	406 × 140 × 39	0	3	819.648
8	7	1.14	406 × 140 × 39	406 × 140 × 39	0	4	858.957
9	7	1.29	406 × 140 × 46	305 × 102 × 33	530	5	957.580
10	7	1.43	406 × 140 × 46	305 × 102 × 33	580	4	991.792
11	7	1.57	406 × 140 × 39	406 × 140 × 39	0	2	975.534
12	7	1.71	406 × 140 × 39	406 × 140 × 39	0	2	1014.324
13	7	1.86	406 × 140 × 39	406 × 140 × 39	0	2	1053.621
14	7	2.00	406 × 140 × 46	305 × 102 × 28	1210	4	1073.830
15	7	2.14	406 × 140 × 46	305 × 102 × 28	1230	4	1099.673
16	7	2.29	406 × 140 × 39	406 × 140 × 39	20	2	1170.809
17	7	2.43	406 × 140 × 46	305 × 102 × 25	1440	4	1102.342
18	7	2.57	406 × 140 × 39	305 × 102 × 28	1210	4	1088.792
19	7	2.71	406 × 140 × 39	305 × 102 × 25	1470	4	1054.707
20	7	2.86	406 × 140 × 39	305 × 102 × 25	950	4	1066.771
21	7	3.00	406 × 140 × 39	305 × 102 × 25	440	4	1078.885
22	7	3.14	406 × 140 × 39	$IPE200$	1860	4	1081.667
23	7	3.29	406 × 140 × 39	305 × 102 × 25	20	3	1117.505
24	7	3.43	305 × 102 × 28	$IPE200$	2030	4	978.983
25	7	3.57	305 × 102 × 28	305 × 102 × 25	1010	4	1041.312
26	7	3.71	305 × 102 × 28	305 × 102 × 25	10	4	1041.423
27	7	3.86	305 × 102 × 28	305 × 102 × 25	30	4	1066.556
28	7	4.00	305 × 102 × 28	305 × 102 × 25	20	3	1090.426

Table A5: Results from genetic algorithm for frames with height of 8 m

Span [m]	**Height** [m]	**S/H**	**Column**	**Rafter**	**Haunch Length** [mm]	**Pitch** [deg]	**Total Weight** [kg]
3	8	0.38	406 × 178 × 54	406 × 140 × 39	280	6	993.813
4	8	0.50	406 × 178 × 54	406 × 140 × 46	180	5	1058.537
5	8	0.63	406 × 178 × 54	406 × 140 × 46	250	5	1107.795
6	8	0.75	406 × 178 × 54	406 × 140 × 46	270	5	1163.906
7	8	0.88	406 × 178 × 60	406 × 140 × 39	320	4	1247.591
8	8	1.00	406 × 178 × 60	406 × 140 × 39	560	6	1296.964
9	8	1.13	406 × 178 × 60	406 × 140 × 39	670	5	1339.759
10	8	1.25	406 × 178 × 54	406 × 140 × 46	880	4	1366.927
11	8	1.38	406 × 178 × 60	406 × 140 × 39	670	4	1417.661
12	8	1.50	406 × 178 × 60	406 × 140 × 39	770	4	1460.773
13	8	1.63	406 × 178 × 60	406 × 140 × 39	650	5	1495.731
14	8	1.75	406 × 178 × 60	406 × 140 × 39	670	4	1534.946
15	8	1.88	406 × 178 × 60	406 × 140 × 39	650	5	1573.951
16	8	2.00	406 × 178 × 54	406 × 140 × 39	1340	5	1544.283
17	8	2.13	406 × 178 × 54	406 × 140 × 39	1150	4	1574.952
18	8	2.25	406 × 178 × 54	406 × 140 × 39	960	4	1606.676
19	8	2.38	406 × 178 × 54	406 × 140 × 39	700	4	1635.631
20	8	2.50	406 × 140 × 46	406 × 140 × 39	1680	4	1583.191
21	8	2.63	406 × 140 × 46	406 × 140 × 39	1710	4	1623.495
22	8	2.75	406 × 140 × 46	406 × 140 × 39	890	4	1630.688
23	8	2.88	406 × 140 × 46	305 × 102 × 33	2260	4	1566.239
24	8	3.00	406 × 140 × 46	305 × 102 × 28	1900	4	1467.835
25	8	3.13	406 × 140 × 39	305 × 102 × 28	2440	4	1399.360
26	8	3.25	406 × 140 × 39	305 × 102 × 25	1600	4	1309.931
27	8	3.38	406 × 140 × 39	305 × 102 × 25	1720	4	1337.742
28	8	3.50	406 × 140 × 39	305 × 102 × 25	1630	4	1360.495

Appendix B

Hand Calculations for Critical Column

Appendix B includes the hand calculations for a critical column analysed as a beam-column in accordance with SANS 10162-1:2011 to compare with the results obtained from the Genetic Algorithm and prove that the Genetic Algorithm provide accurate and trustworthy results.

Table B1: Results from genetic algorithm for critical column calculations

Description	Magnitude	Unit
Span	26	m
Height	6	m
Span/Height	4.333	
Vertical Limit	0.144	m
Horizontal Limit	0.030	m
Column	305 x 102 x 25-I	
Rafter	305 x 102 x 25-I	
Haunch length	0	mm
Pitch	2	deg
Total Weight	943	kg
Column1	0.334	
Column2	0.934	
Rafter1	0.386	
Rafter2	0.698	
Vertical	0.808	
Horizontal	0.453	

Table B2: Input values for capacity calculation of 305 x 102 x 25 column

Description	Magnitude	Unit
C_u	33.685	kN
M_u	100.303	kNm
f_y	355	MPa
E	2.10^5	MPa
L	6	m
b	101.6	mm
h	305.1	mm
t_f	6.7	mm
t_w	5.8	mm
r_x	118	mm
r_y	19.6	mm
A	3120	mm^2
Z_{pl}	336.10^3	mm^3
Z_e	286.10^3	mm^3
I_x	$43.6.10^6$	mm^4

Axial Compression Classification (SANS 10162-1:2011 §11.2)

Flanges

$$\frac{b}{t} = \frac{101.6}{2 \times 6.7} = 7.582 \leq \left[\frac{200}{\sqrt{f_y}} = \frac{200}{\sqrt{355}} = 10.615\right] \quad \textbf{Class 3}$$

Webs

$$\frac{h - (2.t_f)}{t_w} = \frac{305.1 - (2 \times 6.7)}{5.8} = 50.293 \geq \left[\frac{670}{\sqrt{f_y}} = \frac{670}{\sqrt{355}} = 35.56\right] \quad \textbf{Class 4}$$

Flexural Compression Classification (SANS 10162-1:2011 §11.2)

Flanges

$$\frac{b}{t} = \frac{101.6}{2 \times 6.7} = 7.582 \leq \left[\frac{145}{\sqrt{f_y}} = \frac{145}{\sqrt{355}} = 7.696\right] \quad \textbf{Class 1}$$

Webs

$$\frac{h-(2.t_f)}{t_w}=\frac{305.1-(2\times 6.7)}{5.8}=50.293\leq\left[\frac{1100}{\sqrt{f_y}}.\left(1-0.39\frac{C_u}{\phi.A.f_y}\right)=57.613\right]\quad\textbf{Class 1}$$

Class 4 Web (SANS 10162-1:2011 §13.3.3)

$$f=\frac{C_u}{\phi.A}=\frac{33.685.10^3}{0.9\times 3120}=11.996\,\text{MPa}$$

$$W_{lim}=0.644\times\sqrt{\frac{k.E}{f}}=0.644\times\sqrt{\frac{4.0\times 2.10^5}{11.996}}=166.31\,\text{MPa}$$

$$W=50.293\,\text{MPa}\leq[W_{lim}=166.31\,\text{MPa}]$$

$$A_{new}=A=3120\,\text{mm}^2$$

Cross-Sectional Strength (SANS 10162-1:2011 §13.8.2 a)

$$C_r=\phi.A.f_y.\left(1+\lambda^{2.n}\right)^{-1/n}=0.9\times 3120\times 355\times\left(1+0^{2(1.34)}\right)^{-1/1.34}=996.84\,\text{kN}$$

$$M_r=\phi.Z_{pl}.f_y=0.9\times 336.10^3\times 355=107.352\,\text{kNm}$$

$$\frac{C_u}{C_r}+\frac{0.85U_{1x}M_u}{M_r}=\frac{33.685}{996.84}+\frac{0.85\times 1.0\times 100.303}{107.352}=0.828$$

$$\frac{M_u}{M_r} = \frac{100.303}{107.352} = 0.934$$

Overall Member Strength (SANS 10162-1:2011 §13.8.2 b)

$$\lambda = \frac{KL}{r_x} \times \sqrt{\frac{f_y}{\pi^2 E}} = \frac{1.0 \times 6000}{118} \times \sqrt{\frac{355}{\pi^2 \times 2.10^5}} = 0.227$$

$$C_r = \phi.A.f_y.\left(1 + \lambda^{2.n}\right)^{-1/n} = 0.9 \times 3120 \times 355 \times \left(1 + 0.227^{2(1.34)}\right)^{-1/1.34} = 983.033\,\text{kN}$$

$$M_r = \phi.Z_{pl}.f_y = 0.9 \times 336.10^3 \times 355 = 107.352\,\text{kNm}$$

$$\frac{C_u}{C_r} + \frac{0.85U_{1x}M_u}{M_r} = \frac{33.685}{983.033} + \frac{0.85 \times 1.0 \times 100.303}{107.352} = 0.828$$

$$\frac{M_u}{M_r} = \frac{100.303}{107.352} = 0.934$$

Appendix C

Code for JAVA Program on CD